Multi-Organ-Chip Based Skin Models for Research and Substance Testing

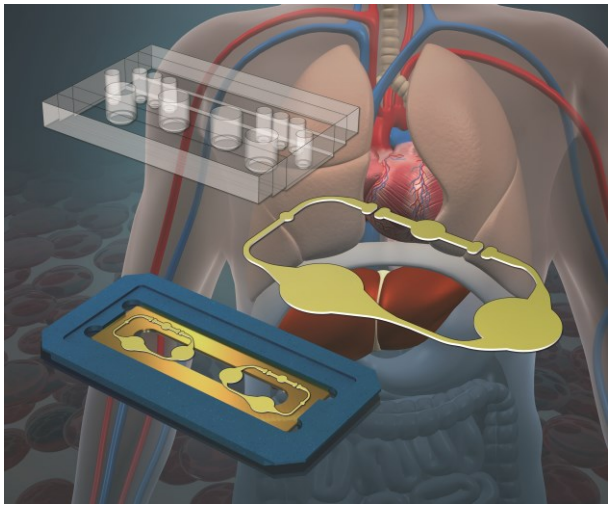

vorgelegt von
Diplom-Ingenieurin, Master of Science
Ilka Wagner
aus Berlin

von der Fakultät III - Prozesswissenschaften
der Technischen Universität Berlin
zur Erlangung des akademischen Grades
Doktor der Ingenieurwissenschaften
- Dr.-Ing. -
genehmigte Dissertation

Promotionsausschuss:

Vorsitzende: Prof. Dr. V. Meyer
Berichter: Prof. Dr. R. Lauster
Berichter: Prof. Dr. P. Neubauer
Berichter: Dr. Otto von Stetten
Tag der wissenschaftlichen Aussprache: 29.11.2013

Berlin 2014
D 83

I. Table of Contents

II. Abbreviations

µCCA	Micro cell culture analogue
µFCCS	Microfluidic cell culture system
2D	Two-dimensional space
3D	Three-dimensional space,
ANOVA	Analysis of variance
BioVaSc	Biological vascularised scaffold
BPE	Bovine pituitary extract
CCA	Cell culture analogue
CD	Cluster of differentiation
DFG	Deutsche Forschungsgemeinschaft
DMEM	Dulbecco's modified eagle medium
DMSO	Dimethylsulfoxid
DNA	Deoxyribonucleic acid
DoE	Design of experiment
DP	Dermal papillae
PBS	Phosphate-buffered saline
ECGM	Endothelial cell growth medium
ECM	Extracellular matrix
ECVAM	European centre for the validation of alternative methods
EDTA	Ethylenediaminetetraacetic acid
EGF	Epidermal growth factor
ELISA	Enzyme-linked immunosorbent assay
EtOH	Ethanol
EU	European union
FcR	Fc receptor
FCS	Fetal calf serum
FGF2	Fibroblast growth factor
FITC	Fluoresceinisothiocyanat
FT	Full thickness
FUE	Follicular unit extractions
GAG	Glycosaminoglycan
GI	Gastrointestinal

H/E	Haematoxylin/eosin
HBSS	Hank's balanced salt solution
HDMEC	Human dermal microvascular endothelial cells
hEGF	Human epidermal growth factor
HHSteC	Human hepatic stellate cells
HRP	Horseradish peroxidase
HTS	High-throughput screening,
IGF	Insulin-like growth factor
IL	Interleukin
KGF	Keratinocyte growth factor
KGM	*Keratinocyte* growth medium
LDH	Lactate dehydrogenase
MACS	Magnetic activated cell sorting
MOC	Multi-organ-chip
mRNA	Messenger ribonucleic acid
MRP-2	Multidrug resistance-associated protein 2
OECD	Organisation for economic co-operation and development
PBPK-PD	Physiologically based pharmacokinetic pharmacodynamics
PDMS	Polydimethylsiloxane
PEEK	Polyether ether ketone
PFTE	Polytetrafluoroethylene
POM	Polyoxymethylene
qPCR	Quantitative polymerase chain reaction
REACH	Registration, evaluation, authorization of chemicals
TG	Test guideline
TGF	Transforming growth factor
TNF	Tumor necrosis factor
TUNEL	TdT-mediated dUTP-digoxigenin nick end labelling
VEGF	Vascular endothelial growth factor

II. Abstract

Current *in vitro* and animal tests for drug development are failing to emulate the systemic organ complexity of the human body and, therefore, to accurately predict drug toxicity. To ban the ever increasing dilemma of poorly predictive preclinical substance evaluation, new solutions are needed. These have to avoid the phylogenetic distance between laboratory animals and humans and eliminate the discrepancy between current *in vitro* test systems and the human body. Only few multi-compartment cell culture flow systems have been described so far, even less on a miniaturised scale. In the development of skin equivalents, substantial progress has been achieved in the last few decades. However, static culture of the skin limits the emulation of essential physiological properties which are crucial for toxicity testing and compound screening. The dynamically perfused chip-based multi-organ-chip developed in this study is capable of applying variable mechanical shear stress and, therefore, can extend culture periods. This improves culture conditions of integrated *in vitro* skin equivalents and skin biopsies which have been proven to be viable as long-term cultures of up to 28 days in the multi-organ-chip. The system supports two different culture modes: i) tissue exposed to the fluid flow, or ii) tissue shielded from the underlying fluid flow by standard Transwell® cultures. Hence, skin can either be cultured in the flow or at air/liquid interface with less shear stress which was shown to be beneficial for the skin's epidermal structure and, hence, its barrier function. The multi-organ-chip was further developed to combine the skin equivalent with a human artificial liver microtissue in co-culture, each a $^{1}/_{100.000}$ of the biomass of their original human counterparts. This co-culture successfully showed stable long-term performance of 28 days. In comparison, most other systems are only stable for 72 h. Crosstalk between the two tissues was observed in 14-day co-cultures exposed to fluid flow. Then, troglitazone, a hepatoxic anti-diabeticum, was chronically applied to the skin and liver co-cultures and showed sensitivity at different molecular levels within a 6-day exposure time. Finally, the skin and liver co-cultures were combined with a fully endothelialised multi-organ-chip. Endothelial cells covered all walls of the channels in the multi-organ-chip, as known from blood vessels. This combination of 3 tissues in one co-culture was stable for 28 days, fulfilling the requirement of 21-28 days of exposure that is defined in OECD guidelines for dermal subsystemic repeated dose toxicity testing of chemicals and cosmetics in animals. Thus, in this study, a potential new tool for systemic substance testing has been developed.

1. Introduction

1.1 The Skin

The skin is the outer cover of the human body and has an area of 1.5 to 2 m². Though it only has a thickness of 1.5 to 4 mm, it is the heaviest organ in the human body with about 16% of the body's weight. The skin is responsible for several complex functions: It has a barrier function which avoids dehydration of the body and penetration of liquids. It protects the body from chemical, biological and physical interactions. Further it acts as a regulatory system for temperature, electrolyte and water balance. Its appendages, like hair follicles and sweat glands, can act as immune and sensory organs. The embedded Merkel and nerve cells can sense temperature, pain and pressure (Elias, 2005), while blood vessels supply the skin with nutrients and are also involved in the thermoregulation. Further, antigen-presenting immune cells, the Langerhans cells and anti-microbial substances support the immune system (Boulais und Misery, 2008; Johnston *et al.,* 2000). Melanocytes in the epidermis are responsible for the pigmentation of skin and hair and thereby provide protection from damage by ultraviolet radiation and contribute to the appearance of skin. Vitamin D3 is produced photochemically in the skin. Moreover, the skin is constantly regenerating which is regulated by growth factors, cytokines and hormones (Blanpain und Fuchs, 2006; Giangreco *et al.,* 2008).

1.1.1 The Morphology of the Skin

The skin is composed of three primary layers, the epidermis, the dermis and the subcutis (Figure 1.1). The epidermis is a stratified squamous epithelium, composed of proliferating basal and differentiated suprabasal keratinocytes. It is separated from the dermis by the basement membrane. The underlying subcutis serves as a supporting and connective tissue and stores fat tissue for isolation and as an energy stock.

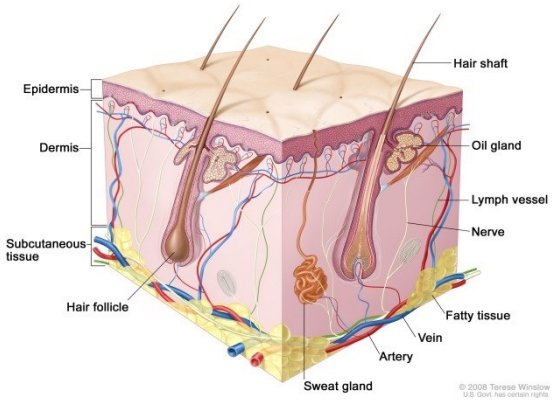

Figure 1.1) Schematic anatomy of the skin, showing the epidermis, dermis, and subcutaneous tissue. (www.cancerinfo.tri-kobe.org)

1.1.1.1 The Epidermis

The epidermis is the outermost layer of the skin and is ectoderm in its origin. It consists of 95% keratinocytes but also contains melanocytes, Langerhans cells and Merkel cells (McGrath *et al.,* 2004). It is avascular and nutrients are provided from the dermis by diffusion. Histologically the epidermis can be divided into four different layers: the *stratum corneum*, *stratum granulosum*, *stratum spinosum* and the *stratum basale* (Figure 1.2). The *stratum basale* is connected to the basement membrane by hemidesmosomes and is single layered. It is the only layer in the epidermis which is mitotically active. The *stratum basale* is apically connected to the *stratum spinosum* which consists of 2-5 cell layers. Cells flatten and start to store keratinosoms, the „odland bodies“ (Odland, 1960). These vesicles originate from the golgi apparatus and contain enzymes, glycoproteins and lipids which are important for the formation of an intact *stratum corneum*. The bordering *stratum granulosum* has 1-5 layers of flattened keratinocytes which contain plenty of basophil keratohyalin granules which give the cells the typical granular structure. At the border to the *stratum corneum*, proteases and nucleases degrade the nuclei and nearly all cell organelles, the cells dehydrate, form a lipid barrier, cornify and thereby form the actual protective layer of the skin (Fuchs and Green, 1980). During the differentiation of the epidermis, the cytokeratin expression profile changes according to the cell layer and differentiation status

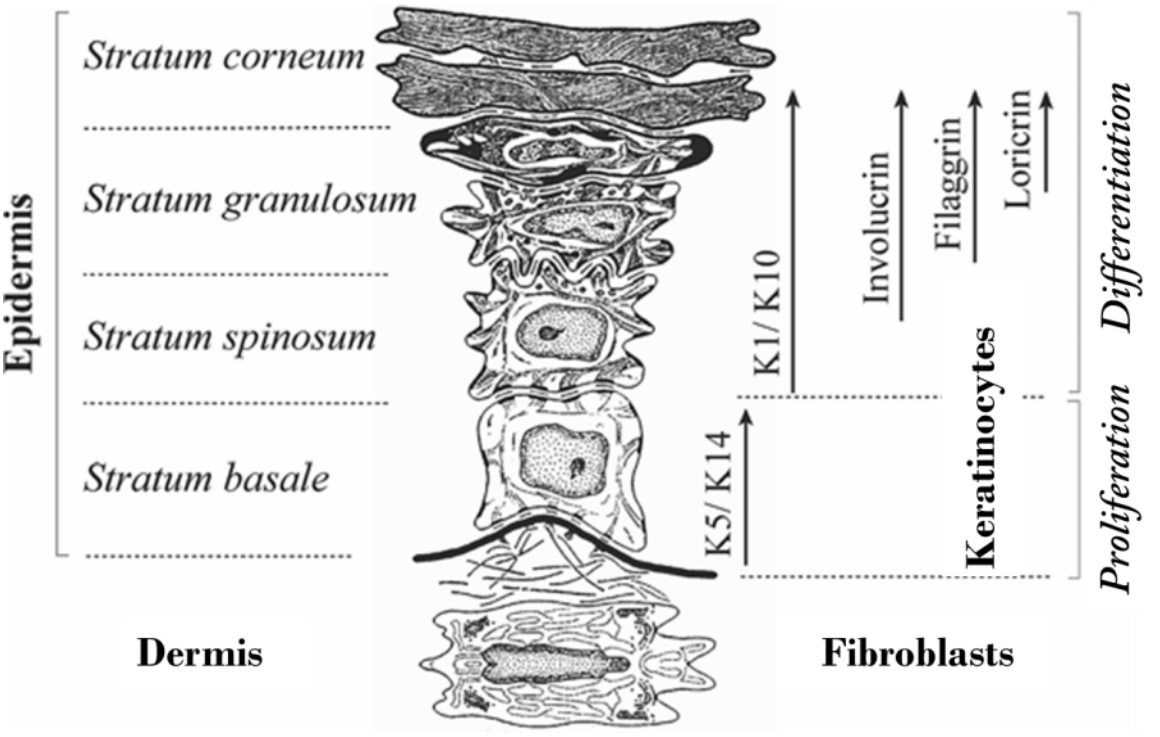

Figure 1.2) Schematic cross section of the human epidermis and its four layers: Keratinocytes express different proteins depending on their location in the epidermis. Below the epidermis is the basement membrane which is connected to the dermis (adapted from *Bowden et al.,* 1987).

(O'Guin *et al.,* 1987; Fuchs and Green 1980). The cytokeratins 5, 14 and 15 are exclusively expressed in the basal layer, while cytokeratin 1 and 10 are found in the *stratum spinosum* and above, where cells are terminally differentiated and cornified (Lampe *et al.,* 1983, Firgure 1.2). The expression profile can therefore provide information about the hierarchical organisation and the grade of differentiation of the epithelial tissue.

1.1.1.2 The Basement Membrane

The basement membrane is composed of a network of specific extracellular matrix which connects the epidermis with the dermis (Figure 1.3), but also separates both compartments (Kalluri, 2003; McMillan *et al.,* 2003). It consists of a tight net of collagen fibres (collagen type IV and VII), laminin, fibronectin, heparan sulphate proteoglycan (perlecan) and glycoproteins (nidogen). Laminin connects the epithelial cells to the basal lamina through integrin molecules. All components of the basement membrane are produced by keratinocytes in the epidermis and fibroblasts in the dermis (Marionnet *et al.,* 2006). Using the electron microscope, the basement membrane of the skin can be divided into four zones: 1) the plasma membrane and the hemidesmosomes of the basal keratinocytes, 2) the *lamina lucida*, with the anchoring fibrils which appear transparent in the electron microscope, 3) the *lamina densa*, a zone with a high electron density and below the 4) *sublamina densa*, as an electron-lucent zone (Woodley and Chen, 2001).

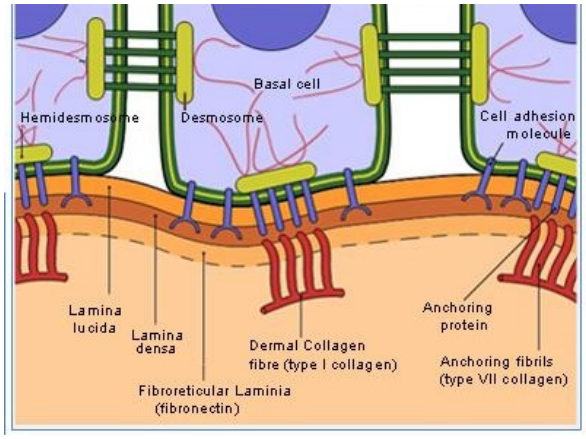

Figure 1.3) Schematic of the basement membrane zone
(http://raregeneticdisorder.blogspot.de)

1.1.1.3 The Dermis

Below the basement membrane is the dermis, an areolar connective tissue mainly made of extracellular matrix which is secreted by the main cellular component - the dermal fibroblasts. These matrix components are constantly rearranged and reorganised, in normal

skin as well as in pathological situations. The dermis can be divided into *stratum papillare* and the *stratum reticulare*. Both layers have a tight network of type I and III collagens which are loaded with water binding glycosaminoglycans like hyaluronic acid, dermatan sulphate, chondroitin-4-sulphate and chondroitin-6-sulphate. The *stratum papillare* is directly below the epidermal basement membrane and contains collagen fibrils which connect the dermis with the basement membrane. In this layer thermo receptors and sensory organs, as well as lymphocytes, plasma cells, monocytes, macrophages and mast cells are found. At the border of the *stratum papillare* and the *stratum reticulare* the subpapillar blood vessels with arterioles and venoles can be found. The *stratum reticulare* is composed of dense irregular connective tissue and is rich in strong collagen fibrils (type I collagen) which gives the dermis its properties of strength, extensibility and elasticity. Further, the roots of the hair, sebaceous glands, sweat glands, receptors and nails are located in the reticular region.

1.2 Skin equivalents

The first reports about successful tissue engineering of the skin were published in the 1980s, when keratinocytes were first cultured at the air/liquid-interface (Bell *et al.,* 1981; Coulomb *et al.,* 1989; Fusenig *et al.,* 1981; Mackenzie und Fusenig, 1983; Parenteau *et al.,* 1991; Prunieras *et al.,* 1983). Equivalents of the human skin can serve as an alternative to animal experiments for drug and cosmetic testing as well as to improve the knowledge on biological processes in the skin, like wound healing, pathogenesis of skin diseases and skin cancer. Different skin reconstructs are available, either composed of an epidermal construct (epidermis models) or an epidermal and dermal construct (full thickness models). Examples for epidermis models which have been validated by the OECD (TG 431) are EpiSkin™ (L'Oreal, France), Epiderm SIT™ (MatTek Corporation, USA) and EST-1000 (CellSystems, Germany). There are some epidermis models which are accredited for transplantation, like Myskin™ (Celltran, UK) and CellSpray® (Clinical Cell Culture, UK). There are no validated full thickness equivalents so far, though tissue engineering is focussing on the development of dermal equivalents on the basis of absorbable materials like AlloDerm® (LifeCell, USA) and Dermagraft® (Advanced BioHealing, USA). The first step of skin equivalent generation is the isolation of cells from skin, like keratinocytes and fibroblasts, but also melanocytes and endothelial cells. Commonly, breast and foreskin from surgical operations is used. Keratinocytes are grown in culture and then differentiated on acellular or fibroblast-populated dermal substrates, like collagen matrices (Bell *et al.,* 1981; Fusenig *et al.,* 1981), de-

epidermised dermis (Ponec *et al.,* 1988; Prunieras *et al.,* 1983), inert filters (Cannon *et al,* 1994, Rosdy *et al.*, 1990) and lyophilised collagen-GAG membranes (Boyce *et al.,* 1988; Shahabeddin *et al.,* 1990). However, a major difference between *in vivo* skin and skin substitutes is the presence of skin appendages such as hair follicles, sebaceous glands and sweat glands. Appendages can change the permeability of the skin, as their organisation differs from that of the epidermis (Schäfer and Lademann, 2001). For example, the transepidermal diffusion follows an inter- or transcellular pathway across the *stratum corneum*, whereas the transappendageal diffusion uses the route through the hair follicles and their associated sebaceous glands (Scheuplein *et al.,* 1967). Standardised full thickness skin equivalents are produced in Transwell®-plates with inserts for the cultivation of keratinocytes at the air/liquid-interface. This is a batch system, where nutrients are not supplied continuously, but exchange of the media only occurs in defined time intervals. So far only few attempts were made to generate skin equivalents in bioreactors with a continuous flow. A first trial was done by Kalyanaraman and Boyce in 2007, who produced an automated bioreactor system to expand keratinocytes for the later use in skin equivalents (Kalyanaraman *et al.,* 2007). In further experiments the effect of the continuous media flow on the anatomy and physiology of full skin equivalents at air/liquid-interface was analysed. These results showed that perfusion rates of skin equivalents at low flow rates (5 ml/h) increased the cell viability and maintained an epidermal barrier suitable for grafting. Skin equivalents cultured at flow rates of 15 ml/h showed a comparable viability to the control. Higher flow rates (50 ml/h) led to deterioration of the skin equivalents' anatomy and physiology (Kalyanaraman *et al.,* 2008). Another perfused bioreactor system was described by Groeber *et al* in 2013 (Figure 1.4). A decellularised porcine jejunal segment served as a biological vascularised scaffold, where the vascular pedicle was explanted and cannulas were inserted into the artery and vein. Human dermal microvascular endothelial cells (HDMECs) were injected into the arterial inflow and cultured in the bioreactor for 14 days at a physiological medium flow between 80 and 120 mmHg. This bioreactor provided perfusion of the upper and lower compartment, allowing the equivalent to be either covered with medium or cultured at air/liquid-interface where a constant air flow could be generated (Groeber *et al.,* 2013).

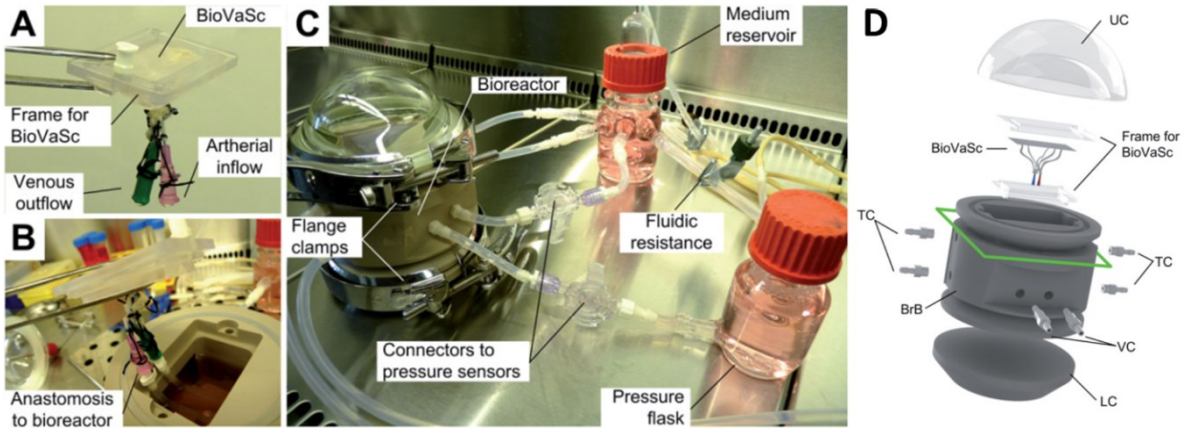

Figure 1.4) Bioreactor system for the culture of vascularised tissue equivalents: BioVaSc integrated in the polycarbonate frame (A). Anastomosis between the vascular system of the BioVaSc and the bioreactor (B). Complete bioreactor system with periphery (C). Overview of the three-dimensional design of the bioreactor components for the culture of vascularised tissue equivalents (D). UC, upper cover; BioVaSc, biological vascularised scaffold; TC, tube connectors; BrB, bioreactor body; VC: vascular connectors; LC, lower cover. From: Groeber *et al.,* 2013

1.3 Testing of Chemicals and Regulatory Environment

Conventional tests for toxicity, safety and efficacy of chemicals have been performed in animals. Among others, these tests include LD_{50}, Draize rabbit eye and Draize skin irritation tests. However, several concerns exist regarding animal tests: i) they are expensive, ii) results have a limited application to humans and iii) there is substantial suffering of animals. The development and validation of *in vitro* skin equivalents for corrosion and irritation test helped to reduce the number of animal experiments. However, still a great number of chemicals need to be classified regarding their capacity to harm the skin and the body. For many drugs and cosmetics which are currently applied to the skin, the amount of substance that reaches the target site often remains unclear. It is, therefore, of great interest, e.g. for the cosmetic industry, to develop an *in vitro* system which could predict the rate of penetration of cosmetic formula through the epidermal layers into the skin. The HET-CAM test was developed as a first *in vitro* test for skin irritation and replaced the Draize rabbit eye test. This *in vitro* test uses fertilised eggs (Lüpke, 1985) and underwent a lengthy validation process. During this validation, public concerns about animal suffering increased. To enhance the progress of animal replacement in testing cosmetics, the EU stated in the 7th amendment of the "Cosmetics Regulation" that from March 2013 on all animal experiments are prohibited when testing cosmetic ingredients and finished cosmetic products (76/768/EEC, 2003.) Already in 1959 Russell and Burch suggested the 3R-principles "replace,

reduce and refine" (Russell and Burch, 1959) which was implemented in the European Council Directive 86/609/EEC in 1986 and more firmly in 2010 in the new Directive 2010/63/EU. The three "Rs" refer to Replacement, where non-animal tests are preferred to animal tests whenever possible, to Reduction, where comparable amounts of information can be obtained from fewer animals, or more information from the same amount of animals and to Refinement, where potential pain, suffering and distress should be minimised by adequate housing, health care and the use of anaesthesia. In great contrast to this approach, the substances required for testing of possible harmful side effects increase. The public's concern about safety of chemicals led to the regulation No. 1907/2006 which requires the evaluation of existing as well as new chemicals (EU, Regulation No. 1907/2006). Therefore, the European program for the Registration, Evaluation, Authorization and Restriction of Chemicals (REACH) was adopted in 2007 and will lead to the reassessment of the hazard potential of up to 100.000 chemicals (Rovida and Hartung, 2009) in order to improve the protection of the environment and human health. Using conventional test methods, this would need an extremely high number of toxicity tests and would be time and cost consuming. Driven by this regulatory pressure, a number of scientific initiatives have been founded with the main focus on integrating existing *in vivo* data with *in vitro* and *in silico* approaches. However, so far, only reconstructed human epidermis models have been validated by the OECD for corrosion and irritation studies which can be exposed to test substances in static Transwell® systems for 7 up to 72 hours. These tests do not provide any information about the substance's absorption or penetration through the skin. Other substance testing methods include single layer or single cell-type cultures in micro wells or cell culture plates which make the system robust and suitable for high throughput testing, but due to their simplicity, these models fail to mimic key aspects of the human body. This leads to misinterpretations and false conclusions. Exchange of metabolites between different cell types, the three-dimensional extracellular matrix environment and physiological shear stress are not taken into account. Existing assays ignore the complexity of biological tissues of the human body with its multiple organs and their interactions. Yet, including more cell types will inevitably lead to a decreased robustness and throughput of the system. However, skin equivalents cannot be used to replace all animal models related to skin, as long as systemic response of applied substances cannot be investigated. It has been shown, that *in vitro* models can be improved by an artificially engineered microenvironment of cells and tissues (Anderson and Berg, 2004 and Khademhosseini *et al.,* 2006). This microenvironment can induce self-organisation and more realistic behaviour in healthy and

diseased cells, without decreasing the robustness and throughput of the testing system. Still, including more tissue types makes the system more complex and can lead to an uncertain behaviour, as each tissue interacts with the other in an unpredictable way which leads to less robust measurements (Manson, 2001). This challenge was addressed by researchers by new, integrated micro engineered *in vitro* platforms: the "organs-on-a-chips".

1.4 Organs-on-a-chip Platforms

Organs-on-a-chip platforms are micro devices to culture *in vitro* tissue with a physiologically relevant but engineered micro-environment. These devices are called "chips", as they are based on microchip technology, featuring several controllable parallel micro-channels which are splitting and merging, pumps, valves and integrated electrical and biochemical sensors. Developing organs-on-a-chip reliably and reproducibly with different kinds of human cells within a defined micro-environment is a major challenge. The cells have to be built together in 3D organoid structures and measuring and monitoring of the interactions between the cell types needs to be possible. Cells need to be cultured over a long period of time for cell differentiation and development of normal tissue architecture for healthy and diseased tissue models. For animal replacement, a self-reliant long-term homeostasis of groups of organs at miniaturised levels needs to be provided in the chip without decreasing the robustness of measurements in the system. The chip should be fully compatible with a microscope and be able to measure cellular response in real time and quantifiable manner. Further, the organ-on-a-chip platform should be medium to high throughput, while results have to be highly reliable and reproducible. In the following I will present the most promising systems.

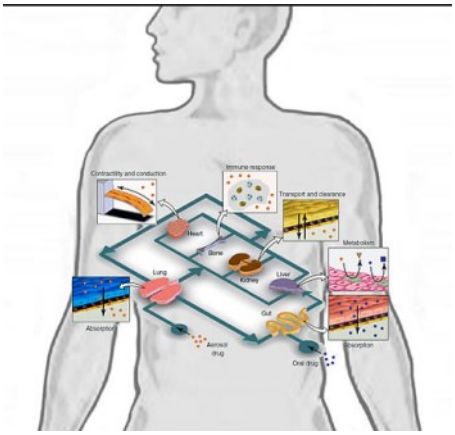

Figure 1.5) Conceptual Schematic of a Human-on-a-Chip: Designing a whole body biomimetic device will potentially correct one of the most significant limitations on organs-on-chips: the isolation of organs. From: Timothy.ruban

1.4.1 The Micro Cell Culture Analogue (µCCA)

The first dynamic micro-scale system combining cultures of different human tissues into a common media flow with around 10.000 cells per culture compartment was proposed in

2002 by the group of Sweeney and co-workers (patent US7288405B2). The concept of this chip is based on a physical analogue of physiologically based pharmacokinetic pharmacodynamics (PBPK-PD). A PBPK model mathematically simulates the absorption, distribution, metabolism and elimination kinetics of chemicals in interconnected tissue compartments. Combining this with a cell culture analogue (CCA) system provides the possibility to predict human response in clinical trials. A CCA contains multiple chambers, each representing a tissue or group of similar tissues in micro-scale (Figure 1.6 A) which are connected by recirculating tissue culture medium as a blood surrogate (Sin, 2004). The size of the compartments and the fluid flow inside each compartment are designed in the same ratio as in the human body. In the initial devices cell lines in 2D culture were used. Recent devices included 3D tissue constructs based on hydrogel entrapped cells, though cells are derived from cell lines which resulted in a different mix of cell types compared to real tissue. The µCCA supports the culture of different cell types and tissues which can be cultured for up to 4 days. The most realistic tissue construct of this group is their "GI tract" containing

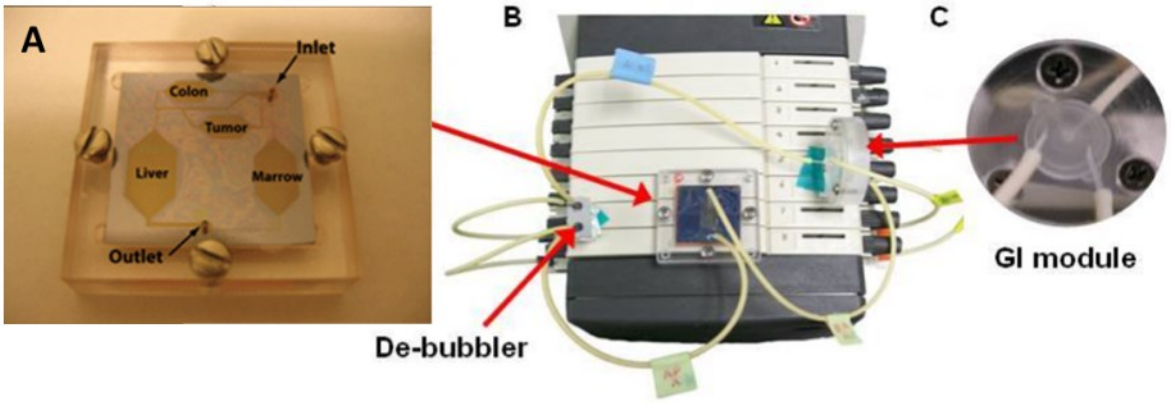

Figure 1.6) Image of the systemic µCCA. Organ chambers and channels are fabricated to accurately scale the chamber size and the interconnecting channels so they are representative of *in vivo* circulating conditions for those organs (A). The other tissues of the body were represented by the external de-bubbler which was a 200 µl reservoir (B). The GI module housed in a plexiglas chamber with cells seeded on a semiporous membrane (C). Images provided by M. Shuler in Biomimetic Sensors for Rapid Testing of Water Resources

cell lines and mimics three or more cell types in appropriate ratios (Shuler, 2012). The "GI-tract" contains the following cell types: the early passage intestinal epithelial cell line Caco-2, the mucus-producing goblet-like cell line HT29-MTX and Raji B lymphocytes which form an M-cell when cultured with Caco-2 cells and are involved in particle uptake (Mahler *et al.,* 2009). This has been coupled to a liver compartment with systemic circulation. Tests with acetaminophen showed similar results to that observed in rodent studies (Mahler *et al.,* 2009 (2)).

1.4.2 Kidney-, Gut- or Lung- "on-a-Chip"

In 2010 the group around Huh and Ingber published a system for chip culture of human lung (Huh *et al.,* 2010). The same system was later adapted for gut and kidney single-culture (Kim and Ingber, 2013 and Jang *et al.,* 2013). The chip consists of a microfluidic system containing two micro channels for cultivation, separated by a porous, flexible, ECM-coated membrane of polydimethylsiloxane (PDMS) and side channels for vacuum application (Figure 1.7). Cells can be seeded on both sides of the membrane, therefore allowing the co-culture of two different cell types. Both sides can be cultured in different media or, in case of the lung, one side can be cultured at the air, while nutrition is supplied by media from the lower layer. The vacuum application at the side of the culture can cause a cyclic mechanical strain (10%; 0.15 Hz) and therefore simulate breathing or gut shear stress in the culture. The culture is perfused by a syringe pump at a volumetric flow rate of 30 - 50 µl/hour (fluid shear stress ~0,2 dyne/cm²). Cells in the system can be cultured for up to 14 days.

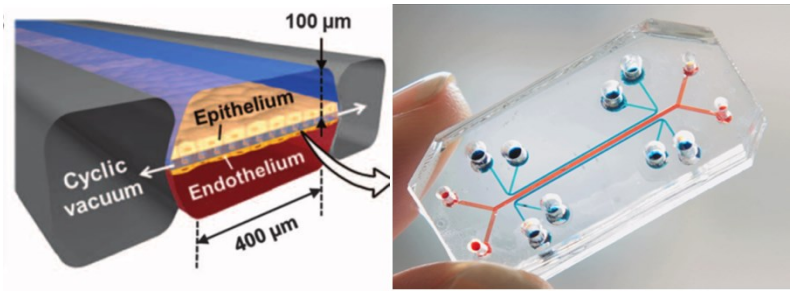

Figure 1.7) „Lung-on-a-chip": A micro engineered lung-on-a-chip that reproduces the lung microarchitecture and breathing-induced cyclic mechanical distortion of the alveolar-capillary interface. The top "air" compartment is the alveolar channel; the bottom "liquid" compartment is the vascular channel. From Huh *et al.,* 2011

1.4.3 Microfluidic Cell Culture System (µFCCS)

Zhang and co-workers from the Institute of Bioengineering and Nanotechnology, Singapore, developed a multi-channel 3-D microfluidic cell culture system (µFCCS, Figure 1.8 C). It has four separate channel-based cell culture spaces, each can be loaded with 10^5 cells to culture different 3D cellular aggregates simultaneously (Figure 1.8 A). Cell line derived human liver, lung, kidney and adipose tissue (C3A, A594, HK-2 and

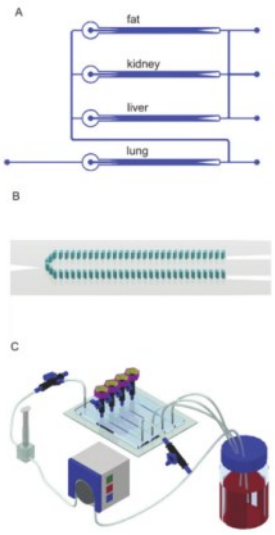

Figure 1.8) µFCCS setup. The schematic representation of the multi-channel 3D-µFCCS (A), the geometry of the 3D-µFCCS (B) and the close-loop perfusion culture of cells (C). From Zhang *et al.,* 2009

HPA, respectively) are shielded from the direct shear stress in the channels (Figure 1.8 B). To support different cell types with specific growth factors, gelatine spheres carrying growth factors are mixed with cells and released the growth factors in the specific microenvironment. Diffusion is the main transport system of nutrients and test substances between the cell compartments (Zhang *et al.,* 2009).

1.4.4 Micro Total Bioassay System

Another chip-system comprises a micro-intestine for intestinal absorption (CaCo-2 cell line), a micro- liver for hepatic metabolism (HepG2 cell line) and a human breast carcinoma cell for the assessment of the responsiveness (MCF-7 cell line) and was designed by Imura and

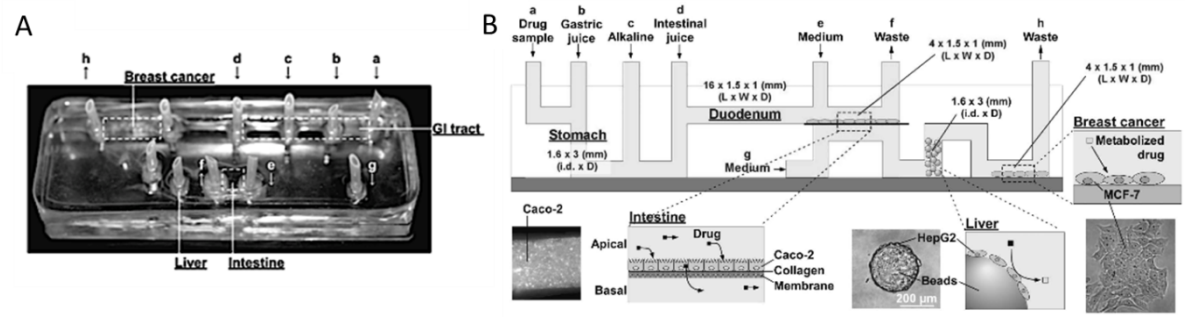

Figure 1.9) Photograph (A) and cross-sectional illustration of the micro total bioassay system (B) from Imura *et al.,* 2012

co-workers in Tokyo, Japan. Their chip has the size of a microscope slide and provides a unidirectional flow which supports the constant perfusion of the cells (Figure 1.9 A). The absorptive properties of the human intestine are represented by a tightly closed monolayer of human intestinal epithelial cells which absorb the drugs into the lower culture medium flow before the liver compartment (Figure 1.9 B). Two day exposure was achieved and led to discrete biological effects on the breast carcinoma cells (Imura *et al.,* 2010 and 2012). A new feature representing the gastrointestinal digestion was added by employing synthetic digestive juices to the latest system (Imura *et al.,* 2012).

1.5 Aim of this Study

During this project a multi-organ-chip system should be established and different kinds of skin equivalents should be tested for proof of principle. Another step forward to animal replacement is the combination of two organoids in one perfused bioreactor system. This should be shown by combining liver and skin culture and later by implementing these two tissues into a completely endothelialised bioreactor system. Testing a hepatoxic substance will complete this work.

Toxic side effects lead to unsuccessful drugs due to lack of efficacy or because they are clinically not safe. Estimations state that only about 1 of 10,000 compounds tested is introduced into therapy. Current *in vitro* and animal tests for drug development are failing to emulate the systemic organ complexity of the human body and, therefore, to accurately predict drug toxicity. Present cell based assays indicate the beneficial therapeutic effect on the target tissue, but never on the whole body: for example they do not include the crosstalk of different organs and the metabolic changes of the drugs. Animal models on the other hand, show effect on the whole body but often cannot be extrapolated to humans. Therefore, the goal of this study is, to provide a chip-based system which is biocompatible, microscopable, chemically resistant, sterilisable, cost effective and easy to produce, as well as being able to perfuse organoids, the smallest functional unit of an organ and possibly combining several organoids in one system. An on-chip pump would reduce the total media volume and would advance the system to more physiological tissue/volume ratios. This chip system should further be able to culture 3D cultures of different origin, like cell lines, primary cells and tissue biopsies. To prove this system, skin was chosen as a first organ, since several unwanted side effects appear on the skin, e.g. toxic epidermal necrolysis, exfoliative dermatitis and erythema multiforme. In order to include the skin into the chip system, skin samples needed to be miniaturised, but had to be big enough to integrate a hair follicle. Cultures of skin in form of own downscaled skin equivalents, commercially available skin models and skin biopsies should be tested and the system should possibly allow culture at the air/liquid interface. During drug application, the original substance, is metabolised in the liver. This metabolite, together with the original substance is then distributed to other organs, like the skin. Moreover, hepatoxicity is one of the major reasons for drug failure and withdrawal from the market. Combining the liver organoid with the skin organoid in the same circuit of the chip system will allow the analysis of this interaction between the organoids. These co-cultures need to be conducted in the same medium and should possibly be executed as long-term cultures. Combining them with endothelialised

channels in the multi-organ-chip system will further advance this system and should prove long-term stability (≥ 14 days) of the established system. Substance testing should provide data for successful drug toxicity prediction of a failed anti-diabetic drug.

2. Material and Methods

2.1 Materials

2.1.1 Devices and Technical Support

Table 1: Devices and technical support

Device	Type	Manufacturer
2-photon-microscope	TrimScope II	LaVision
CO_2-Incubator		Sanyo
Digital camera	E-3	Olympus
Fluorescence microscope	Biorevo	Keyence
Fluorescence quenching	BZ-9000	Presens GmbH
Light microscope	Axiovert 40c	Zeiss
Micromanipulator	T25	Luigs & Neumann
Microplate-reader	FLUOstar Omega	BMG Labtech
Microtome	HM 500OM	Fischer Scientific
Neubauer counting chamber	Improved	A. Hartenstein
Vi-Cell™ viability counter		Beckman Coulter

Table 2: Materials of the Multi-Organ-Chip

Equipment	Type	Manufacturer
Casting station		GeSiM
Channel master	A040-705	GeSiM
Channelplate	M3	SMC
	M5	GeSiM
Control unit of the pump		Capitalis Technology
Hexagon Socket Head Male Connector	M3	SMC
I-Fitting, PEEK	A040-706	GeSiM

Insert spacer	A040-708	GeSiM
Lid incl. O-Ring	A040-709	GeSiM
Membrane spacer, POM	A040-710	GeSiM
MOC-Support	MOC-I J–28 UNF6 M10 (PEEK)	GeSiM
Multi-Organ-Chip	A040-712	GeSiM
Needle, unbevelled		Fraunhofer IWS/GeSiM
Object glass slide	76x26mm	Menzel
Object slide	1 ml	BD
Peristaltic pump I and II	76x26mm	Thermo
Plasma-chamber		Capitalis Technology and BioClinicum
Plasma-pen	Femto	Diener
Plastipak™ luer slip syringe	Kinpen09	Neoplastools
Reservoir spacer	3 ml, 10 ml	BD
Reservoir, PEEK	A040-707	GeSiM
Reservoir, POM	A040-701	GeSiM
Surgical scalpel, disposable	A040-702	GeSiM
Syringe		Menzel
Syringe adapter	Female luer x 1-4-28 Male	IDEX
Transwell®-holder, PEEK	A040-716	BBraun
Transwell®-holder, POM	A040-703	GeSiM

Figure 2.1) Materials for MOC casting

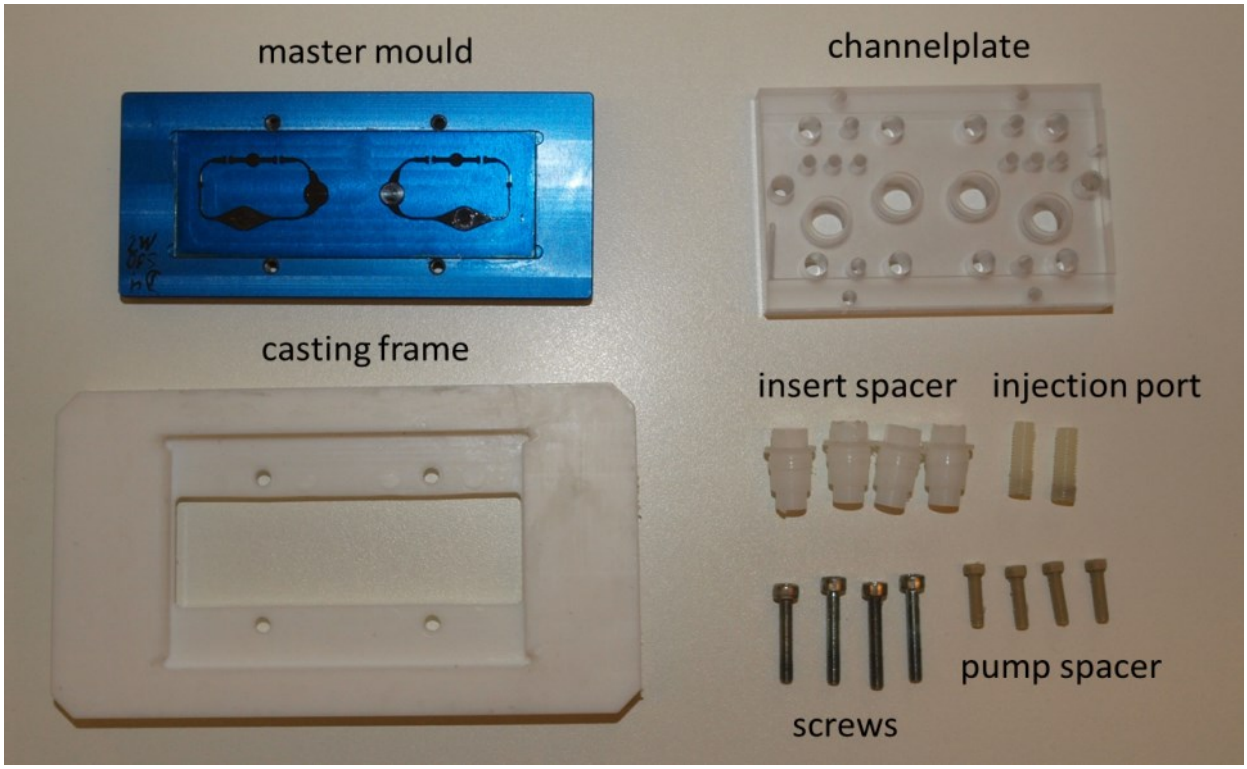

2.1.2 Solvents and Chemicals

Table 3: Solvents and chemicals

Product	Manufacturer
Acetone	Sigma Aldrich
Ammonium acetate (5M)	AppliChem
Aprotinin (bovine lung)	Sigma
$CaCl_2$	Roth
Chloroform	Sigma
Collagen A	Biochrom
Collagen, Type-I, 4mg/ml	Serva, PAA
Collagenase 1a	Sigma
Dispase II	Sigma
DNAse	Macherey Nagel
DNAse reaction buffer	Macherey Nagel
Elastosil® RT 601 (A+B)	Wacker
Ethanol (EtOH)	Roth

FCS	PAA
Fibrinogen (Type I-S, bovine plasma)	Sigma
Fibronectin	Sigma
HBSS incl. phenol red	Gibco
Human insulin	PAA
Hydrocortisone hemisuccinate	PAA
Isopropanol	Sigma
L-ascorbic-acid-2-phosphate	Sigma
L-glutamine	PAA
MaxGel™ ECM mixture	Sigma
PBS	PAA
PDMS Casting Sylgard® 184	Dow Corning
RNAse free water	Macherey Nagel MN
Thrombin (bovine)	Sigma
Trizol	Qiagen
Trypan blue	Sigma
Trypsin/EDTA	PAA
Wacker® primer G790	Wacker

2.1.3 Antibodies, Sera and Solutions

Table 4: Antibodies, sera and solutions for immunohistochemistry

Product	Manufacturer
Acetone, 99,7 %	Roth
ApopTag ® Fluorescein In Situ Apoptosis Detection Kit	Merck Millipore
CellTrace™ calcein red-orange AM	Life Technologies
ClearMount™ solution	Life Technologies
Collagen IV, mouse anti-human, 6,6 mg/ml	Sigma
Cytokeratin 10, mouse anti-human, 1mg/ml	Chemicon
Cytokeratin 15, rabbit anti-human, 100 µg/ml	Chemicon
Goat serum	Sigma

Hoechst 33342, 10 mg/ml	Life Technologies
IgG (Fab‘2) – Alexa 594, goat anti-mouse, 2 mg/ml	Sigma
IgG (Fab‘2) – FITC, goat anti-mouse, 4 mg/ml	Chemicon
IgG (H+L) – Alexa 594, goat anti-rabbit, 4 mg/ml	Sigma
Ki67, IgG, rabbit anti human, 400 µg/ml	Abcam
panCytokeratin – FITC, IgG	Abcam
Tenascin C, rabbit anti human, 200 µg/ml	Santa Cruz
Vimentin C-20 R, IgG, rabbit anti human, 200 µg/ml	Santa Cruz
Vimentin, IgG, rabbit anti-human, 1,1 mg/ml	Santa Cruz

Table 5: Antibodies, sera and solutions for haematoxylin and eosin stain

Product	Manufacturer
Eosin G-solution 0.5%	Merck
Ethanol 70, 90 and 99%	Roth
Haematoxylin -Solution, Meyer	Roth
Roti®-Histol	Roth
Roti®-Histokitt	Roth

2.1.4 Consumables

Table 6: Consumables

Product	Type	Manufacturer
Albumin ELISA Quantitation Set		Bethyl Laboratories
Cannula for Micromanipulation	Bend, bevelled, 110 µm	Eppendorf
Cell culture dish	CellstarR 6, 12, 24 Well	Greiner Bio-One
Cryomold	Tissue-Tek	Sakura
Deep Well Plate	96-Well, 500 µl	BD
EpiDermFT™		Mattek
Glucose LiquiColor®	(Oxidase) kit	Stanbio
HTS Transwell® Permeable Supports	96-Well, Polyester-Membrane, Pore size: 0,4; 1,0; 8,0 µm	Corning

HTS Transwell® Receiver plate	96-Well	Corning
LAC 142 Kit		Diaglobal
LDH Liqui-UV kit		Stanbio
Microtitre-plates	96-well	Greiner Bio-One
Nylon cell filter	Pore size 70 µm	BD Falcon Bioscience
O.C.T.™ Compound		Tissue-Tek
Object slide	SuperFrost R Plus	Thermo Scientific
PAP-Pen		Pen Science Services
Perfecta3D® Hanging Drop Plate	384-Well	3D Biomatrix
Petri dish	60 mm	Greiner Bio-One
Punch	4 and 5 mm diameter	Stusche
Tissue culture flask	T 25, T 75,	Greiner Bio-One, Corning
Ultra-low attachment plate	24-well	Corning

2.1.5 Media

Table 7: Media

Media	Components	Conc.	Manufacturer
Derma Life	Derma Life Basal Medium	480 ml	Cell Systems
	L-glutamine	6 mM	
	ExtractP™	0,4 %	
	Epinephrin	1 µM	
	rh TGF-α	0,5 ng/ml	
	Apo-Transferrin	5 µg/ml	
	Hydrocortisone hemisuccinat	100 mg/ml	
DMEM (Dulbecco´s	DMEM incl. glutamine, high glucose		Invitrogen
	FCS	5 and 10 %	

Modified Eagle Medium)	Penicillin Streptomycin	100 units/ml 100 µg/ml	
EFT-400-MM	DMEM-based maintenance medium		MatTek
HDMEC-Medium	Endothelial Cell Growth Medium MV2		Promocell
	FCS	5 %	
	hEGF	5 ng/ml	
	R3 IGF	20 ng/ml	
	Hydrocortisone	0.2 µg/ml	
	Ascorbic acid	1 µg/ml	
	VEGF	0.5 ng/ml	
	hbFGF	10 ng/ml	
	Penicillin Streptomycin	100 units/ml 100 µg/ml	
HepaRG-Medium	William's Medium E		PAA
	FCS	10 %	
	Human insulin	5 µg/ml	
	L-glutamine	2 mM	
	Hydrocortisone hemisuccinate	5 x 10-5 M	
	Penicillin	100 units/ml	
	Streptomycin	100 µg/ml	
Keratinocyte Growth Medium 2 (KGM2)	Bovine pituitary extract	0.004 ml / ml	PromoCell
	Epidermal growth factor (recombinant human)	0.125 ng/ml	
	Insulin (recombinant human)	5 µg/ml	
	Hydrocortisone	0.33 µg/ml	
	Epinephrine	0.39 µg/ml	
	Transferrin, holo (human)	10 µg/ml	
	$CaCl_2$	0.06 mM	

2.2 Cell Cultivation

2.2.1 Cell Isolation from the Hair Follicle

Follicular units of hair were obtained with informed consent from healthy donors at the age of 23-42 years after follicular unit extraction for hair transplantation. The isolation of dermal papillae (DP) from human hair follicles was performed according to the protocol of Magerl *et al*., 2002, with slight variations. The hair follicle was pressed slightly with a forceps at the suprabulbular region, whereby the bulbus was slightly squeezed. Thus, the proximal part of the bulbus, including the dermal papilla, could be separated from the remaining hair follicle with a cannula. The dermal papilla was separated from the surrounding tissue and transferred to a 6-well cell culture plate (2-4 DPs/well) and pressed to the well's ground in order to burst the basal lamina and allow the DP-cells to migrate. DP-cells were cultivated in DMEM 10% FCS and medium was changed after 1 week of isolation. When cells were grown out of the dermal papilla, medium was changed twice a week. When the cells reached 80% confluence, they were passaged with trypsin/EDTA and moved to a T25-cell culture flask. Cells were used from passage P2 to P4 for further experiments.

2.2.2 Cell Isolation from the Prepuce

Human juvenile prepuce was obtained, with informed consent and ethics approval, from a paediatric surgery after routine circumcisions. Prepuce samples were stored and transported in 10 ml phosphate-buffered saline (PBS) at 4°C and prepared for further culture within 6 hours following surgery. Prepuce samples were sterilised in 80% ethanol for 30 sec and then rinsed in PBS. The skin ring was cut open and the subcutaneous tissue removed mechanically. The skin was treated with Dispase II (5 mg/ml in DMEM) overnight at 4°C to enable the separation of the epidermal layer from the dermis. Once separated, dermis was cut into stripes and incubated in Collagenase I solution (4 mg/ml in DMEM) for 70 min, while the epidermis was cut into small pieces and incubated in trypsin/EDTA for 30 min. Suspensions were then passed through a 70 µm nylon filter and centrifuged for 5 min at 300×g. Supernatants were aspirated and pellets suspended according to the cell types isolated: keratinocytes isolated from epidermis were suspended in 10 ml DermaLife medium, fibroblasts isolated from dermis in 10 ml DMEM 10% FCS and endothelial cells isolated from dermis in 10 ml HDMEC medium supplemented with 0,01% fungizone. All media contained 100 units/ml penicillin, 100 µg/ml streptomycin and cells were moved to T75

tissue culture flasks and incubated at 37°C and 5% CO_2. Medium was changed after 24 h and fungizone was removed from endothelial cell culture.

2.2.3 MACS for Endothelial Cell Isolation

Endothelial cells cultures were purified by MACS at day 4 and 7 of culture. Therefore, cells were detached and cells resuspended in HDMEC Medium, counted and centrifuged at 300×g for 3 min. The supernatant was completely removed and a maximum number of 1 x10^7 cells was resuspended in 60 µl medium. 20 µl of FcR Blocking Reagent was added and vortexed briefly before 20 µl of CD31 MicroBeads were added and incubated for 14 min at 4°C. 1 ml of medium was added and cells were centrifuged at 300×g for 3 min, to subsequently be resuspended in 1 ml of medium. An LS Column was placed in the magnetic field of a MidiMACS Separator and rinsed with 3 ml of medium. Then, the cell suspension was applied onto the column. Unlabelled cells passed through the column and were washed out with 3 x 3 ml of medium. The column was removed from the separator and placed into a collection tube. 5 ml of medium was added onto the column and the labelled cells were flushed out by pushing the plunger into the column.

2.2.4 Cell Culture

Cells were cultured in incubators at 37°C, 5% CO_2 and 98% air humidity in their respective medium. Medium was changed every 3 days. Medium was removed and cells were passaged, when cell cultures reached 80% confluence. In detail, cell cultures were treated with trypsin/EDTA for 3 to 5 min at room temperature until cells dissociated. Then, cells were diluted with medium, three times the amount of trypsin/EDTA, to stop the proteolytic activity of trypsin. Cell counting was performed using the Vi-Cell™ Cell Viability Analyser (see chapter “Cell Counting”), using the trypan blue dye exclusion method. Cells were centrifuged at 300×g for 5 min and cells were seeded at a density of 10^5 cells/cm² or used for further experiments. Keratinocytes were cultured on collagen-coated flasks (see chapter “Matrices for Cell Culture”)

2.2.5 Matrices for Cell Culture

Tissue culture flasks were coated with collagen I for keratinocyte cultures. Therefore, collagen I solution was diluted in water to a concentration of 0.1 mg/ml and 2,5 ml/75 cm^2 were distributed equally and were incubated overnight at 37°C. The next day, the solution

was removed and the flask was used directly for culture of keratinocytes or was covered with parafilm and stored at 4°C for a maximum of 4 weeks.

2.2.6 Cell Counting

ViCell™ Viability Analyser, an automated haemocytometer, was used for automated cell quantification. For every sample run, 500 µl of cell suspension were supplied. The suspension was taken up by the analyser and mixed 1:1 with trypan blue which only stains dead cells. The mixture was then delivered to a flow cell with a camera for imaging of differences in grey scale between live and dead cells which were determined by the software. 50 images were taken to evaluate the cell concentration and viability.

2.2.7 Cryosections

Tissues were frozen in cryomedium for further immunocharacterisation. Skin tissues were oriented vertically in the cryosections and embedded in the cryomedium, snap frozen with liquid nitrogen and were stored at -80°C until they were cut for immunohistochemistry. Cutting was performed on a Cryotome at -16°C chamber temperature and -11°C sample temperature. Samples were sliced to a size of 8 µm thickness and moved to a SuperFrost object slide to be subsequently stored at -20°C for further analysis.

2.3 Skin Equivalents

2.3.1 Dermis Equivalent: Fibrin-Gel

The fibrin-gel consists of fibrinogen which is polymerised to fibrin when adding the enzyme thrombin. The addition of aprotinin avoids the proteolytic degradation of the generated three-dimensional structure and needs to be performed continuously.
Fibroblasts were treated with trypsin/EDTA, counted, centrifuged and resuspended in DMEM with 5% FCS to the desired cell concentration. The solutions of fibrinogen, aprotinin, cells and thrombin were mixed in the given concentrations (see table 8). An amount of 75 µl of the mixture was transferred to a 96-well insert and incubated at 37°C in the CO_2-incubator for complete polymerisation. DMEM Medium containing 5 % FCS and 2% Aprotinin was used to feed the cells in the dermis equivalent.

Vol.-%	Solution	Final Concentration
85,5	Fibrinogen	3 mg/ml
10	Cell suspension	250.000 or 100.000 /cm²
2	Aprotinin	20µg/ml
2,5	Thrombin	1,25 U /ml

Table 8: Solutions and concentrations of fibrin-gels

Fibrinogen-Solution

35 mg of fibrinogen were transferred to the surface of 10 ml PBS and rehydrated for 30 min at room temperature. Then, the solution was slightly shaken until the powder was completely dissolved in PBS and kept for 30 min at 37°C. Subsequently the solution was sterile filtered (0.2 µm pore size) and stored at 4°C.

Thrombin-Solution

10 mg Thrombin were dissolved in 10 ml $CaCl_2$-Solution (20 mM in bidest water) for 30 min at 37°C, filtered sterile (0,2 µm pore size) and stored at 4°C.

Aprotinin-Solution

1 mg of aprotinin was dissolved in 1 ml bidest water and stored at -20°C.

2.3.2 Dermis Equivalent: Collagen-Gel

All solutions, tubes and pipettes were cooled on ice before use.
Fibroblasts were treated with trypsin/EDTA, counted, centrifuged and resuspended in DMEM with 5% FCS to a cell suspension of 500.000 cells/cm². First, 1 ml of the collagen-solution (4 mg/ml) was mixed with 125 µl of HBSS Puffer (pH 5.5) and was then titrated with a 1 molar sodium hydroxide solution until a pH of 7 was reached. 125 µl of the cell suspension were added and mixed carefully while avoiding air bubbles. 75 µl of the collagen solution were transferred to 96-Well inserts or 150 µl to a 24-Well insert. The collagen solution was transferred to the incubator for polymerisation for 45 min before the medium was added.

2.3.3 Epidermis Equivalents

After 3 days of submersed culture of the dermis equivalents, keratinocytes were harvested and suspended in KGM 2 media with 5% FCS. Keratinocytes were seeded on top of the dermis equivalents, with a concentration of 250.000 cells/cm² and were cultured submersed

for another 5 days. Medium exchange was performed every day, whereat FCS was continuously diluted (5%, 3%, 2%, 1% and 0%). Then, medium level was lowered to culture skin equivalents at an air/liquid interface, where the epidermis was dried and in contact to the air, while the dermis was in contact with the media, allowing diffusion of nutrition. EGF, TGF-α and BPE were diluted in 4 steps with daily media exchange (100%, 50%, 25%, 10%, 0%) and 1,88 mM $CaCl_2$ was added to the media to support differentiation of the epidermis.

2.3.4 Production of Hair Follicle Equivalents

Dermal papilla cells were harvested and 100.000 cells resuspended in 2 ml DMEM 10% FCS. They were cultured in 6-well ultra-low attachment plates to avoid adhesion to the culture surface. After 48 hours of aggregation, collagen IV (100 µg/ml) was added and 24 hours later 50.000 keratinocytes per well were added. Another 24 hours later, the formed aggregates were used for further experiments.

2.3.5 Integration of Hair Follicle Equivalents into Skin Equivalents

Integration of hair follicle equivalents into skin equivalents was performed with a micromanipulator. All steps were performed under a stereo microscope. Aggregates of an approximate diameter of 150 µm were carefully taken up by a bevelled glass cannula, with as little medium as possible, positioning the hair follicle equivalents as close to the cannulas tip as possible. The cannula was then moved to a plate containing skin equivalents cultured at air/liquid interface and was moved onto the skin equivalent, where enough speed was needed to overcome the surface tension, but as little as possible, to avoid disruption of the epidermis. Skin equivalents were then cultured for two days and analysed with the two-photon microscope.

2.3.6 Punch Biopsies

Skin was punched, when biopsies were used in MOC experiments. Therefore, prepuce samples were sterilised in 80% ethanol for 30 sec and the ring was cut open. Samples with an average height of 2 mm were punched to biopsies with 4 or 5 mm diameter, depending on the culture setup chosen. One biopsy was loaded into a single MOC culture compartment for cultivation. Samples from one donor were used for each MOC-based test series and the respective control in the static culture.

2.4 Preparation of Liver Equivalents

Liver equivalents were prepared by Eva-Maria Materne in our laboratory. Briefly, liver microtissue aggregates were formed in Perfecta3D® 384-Well Hanging Drop Plates, according to the manufacturer's instructions: 20 µl cell suspension containing 4.8 x 10^4 hepatocytes and 0.2 x 10^4 HHSteC were pipetted to each access hole. After two days of hanging drop culture, aggregates were transferred to ultra-low attachment 24-well plates with a maximum of 20 aggregates per well. Following culture in ultra-low attachment wells for 3 days, 20 aggregates were loaded into a single tissue culture compartment of the MOC.

2.5 Development of Multi-Organ-Chip

In order to develop a new Multi-Organ-Chip, several requirements had to be considered: It should have the size of a glass object slide, be microscopable, biocompatible and should be able to culture skin equivalents, preferably at air/liquid interface. Therefore, together with the Fraunhofer IWS, a design was created which was developed further with different prototypes during this thesis.

2.5.1 MOC casting

The Multi-Organ-Chip is composed of 4 main components: A polycarbonate channelplate, a 2 mm thick PDMS layer (PDMS; Sylgard® 184, Dow Corning), a glass object slide and a support (Figure 2.2 B). The Channelplate has several boreholes to provide screws for the on-chip pump connection and the Transwell®-holders. The disposable PDMS slice contains the microfluidic, including the two tissue culture compartments and the pump membranes (Figure 2.2 A). The glass object slide closes the system from the bottom and supports the complete access via microscope. The support protects the MOC and helps to align the PDMS to the glass object slide. The MOCs were fabricated applying standard soft lithography and replica moulding of PDMS: A master mould was fabricated in Dresden by our cooperation partners by bonding a silicon wafer to a glass wafer. Photoresist was applied to the silicon wafer and patterned by using a photomask and UV light. Subsequently, unprotected silicon regions were etched and the photoresist was stripped. The fabrication of the microsystem was as follows: The channelplate was treated with a silicon rubber additive (WACKER® PRIMER G 790) for 20 min at 80°C. This film of silicon resin adhered firmly to the surface and formed a tight bond to the later added PDMS. Teflon screws were

inserted to create four PDMS-free compartments for culture and six 500-µm thick PDMS membranes to connect the

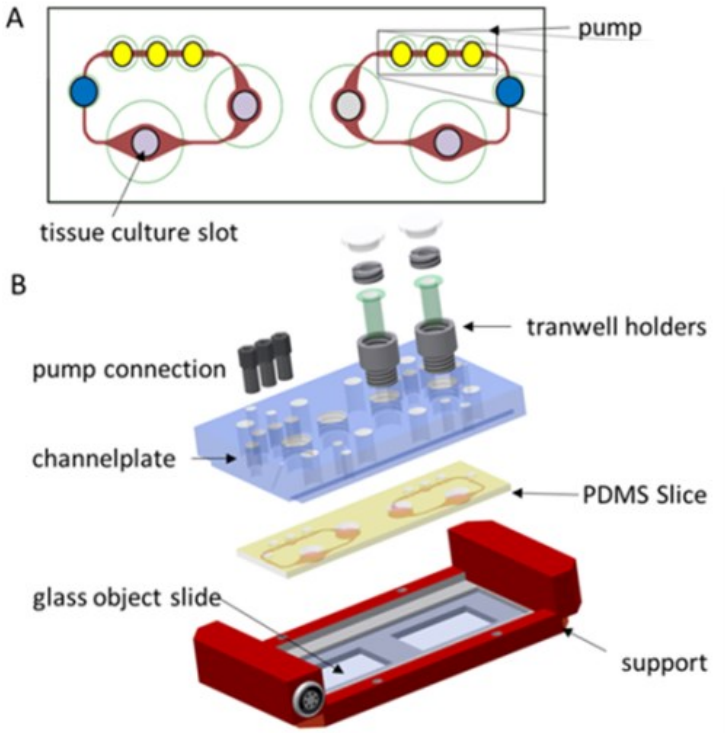

Figure 2.2) The Multi-Organ-Chip: Schematic of the micro-circulation showing the two microfluidic circuits each accompanied by two tissue culture slots and the pump (A). Schematics of the Multi-Organ-Chip: channelplate holding pump connections and Transwell®-holders; PDMS slice, with the negative of the microfluidic; the glass object slide and the support (B).

micropumps. The prepared channelplate was plugged to a lithographically produced master mould (channel height 100 µm, width 500 µm) and PDMS (10:1 v/v ratio of PDMS to curing agent) was injected into this casting station. The setup was incubated at 80°C for at least 60 min and the master was removed from the channelplate with the attached PDMS.

2.5.2 MOC Bonding

Treating surfaces with plasma eases the loading of the chip, supports tight bonding of the PDMS to the glass and the cultivation of cells on the PDMS. Due to the high energy introduced to the gas, electrons are released from the gas atoms and an ionised gas is formed which is called plasma and has a high responsiveness (Strobel *et al.,* 1993). The channelplate with the attached PDMS as well as a glass object slide were exposed to plasma, thus forming the respective fluid-tight microfluidic MOC device with standard channel heights of 100 µm.

2.5.2.1 Plasma Pen

The plasma pen produced atmospheric pressure plasma with a length of ca. 2 mm at the pen's tip. Argon was used as process gas and was ionised over an electrode head (Häckel *et al.*, 2010). To avoid bonding of the pumping membranes, a tape pad was affixed to the glass

slide and was removed after plasma treatment. The whole area of the object slide and the PDMS were scanned with the plasma except the pumping area. Then, the object slide was adjusted in the support and the channelplate with the PDMS was pressed against it for tight bonding.

2.5.2.2 Low-Pressure Plasma Chamber

Magnetic spacers were screwed onto the pumps membrane of the channelplate and small metal plates were added on the PDMS to avoid plasma forming and therefore bonding of the pump membranes to the object slide. The channelplate with the attached PDMS and the object slide lying in the support, were then placed into the plasma chamber. A pressure of 0,1-2 mbar was induced, whereby low-pressure plasma was produced in the vacuum chamber. Then the chamber was filled with process gas (air) and an electric field formed a high frequent current. The energy was transferred to the process gas which was then ionised and, in case of air, formed reactive oxygen radicals. After 30 seconds of ionisation, the vacuum was removed. The magnetic screws and the metal plates were removed immediately and the channelplate pressed onto the object slide, forming a tight and permanent bonding.

2.5.3 MOC Activation

Injection-fittings were screwed into the channelplate and female luer adapters were connected. Medium was immediately injected with a syringe to avoid neutralisation of the plasma. When the channels were completely filled with medium and no air bubbles were visible, the injection-fittings were replaced by Transwell®-holders, designed to hold a 96-well Transwell® insert from Corning. 300 µl medium were added to each culture space to incubate the MOC. Then the lid was screwed onto the Transwell®-holders. Connectors for the pump were screwed into the channelplate and the MOC was connected to the pump. The on-chip micropump was modified from Wu and co-workers and represents three consecutive PDMS membranes (Wu *et al.,* 2008). This implemented peristaltic pump can be operated by applying vacuum and pressure ranging from 900 - 2000 mbar to the membranes on top of the micro-channel, thereby opening or closing the valves of the pump, producing a peristaltic flow of defined velocity. MOCs were incubated for 24 hours before loading of the tissue cultures or cells.

2.5.4 Setup MOC Cultivation

The MOC system supports two different culture modes: tissue exposed to the fluid flow and tissue shielded from the underlying fluid flow by standard Transwell® cultures. The chip casting, bonding and connection to the peristaltic pump is identical for both setups.

2.5.4.1 Transwell®-Based MOC Cultivation

Tissues were cultured each in a separated single insert of a 96-well Transwell® unit which was hung inside the chip with the membrane fitting directly above the circuit. Compartments for tissue culture were filled with 200 µl medium each to incubate the MOC. Two wells per circuit from a 96-well Transwell® plate (0.4 µm pore size) were cut below the bracket with an incandescent knife and removed. Prepared tissues were transferred into the excised Transwells® which were positioned into the Transwell®-holders and screwed into the MOC.

2.5.4.2 Exposed to Fluid Flow

Tissues were loaded into the respective culture compartment of the two circuits of each MOC device for co-culture. Subsequently, 300 µl of medium was added to each culture compartment which was then hermetically sealed by a lid.

2.5.4.3 Static Control

Transwells® were loaded with tissue and hung into a receiver-plate or a 500 µl-deepwell plate for static control. Two wells (equivalent to two compartments) of a receiver-plate were connected by melting the plastic connecting wall, as a static control for two-tissue cultures. 450 µl of medium were added and Transwells® holding tissues were placed in the combined wells to function as control for Transwell®-based culture. For Transwell®-free co-cultures 650 µl of medium were added and each organ-tissue was put into one of the connected wells. The stationary control was treated the same as the Multi-Organ-Chip, except no flow was added to the culture.

2.6 MOC Cultivation of Skin Equivalents

2.6.1 MOC Cultivation of Fibrin- and Collagen-gels

Skin equivalents which were cultured in 24-well inserts, but shrank over the cultivation time, were carefully transferred to a single 96-well Transwell® insert, epidermal side up. Skin equivalents which were cultured in 96-well Transwell® inserts were cut below the bracket of the Transwell®. In both cases Transwell® inserts were transferred to the chip as described above (see "Transwell®-based MOC cultivation") and cultured in 500 µl of KGM2 medium without EGF, TGF-α and BPE. Medium change was performed every second day and 250 µl of medium were exchanged. Static cultures were performed in a 500 µl deepwell plate and were treated the same as in the MOC, except no flow was added to the culture.

2.6.2 MOC Cultivation of MatTek Skin Equivalents

MatTek's full thickness EpiDermFT™ *in vitro* skin models were used for this setup. Skin equivalents were delivered in 24-well format and were punched to 5 mm biopsies. They were then carefully transferred to the cut 96-well Transwell® insert, cultured in 500 µl of DMEM-based maintenance medium (EFT-400-MM) and 200 µl of the medium were changed every day. Static cultures were performed in a 500 µl deepwell plate.

2.6.3 MOC Cultivation of MatTek Skin Equivalents and Subcutaneous tissue

Skin equivalents with subcutaneous tissue were prepared as described in 2.6.2. Except, before transferring the equivalent to the Transwell®, subcutaneous tissue was cut from a prepuce and added below the skin equivalents in the Transwell® insert.

2.6.4 MOC Adaption to Philpott Assay

Occipital and temporal scalp skin follicular unit extractions (FUEs) containing mainly growing anagen VI hair follicles were obtained from disposed excess skin samples derived from male patients aged between 25–55 years undergoing hair transplantation surgery. FUEs were delivered in Williams's E medium with 100 units/ml penicillin and 100 mg/ml streptomycin and processed within 4 h after surgery by placing them directly in the microcirculation of the MOC system. William's E medium supplemented with 10% FCS, 100 units/ml penicillin, 100 mg/ml streptomycin, 5 mg/ml human insulin, 2 mM L-glutamine and 5 x 10^{-5} M hydrocortisone hemisuccinate was used as the culture medium. An

amount of 350 µl of a total of 600 µl was exchanged every second day during the 14 days of culture.

2.7 MOC Cultivation of Liver and Skin Co-cultures

2.7.1 MOC 14 Day Functionality Test of 2-Tissues-Culture

Skin biopsies and liver equivalents were transferred directly into the culture compartment and were cultured in 650 µl HepaRG Medium. During the first 7 days, a 40% media exchange rate was applied at 12 h intervals. From day 7 onwards, a 40% exchange rate was applied at 24 h intervals. Daily samples were collected for respective analyses. Experiments were stopped at day 14 of co-culture and tissues of the MOCs were subjected to immunohistochemical staining. Experiments were conducted with six replicates.

2.7.2 MOC 28 Day Long-Term Cultivation of 2-Tissues-Culture

Skin biopsies and liver equivalents were transferred into the excised Transwell®-inserts and then screwed into the MOC. The medium was exchanged every 12 hours within the first 7 days and every 24 hours afterwards, as described above. Supernatants were collected every day for lactate and glucose measurements. At the end of the 28-day culture, cell viability and protein expression were assessed via immunohistochemistry. The experiments were conducted in quadruplicate.

2.8 MOC Cultivation of Liver, Skin and Endothelial Cell Co-cultures

Endothelial cells were seeded into the MOC first for co-cultures of liver, skin and endothelial cells. Prior to seeding, each MOC was incubated statically for 3 days in 5% CO_2 at 37°C. HDMECs were harvested from expansion cultures using trypsin/EDTA. The cell suspension was centrifuged and cells counted. Cell viability was ≥ 85% for all experiments. Centrifuged cells were resuspended with complete ECGM-MV2 to a final concentration of $2x10^7$ cells/ml. Afterwards, 200 µl of the cell suspension was transferred to a 1 ml syringe. Injection-fittings were screwed into the channelplate and female luer adapters were connected. An empty syringe was connected to one compartment, while the cells were injected through the other compartments of each circuit. After even cell infusion into both circuits the device was incubated in 5% CO_2 at 37°C under static conditions over head for 3 h to allow the cells to attach to the PDMS channel walls. An amount of 300 µl fresh medium was added to each compartment and then flushed through the channels. The

seeding procedure was repeated and the MOC was cultivated another 90 min, to allow cells to attach to the glass side of the channel. An amount of 300 µl fresh medium was added to each compartment and then flushed through the channels using the on-chip micropump of each circuit. A frequency of 0.476 Hz was applied to every microvascular circuit of the MOCs for continuous dynamic operation. An amount of 300 µl medium per circuit was replaced every second day and cell growth and viability were monitored by light microscopy. After 5 days of proliferation and adaption of the cells to the MOC, approximately when cells reached homeostasis (Schimek *et al*., 2013), HepaRG+ media, including all growth factors of the endothelial medium, was added stepwise with every media exchange, increasing the HepaRG+ medium content slowly (20%, 50% and 80% of HepaRG+). At day 10 of endothelial culture in the MOC, skin biopsies and liver equivalents were added to the culture. Skin biopsies were transferred to Transwell® inserts as described above and liver equivalents were cultured directly in the culture compartment. For co-cultivation of the three different tissues, 80% of HepaRG+ medium and 20% of complete ECGM-MV2 was used and the medium was exchanged every 12 hours within the first 5 days and every 24 hours afterwards, as described above. Supernatants were collected every day for lactate and glucose measurements. At the end of the 15-day culture, cell viability and protein expression were assessed via immunohistochemistry. The experiments were conducted in quadruplicate. Two cultures were cultivated for 28 days. Seeding of endothelial cells was identical, but liver and skin tissues were cultured in Transwell® inserts.

2.9 Toxicity tests

For toxicity test, the antidiabetic drug troglitazone was used. Troglitazone was dissolved in DMSO, stored frozen at a concentration of 20 mM until used and then diluted in culture medium to a level of 0.05% DMSO. Medium containing 0.05% DMSO was used for control cultures.

2.9.1 Troglitazone exposure of skin and liver co-cultures for 7 days

Liver micro tissue and skin biopsy co-cultures in MOCs were prepared, cultured and analysed as described above. The MOCs were cultured for one day prior to exposure and were, subsequently, exposed to 0 µM, 5 µM and 50 µM troglitazone, respectively. Application of troglitazone was repeated at 12 h intervals simultaneously with the medium change. The experiments were completed at day 7.

2.10 Live Image Staining

2.10.1 CalceinAM Staining

Cell viability of endothelial cells in the MOC channels was determined with a Calcein AM assay. The lyophilised calcein was dissolved in DMSO to a final concentration of 5mg/ml. A solution of 1 µg/ml CellTrace™ calcein red-orange AM in medium was added into both compartments of each circuit of the MOC at a volume of 150 µl. The MOC was pumped for 5 min and then incubated under static conditions in 5% CO_2 at 37°C for 25 min. Then, the microchannels were washed twice with 300 µl of medium. Images were obtained using the merge function of the Keyence fluorescence microscope.

2.10.2 CellTracker™ Staining

The lyophilised CellTracker™ was dissolved in DMSO to a final concentration of 10 mM. This stock solution was diluted to a final working concentration of 5 µM in serum-free medium. Cells for staining were harvested with trypsin/EDTA, centrifuged, counted and resuspended in the working solution and incubated for 45 min at 37°C in 5% CO_2. The cells were then centrifuged and the dye working solution was replaced with fresh, prewarmed medium and incubated for another 30 minutes at 37°C. During this time, the chloromethyl group of the dye underwent modification into a cell-impermeant fluorescent dye–thioether adduct or was secreted from the cell. The cells were washed in PBS and then used for the experiments.

2.11 Immunohistochemistry

2.11.1 TUNEL/Ki67 Staining

Tissue behaviour, apoptosis and proliferation were analysed by immunohistological end-point staining at the end of each MOC experiment using TUNEL (TdT-mediated dUTP-digoxigenin nick end labelling)/Ki67 markers. Representative central sections of the tissue of each sample were selected for staining. Eight-micron cryostat sections per sample of skin and liver were stained for apoptosis using the TUNEL technique according to the manufacturer's instructions. The apoptosis staining was combined with a nuclear stain, Hoechst 33342 and, where sections were also stained for proliferation, an antibody against Ki67. The sections were fixed in acetone at -20°C for 10 min, washed with PBS and blocked with 10% goat serum in PBS for 20 min, then incubated with rabbit anti-human

Ki67 antibody at 4°C overnight. The sections were washed and incubated with secondary antibody goat anti-rabbit IgG Alexa Fluor® 594 for 45 min, washed, incubated with Hoechst 33342 dye (10 µg/ml in PBS) for 10 min and washed again before fluorescence imaging.

2.11.2 In-depth Immunohistochemical Endpoint Analyses

In-depth immunohistochemical endpoint analyses were performed by fixing and blocking following the same methods as described for the Ki67 staining. Tissues were then incubated with the primary antibody for 2 hours and washed with PBS. Subsequently, the conjugated secondary antibody and Hoechst 33342 were added, incubated for 45 min and the sections were washed two times in PBS before fluorescence imaging.

2.11.3 Haematoxylin/ Eosin staining

Slides with cryosections of skin biopsies and skin equivalents were stained with haematoxylin/ eosin (H/E) to get an overview of the tissue structure. The slides were fixed in aceton for 10 min at -20°C and were then washed in dest water. The slides were then stained in haematoxylin-solution for 5 min and washed in dest water. The staining turned blue, when tab water was run over the slides for 1 min, whereon the slides were washed in dest water. Staining in eosin followed for 3 min, the slides were washed in dest water and were then dehydrated in alcohol solutions with increasing concentration (70%, 96% and 99% and Roti®-Histol) for 5 min each. Stained slides were covered with roti-histokitt and a cover slip was attached. Analysis was performed with the Keyence microscope.

2.11.4 Microscopy

Microscopic analysis was performed with the Keyence-microscope or the 2-Photon-microscope.

2.12 Oxygen Measurement

PreSens equipment was used for oxygen measurement, applying non-invasive fluorescence quenching methods. The sensor spot (diameter 3 mm) was cut into half and one half was glued into the skin-culture compartment in the MOC. The optical fibres in the transmitter were fixed opposite of the sensor spot and measurements were taken every minute.

2.13 Medium Analysis

Supernatants were collected daily and were immediately monitored for tissue viability by the measurement of the released lactate dehydrogenase (LDH) and then stored at -80°C for further analysis of glucose, lactate and albumin. All absorbance-related measurements were performed in 96-well microtitre-plates in a microplate-reader, if not stated otherwise.

2.13.1 LDH Viability Measurement

LDH concentration in the medium was measured using the LDH Liqui-UV kit. 100 µl of reagent were prewarmed to 37 °C and 1 µl of the sample was added. The average absorbance per minute (ΔA/min) at 450 nm was determined over 3 minutes using medium as a reference.

2.13.2 Glucose

Glucose concentration of the medium was measured using the Glucose LiquiColor® (Oxidase) kit. 100 µl of reagent were added to a 96 multi-well plate and 1 µl of medium was added. After 5 min of incubation at 37°C the glucose concentration was quantified at 500 nm, using water as a reference.

2.13.3 Lactate

Lactate concentration of the medium was measured according to the LOD-PAP Method using the LAC 142 Kit. 100 µl of the reagent were mixed with 1 µl of medium sample and absorbance was measured at 520 nm, using water as reference.

2.13.4 Albumin

For the measurement of the albumin concentration the Albumin ELISA Quantitation Set was used. All steps were carried out at room temperature. 100 µl of diluted coating antibody were added to each well of a microtiter plate, incubated for 1 hour and washed five times. 200 µl of blocking solution were added to each well, incubated for 30 min and washed five times. 100 µl of sample were added and incubated for 1 hour, then washed five times. 100 µl HRP detection antibodies were added and incubated for 1 hour and washed five times. 100 µl of TMB Substrate Solution were added and the plate was kept in the dark to develop for 15 minutes. The reaction was stopped by adding 100 µl of stop solution and absorbance was measured on a plate reader at 450 nm.

2.14 RNA Analysis

2.14.1 RNA Isolation with Trizol

Small tissues (15-35 mg) were cut from the skin biopsies after cultivation, minced with a homogeniser and then transferred into 1 ml of trizol to be stored at -80°C for further use. Samples were then thawed and kept at room temperature for 5 min. 200 µl of chloroform were added, slightly agitated, kept for 5 min at room temperature and then centrifuged at 14.000 × g for 15 min at 4°C. The upper, aqueous phase was moved to another Eppendorf tube and mixed 1:1 with isopropanol. 120 µl of 5 M ammonium acetate were added, slightly agitated for 15 seconds, kept for 10 min at room temperature and then centrifuged at 14.000 × gfor 15 min at 4°C. The supernatant was discarded completely, the pellet was resuspended in 1 ml of ice-cold 70% ethanol and centrifuged at 6.000 × g for 5 min. The supernatant was removed completely and the pellet was air dried for 15 min. Then the pellet was dissolved in 90 µl DNAse reaction buffer, 10 µl of DNAse was added and kept at room temperature for 15 min. 1 ml of trizol was added and the protocol was repeated until the pellet was air dried. The RNA was then dissolved in 15 µl RNAse-free water and the RNA content was measured with the Nanodrop.

2.14.3 qPCR

Real-time qPCR endpoint analyses were performed to evaluate liver gene transcription at mRNA level after the MOC cultures were stopped as follows: Real-time qPCR experiments were conducted by using the Stratagene system and the SensiFast SYBR No-ROX One-Step Kit according to the manufacturer's instructions. The real-time qPCR primers were as follows: cytochrome P450 3A4 forward; 5'-GGAAGTGGACCCAGAAACTGC-3' and reverse 5'-TTACGGTGCCATCCCTTGAC-3', Housekeeping gene: TBP (TATA box binding protein) forward 5'-CCTTGTGCTCACCCACCAAC-3' and reverse 5'-TCGTCTTCCTGAATCCCTTTAGAATAG-3'.

2.15 Statistical Analysis

Statistical analysis was performed by one-way analysis of variance (ANOVA), followed by post-hoc Dunnett's pairwise multiple comparison test. * $P<0.05$ versus control.

3. Results

3.1 Skin Equivalents

Skin equivalents are one of the very few commercially available and the only validated human organ equivalents for substance testing. However, there are no validated full thickness skin equivalents (equivalents with a dermis and an epidermis) and the smallest available equivalent has a diameter of 6.5 mm. In order to minimise the equivalents for the MOC system, the first step was to miniaturise the skin equivalents.

3.1.1 Skin Equivalent Using Fibrin-Gel and Collagen-Gel

In order to down-scale the skin equivalents, two different dermis equivalent matrices were tested: fibrin-gel and collagen-gel. Fibroblasts were embedded in the dermis equivalents and were cultured in 96-well inserts.. Skin equivalents on fibrin-base had a more stable volume and shrank less than the collagen-matrices (Figure 3.1 B and D). However, the fibrin-gel equivalents adhered to the plastic side of the cell culture inserts which led to a strong concave surface of these skin equivalents (Fig 3.1 B). Thus, keratinocytes accumulated at the lowest spot which led to an uneven distribution of keratinocytes and therefore to an uneven population of the epidermis. However, in collagen-gels a similar uneven distribution of epidermis was visible, though less distinct. Patterns of populated and less populated areas of the epidermis could be seen. In the 96-well insert the fibrin equivalents could not be removed from the Transwell® without deformation or destruction of the equivalent, even though different methods of withdrawal and freezing were tested. Hence, the necessary quality control could not be performed for fibrin-gel.

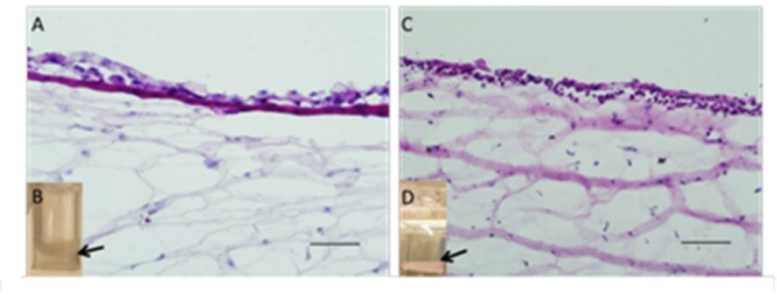

Figure 3.1) Skin equivalents made of fibrin-gel and collagen-gel. H/E staining of fibrin-gel (A) and type I collagen-gel (C) and their side view in the Transwell® (B and D). Scale bars indicate 100 µm.

Different protocols and methods were tested and compared for type I collagen-gels. In every protocol, skin equivalents with a collagen matrix shrank within the culture period. However, matrices shrank evenly in the z-axis, when Mitomycin, a growth inhibitor, was added to the fibroblasts culture before addition to the skin equivalent. Skin equivalents with a collagen matrix were easier to remove from the Transwell® insert and allowed easier access for the

evaluation of the quality criteria. The gel adhered less to the plastic side of the cell culture insert and a less distinctive concave surface allowed keratinocytes to grow a more even epidermis. The formation of the epidermis was visible by eye, though the distribution of the keratinocytes was unregular.

Figure 3.1 A and C shows the haematoxylin-eosin staining of two skin equivalents cultured in the 96-well insert with the dermis made of fibrin-gel (A) or collagen-gel (C), respectively. Both skin equivalents were constructed with a volume of 50 µl and were seeded with 100.000 fibroblasts/ml. The skin equivalent with the collagen-matrix showed the expected structure of the skin equivalent: integrated fibroblasts (violet nucleus) were settled in the gel. On top of the dermis equivalent the keratinocytes had formed a layer of several cells. The skin equivalent with the fibrin matrix, however, was slightly disrupted, fewer fibroblasts were in the dermis and only few keratinocytes in the epidermis were visible.

3.1.2 Punch Biopsies

Skin biopsy preparation was established for more than 30 biopsies with 100% nondissipative and contamination-free preparations and applications per year. Biopsies of 4 and 5 mm diameter – different sizes for technical use – were prepared, representing about $^{1}/_{100.000}$ of the human skin area. A 5 mm diameter biopsy has a tissue volume of 24 µl and consists of approximately five million cells.

3.1.3 Integration of Hair Follicle Equivalents into Skin Equivalents

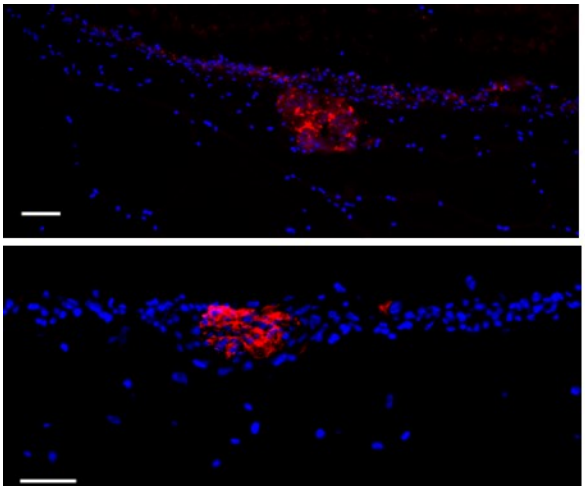

Figure 3.2) Neopapilla seeded into skin equivalents: Neopapilla seeded onto the dermis, below the keratinocytes, stained for versican (red) and cell nuclei (blue). Neopapilla did not sink into the gel but did not grow a hair shaft either. Scale bar: 100 µm

Already in 1998 the first skin equivalents were verified by ECVAM (Fentem and Botham, 2002). Nevertheless, 15 years later, skin equivalents still lack any integrated appendages. Hair follicle stem cells, for example, are involved in wound healing and can further play an important role in uptake and distribution of topically applied substances. Therefore, full thickness skin equivalents with integrated hair follicle equivalents would be of great impact on clinical as well as on pharmacological and toxicological applications. Hence, in a first

approach, dermal papilla aggregates (neopapilla) were seeded onto the dermis equivalents (fibrin and collagen-based) and keratinocytes were added on top 2 days later by Katharina Cierpka, under my supervision. The dermal papilla *in vivo* is the consistent part of the hair follicle and stimulates new hair growth. In both, fibrin-gel and collagen-gel based skin equivalents, the dermal papilla aggregate was still intact after 5 days of cultivation and did not grow out. It did not sink into the dermis, but stayed on the upper part of the dermis, surrounded by keratinocytes of the epidermis. No hair shaft growth could be seen during cultivation (Figure 3.2).

In a second approach, full thickness skin equivalents were produced with CellTracker® red stained keratinocytes in the epidermis. Dermal papilla cells were stained with CellTracker® green to be able to track the neopapilla after integration into skin equivalents. Integration of the neopapilla was performed with a micromanipulator. The neopapilla could be integrated into skin equivalents (Figure 3.3), though the cannula disrupted the epidermis (Figure 3.3 A and B). Further analysis showed that no hair follicle developed from the integrated neopapilla.

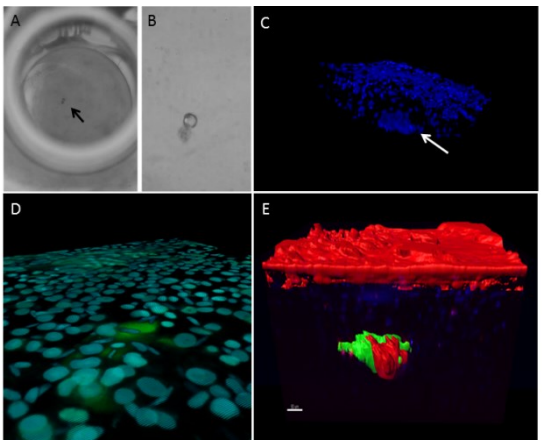

Figure 3.3) Integration of Neopapilla using micromanipulation: Top view of fibrin-gel after injection. (A and B) top view with the 2-photon microscope (D) 3D view of integrated dermal papilla with Hoechst 33342staining and (C) CellTracker® staining – green: Neopapilla, red: Keratinocytes (E).

3.2 Preparation of Liver Equivalents

Preparations as well as all analyses concerning liver equivalents were performed by Eva-Maria Materne in our lab as part of her doctoral thesis.

Consistent disk-shaped liver cell aggregates with a medium diameter of 300–400 µm and a height of 200–300 µm were formed during 2 days of hanging drop culture (Figure. 3.4 A). A reliable production of 300 spheres per plate was achieved. One tissue culture compartment of each MOC circuit was seeded with 20 liver aggregates corresponding to 10^6 cells. Immunohistochemical staining of vimentin and cytokeratin 8/18 showed that the Human Hepatic Stellate Cells (HHSteCs) were distributed equally throughout the whole aggregate (Figure. 3.4 B). ZO-1 staining showed that cell–cell contact supported the development of tight junctions during culture (Figure 3.4 C). Positive staining for MRP-2

demonstrated the polarisation of cells and the existence of rudimentary bile canaliculi-like networks in the generated liver micro-tissues (Figure 3.4 D).

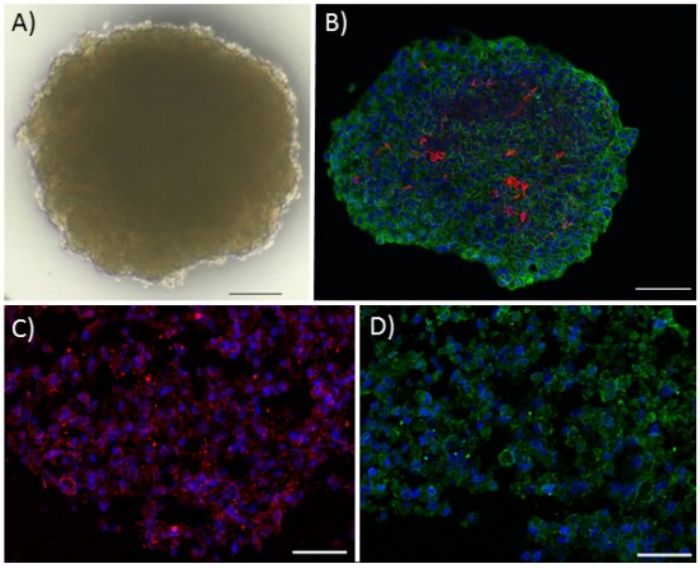

Figure 3.4) Formation of human artificial liver microtissues over 2 days: Light microscopy of a human liver spheroid generated by a standardised hanging drop culture. Scale bar: 100 µm (A). Equal distribution of HHSteCs throughout the HepaRG cell aggregate at a 1 : 24 ratio demonstrated by immunostaining of vimentin (red) and cytokeratin 8/18 (green), blue nuclear staining. Scale bar 100 µm (B). Characteristic formation of tight junctions (protein ZO-1, red), blue nuclear staining. Scale bar 50 µm (C). Expression of canalicular transporter MRP2 (green), blue nuclear staining. Scale bars: 50 µm (D).

3.3 Development of the Multi-Organ-Chip

Within the first years of MOC development, 4 different MOC designs were generated. All designs were designed and developed in close collaboration with and produced from the Fraunhofer Institute for Material and Beam Technology and GeSiM. All designs were biocompatible and microscopable. The first design had six micro bioreactor compartments and consisted of 4 different layers. The first layer was made of PDMS, containing the channels and a reservoir. Below was a double sided lithographically or laser structured silicon layer with integrated channels and the culture compartment for the micro-organoids. The system was closed at the bottom by a glass with integrated sensors for temperature and metabolites and a heating element. Each of the micro bioreactor compartments consisted of 3 separate tissue compartments, each with a volume of 0.5 µl (Figure 3.5 A). Though already a very extensive design, the first experiments revealed a difficult handling due to a small tissue and medium volume. A major drawback of this design was the lack of an active actuator for liquid pumping. Further, an expensive production led to a deferment of the first design. The second generation was a prototype with a pump-diffusor (Figure 3.5 B). Experiments in our lab showed that it was possible to fill the channels of this prototype with endothelial cells and cells adhered, but the inefficient pump principal led to cell death due to malnutrition. The exchange of medium and an optimised on-chip peristaltic pump was first implemented into the third design of MOC

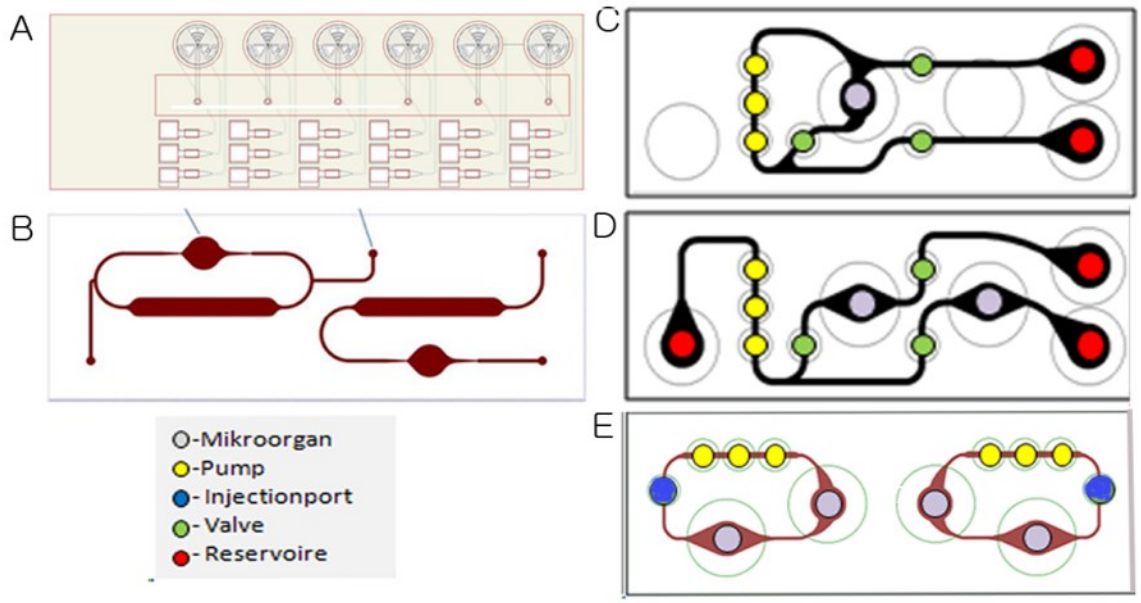

Figure 3.5) Different designs of the Multi-Organ-Chip: The first design had 6 parallel compartments each with 3 different culture compartments, with a volume of 0,5 µl (A). The second design with two parallel cultures and a pump diffusor (B). The third design had an integrated on-chip peristaltic pump and had two versions: one system with one culture compartment which could be cultured as an open or closed system depending on pressure on valves (C) or the other system with two parallel cultures with a common medium supply and separate waste tanks (D). The fourth design had two parallel circuits on one MOC, each with an on-chip peristaltic pump and two consecutive culture compartments and an injection port (E).

(Figure 3.5 C and D). The third design was further developed to integrate a tissue culture compartment for the skin. To realise this, tissue culture compartments were designed, slightly expanding from the channels to a tissue culture space with a diameter of 6 mm. On top of this, a specially designed Transwell®-holder could be screwed into the channelplate, so that a 96-well Transwell® insert could be hung directly above the culture medium which circulated through the channels. The culture in Transwells® reduced shear stress and, further, allowed the culture to be air/liquid interfaced. If a higher shear stress combined with a submerged culture was preferred, the Transwell® could be removed and the tissue could be cultured directly exposed to the fluid flow. This was realised in two different designs: one had one tissue culture compartment and valves could be opened and closed anytime to provide a closed (applied pressure to the valves) or an open circulation (applied underpressure to the valves) of the medium. Reservoirs supplied medium and a waste tank and were also regulated by the valves (Figure 3.5 C). The second design of the third prototype had two parallel culture compartments with a common medium reservoir and separate waste tanks. Medium supply to the different culture compartments could be regulated by the valves (Figure 3.5 D). This design proved to be feasible, though especially

the second version happened to leak, as the channels were too close to the border of the glass slide and bonding was therefore less efficient. To avoid this leakage and further to allow more cultures to be cultured in parallel, the fourth MOC design was established. It had two circulations on one MOC, both connecting two tissue culture compartments with a peristaltic pump (Figure 3.5 E). If only one organoid was cultured, the other culture compartment could be used for medium exchange. If two tissues were cultured together, medium change needed to be done in the same compartment where the organoids were cultured. This design was mainly used in this thesis.

3.3.1 MOC Casting

MOC casting was enhanced within the first year of MOC production of the third and fourth generation of MOC. Contact with latex gloves and a humid environment led to an incomplete polymerisation of the MOC. Therefore, nitrile gloves and polymerisation in a dry chamber at 80°C allowed casting of up to 15 MOCs per day, compared to one MOC at the beginning of the project. Additionally, a syringe pump eased the injection of the PDMS (Figure 3.6).

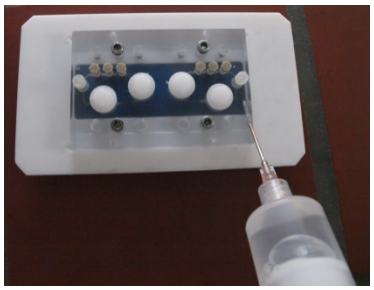

Figure 3.6) Casting of the MOC

3.3.2 MOC Bonding

After casting the MOC, the next step was bonding the PDMS to the glass object slide. This was done by plasma treatment. A high energy level was applied to the gas, ionised it and transported it to the fourth state of matter - plasma. Due to its free electrons, it had a high reaction activity (Strobel, M. *et al.*, 1993). Therefore, plasma-treated PDMS and glass developed a hydrophobic surface. Plasma treatment of the MOC had three positive effects: i) tight PDMS adhesion to the glass object slide ii) facilitating the filling of the microfluidic system and iii) adhesion of cells on the surface of PDMS and glass. Within this study two different ways of plasma bonding were used: The plasma pen and the plasma chamber.

3.3.2.1 Plasma Pen

The plasma treatment with the plasma pen Kinpen was carried out by slowly scanning the PDMS and the glass slide of the MOC from a distance of approximately 0.5 cm (Figure 3.7). Following this procedure and the filling of the fluidic system with medium, leakage occurred in approximately 70% of the bonded MOCs and several air bubbles were visible in

most of the systems. Another problem was the bonding of the pump membrane onto the glass slide and, therefore, the blocking of the micro-channels. This was avoided by using a rather time consuming method of affixing a tape pad onto the glass slide, where the pump membrane was going to be situated after bonding. This method avoided bonding of the membrane to the glass slide, though the tape pads had to be removed by a scalpel and sometimes sticky leftovers could not be removed properly. The whole procedure of bonding one MOC took about 30-40 min. Due to the low yield of only 30% leakage-free MOCs and the time consuming plasma treatment, a new method for bonding was needed.

Figure 3.7) Plasma bonding using the plasma pen

3.3.2.2 Plasma Chamber

A plasma chamber treatment (Figure 3.8) was chosen and tested, to avoid the time consuming progress of plasma bonding. Hence, the channelplate with the PDMS and the glass slide were placed into the plasma chamber, a vacuum was induced, air added and ionised whereon reactive oxygen radicals were formed that reacted with the surface of PDMS and the glass slide, producing a hydrophilic surface. To avoid the bonding of the pump membrane to the glass slide, small magnets were screwed into the pump spaces and, on the PDMS side, magnetic plates were positioned on the pump membrane to avoid reaction with the plasma. This method proved to be a lot faster and could be removed without any residues. The combination of those two new procedures led to an 80% leakage-free production of MOCs and only took about 10 min. Thus, this system proved to be more efficient.

Figure 3.8) Plasma bonding using the plasma chamber

3.3.3 Setup of MOC Cultivation

The MOC designs 3 and 4 enabled the co-culture of different tissues using two possible culture modes: directly exposed to the fluid flow and shielded from the underlying fluid

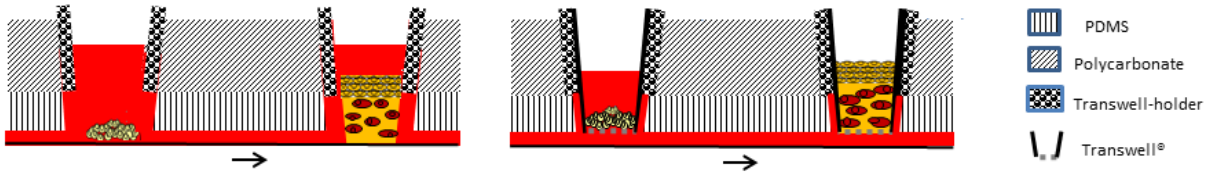

Figure 3.9) Schematic sections through the tissue culture compartments: submersed tissue cultures in the fluid flow (left image) or cultures in Transwell® (right image)

flow by standard Transwell® inserts (Figure 3.9). Both setups were identical in terms of casting, bonding and connection to the peristaltic pump. This allowed easy adaption to the required culture mode.

3.3.3.1 Transwell®-Based Skin Cultivation vs. Exposed to Fluid Flow

Transwell®-based skin culture allowed the tissue to be cultured at air/liquid interface, emulating the *in vivo* situation, where the nutrition is supplied to the dermis by blood through vasculature and by diffusion to the epidermis which is exposed to the air at the *stratum corneum*. Further, the shear stress is reduced when tissues are cultured in the Transwell®. If an air/liquid interface is not required, tissues in the Transwell® can also be cultured submersed, but with reduced shear stress. If a higher shear stress is beneficial for the tissue, it can be cultured exposed to the fluid flow. The culture mode can be changed without any changes of the chip design. For skin biopsies Transwell®-based cultures achieved better results than those exposed to fluid flow: The epidermis was less destructed and cytokeratin 15 (green) was expressed only in the basal layer of the epidermis, while cytokeratin 10 (red) was expressed in the layers above (Figure 3.10, left). In contrast, skin biopsies exposed to fluid flow showed a premature degradation of the epidermis and the disrupted skin showed several cytokeratin 15 positive (red) layers while only few cells were positive for cytokeratin 10 differentiated keratinocytes (Figure 3.10, right).

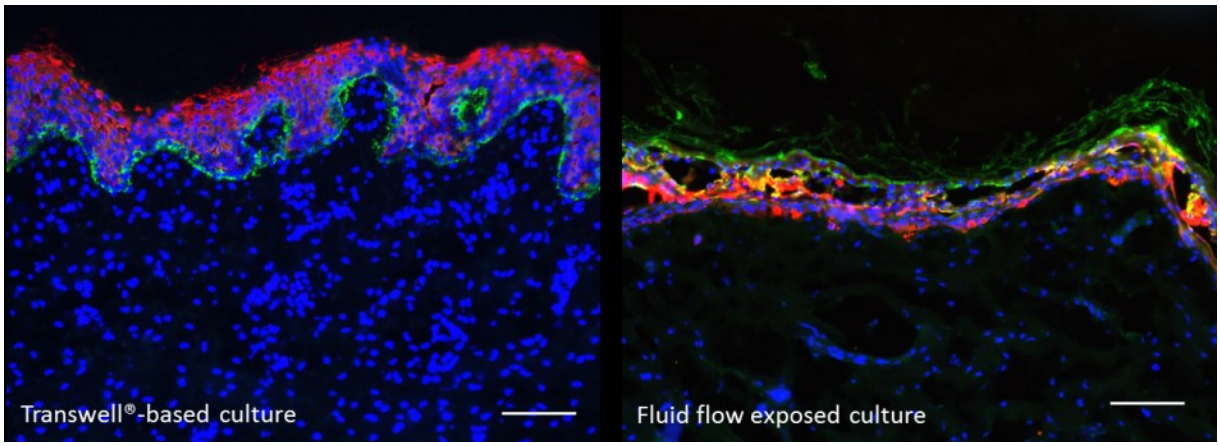

Figure 3.10) Skin biopsies cultured in Transwells® or exposed to fluid flow: Skin biopsies cultured in Transwell®-based culture showed less destructed epidermis Cytokeratin 10 (red), 15 (green) (left) than fluid flow exposed cultures (right) Cytokeratin 10 (green), 15 (red) and nuclei (blue). Scale bars: 100 µm.

3.4 MOC Cultivation of Skin Tissues

The MOC cultivation of skin was operated with different types of skin tissue. Skin models of own manufacture were cultivated, using fibrin-gel as well as collagen as dermal matrices. Further, validated full thickness skin models from MatTek were punched to the appropriate

size for MOC cultivation and were cultivated either alone in the MOC or in combination with subcutaneous tissue. Finally, *ex vivo* full skin biopsies were cultivated for 14 days in the MOC, in Transwell® cultures as well as directly exposed to the fluid flow.

3.4.1 MOC Cultivation of Skin Equivalents

3.4.1.1 MOC Cultivation of Skin Equivalents of Fibrin- and Collagen-Gels

Fibrin-Gel based Skin Equivalents

Skin equivalents with a dermis made of fibrin-gel were constructed in a 96-well Transwell® which was cut below the brackets, inserted into the Transwell®-holder and screwed into the third design of the MOC. Within 24 hours of cultivation in the MOC, skin equivalents were pressed to the side and medium was covering the skin equivalent which was deformed (Figure 3.11). Regulating the pressure and the frequency down to 0.1 bar and 3 Hz, also deformed the fibrin-gel and made further cultivation impossible, as the skin equivalent was completely disrupted. Additionally, it was impossible to remove the fibrin-gel from the insert for analysis.

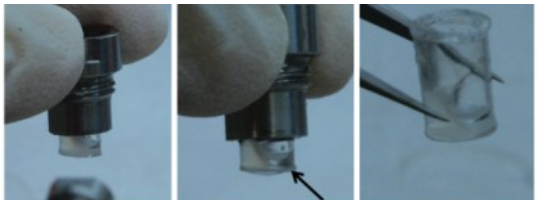

Figure 3.11) MOC cultivation of fibrin-gels: Fibrin-gels were completely disrupted within 24 hours of culture in the MOC system (3rd generation, closed circulation)

Collagen-Gel based Skin Equivalents

Next, skin equivalents with a collagen matrix were inserted into the MOC to test, if these skin equivalents were applicable in the MOC. As collagen-gels tend to shrink in culture, it was difficult to assemble the collagen-gel in the 96-well insert. Therefore, skin equivalents from a 24-well insert were transferred into a 96-well insert and included into the MOC. Both static and dynamic cultures were cultured submersed. This was performed by Martina Fischer under my supervision. Skin equivalents were cultured 14 days in the MOC. Collagen-gels did not deform when cultured in the MOC. Comparing static cultures to the skin equivalents in the

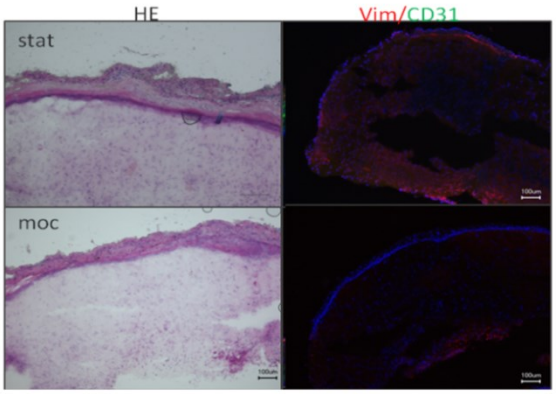

Figure 3.12) MOC cultivation of collagen-gels: Skin equivalents after 14 days of static culture (stat) or perfusion in the MOC (moc). H/E staining (left) revealed no differentiated epidermis in both equivalents. Vimentin staining (right) was stronger expressed in static than in MOC cultures. Scale bars: 100 µm

MOC, the epidermis in the static cultures had a thicker, but less organised epidermis. H/E staining revealed that both cultures did not show a differentiated epidermis. The top layer in both cultures showed cells with cell nuclei, not representing the nuclei free *stratum corneum*. Vimentin expression in static cultures was higher than in the MOC cultures (Figure 3.12).

3.4.1.2 MOC Cultivation of MatTek® Skin Equivalents

The full thickness skin models "EpiDermFT™" were ordered from MatTek® Corporation. Cells for these models were derived from the same human donor and consisted of a 3D dermis and an epidermis equivalent. MatTek® further promised to deliver a well-developed basement membrane within these models. The delivered models were punched to 5 mm biopsies and moved into Transwells®, epidermal side up. Tissues were cultured in the MOC for a total of 9 days, prolonging the recommended 3-day culture by 6 further days. After the 9 days, tissues were analysed for protein expression by immunohistochemistical means. H/E staining showed a rearrangement and compression of the dermal matrix structure compared to the day 0 control (Figure 3.13 A-C). Additionally, more cell nuclei were visible in the MOC-cultivated skin compared to the static control. The cornified layer increased over time in both, MOC and static culture. The amount of cells in the basal layer of the skin increased. The different layers of the epidermis were then stained for the expression of cytokeratin 15 in basal keratinocytes and cytokeratin 10 in keratinising and non-keratinising stratified epithelia. Both were

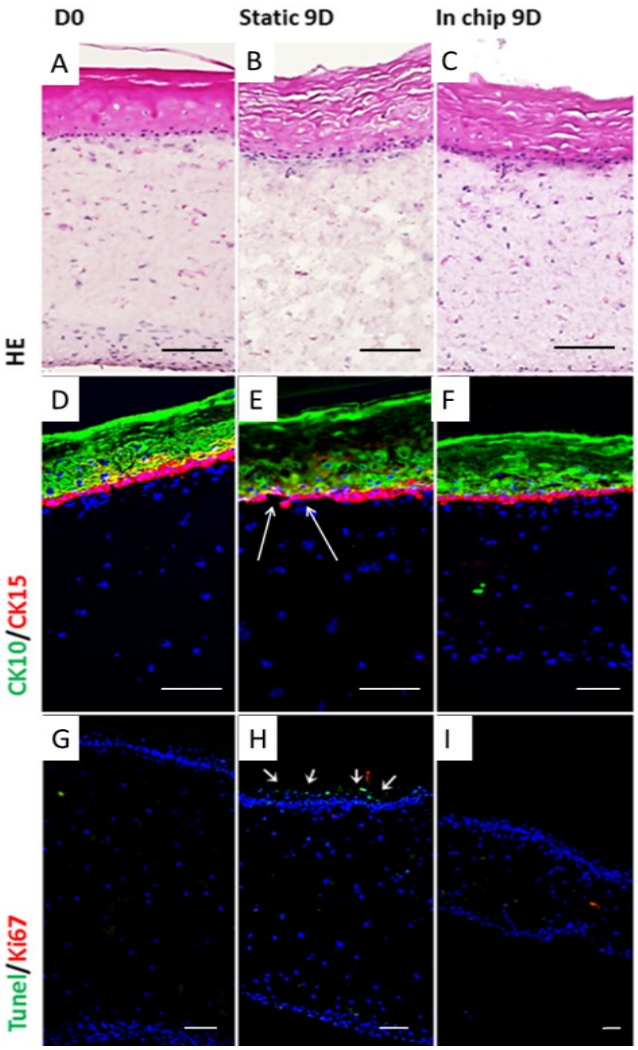

Figure 3.13*) In vitro* skin equivalents cultured in MOC for 9 days: H/E staining for histological comparison of the sections (A–C) and immunofluorescence staining for epidermal markers cytokeratin 10 and 15 (D–F) were applied (arrows indicate discontinuous basal layer of epidermis in E). Ki67 and TUNEL assay for proliferation and apoptosis (G–I) are used for comparison of viability of tissues. Bars indicate 100 µm.

expressed in all tissues similarly, although epidermal barrier function seemed to be better preserved in the MOC cultures (Figure 3.13 D-F). Tissues were stained for Ki67 and TUNEL, to detect proliferation and apoptosis (Figure 3.13 G-I). Hardly any proliferating cells were visible in the stationary controls or in MOC cultures, but the static culture showed selected apoptotic cells in the epidermal layer (Figure 3.13 H, arrows).

3.4.1.3 MOC Cultivation of MatTek® Skin Equivalents in Combination with Subcutaneous Tissue

A further analysis was performed by adding subcutaneous tissue of a prepuce under the EpiDermFT™ skin equivalent. One advantage of this combination was the lifting of the tissue within the Transwell® and therefore a reduced risk of moistening of the cornified layer. The subcutaneous tissue is composed of mainly adipocytes, fibroblasts and macrophages (Lee *et al.,* 2012). Hence, the support of the lipid metabolism and the paracrine effects of adipose-derived cells on the skin model were expected. Skin equivalents with and without subcutaneous tissue in static culture were run under the same condition, though without fluid flow, as a control. H/E staining showed that the subcutaneous tissue aligned and connected well to the skin model in the MOC (Figure 3.14 C), while

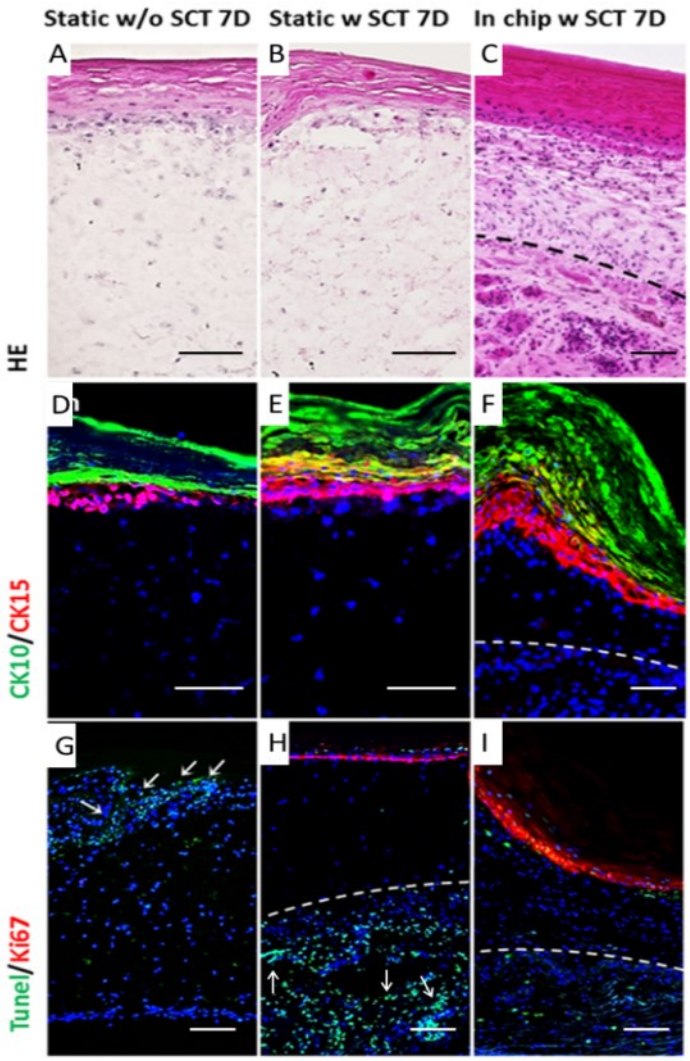

Figure 3.14) *In vitro* skin equivalents cultured for 7 days in MOC with subcutaneous tissue (SCT) from prepuce: H/E staining for histological comparison of the sections (A–C) and immunofluorescence staining for epidermal markers cytokeratin 10 and 15 (D–F) were applied. Ki67 and TUNEL assay for proliferation and apoptosis (G–I) was used for comparison of viability of tissues (arrows indicate TUNEL positive apoptotic cells in the epidermis in G and in the subcutaneous tissue in H). Dashed lines mark the border between skin equivalents and SCT. Scale bars indicate 100 µm.

the integration was poor in the static control. The dermal matrix was compressed and more cell nuclei were visible in the MOC culture compared to both static cultures (Figure 3.14 A-C). But also the cornified layer of the MOC-cultivated tissue was thicker and tighter. Tissues from all cultures were stained for cytokeratin 10 and 15, whereof the tissue cultured in the MOC showed the greatest similarity to the native tissue and day 0 controls (Figure 3.14 D-F). The static tissue cultured with subcutaneous tissue also showed an increase of undifferentiated keratinocytes compared to the regular static control. Staining for TUNEL and Ki67 showed proliferating cells in the basal layer of the epidermis in both tissues cultured with subcutaneous tissue, though more proliferating cells were seen in tissues cultured in the MOC (Figure 3.14 G-I). The subcutaneous tissue in the static culture showed a strong increase of apoptotic cells (Figure 3.14 H, arrows).

3.4.2 MOC Cultivation of Skin Biopsies

After cultivation of skin equivalents in the MOC and adding subcutaneous tissue, the next step was the cultivation of 5 mm skin punch biopsies including subcutaneous tissue for 14 days in the MOC. As control, skin biopsies were cultured under the same conditions though

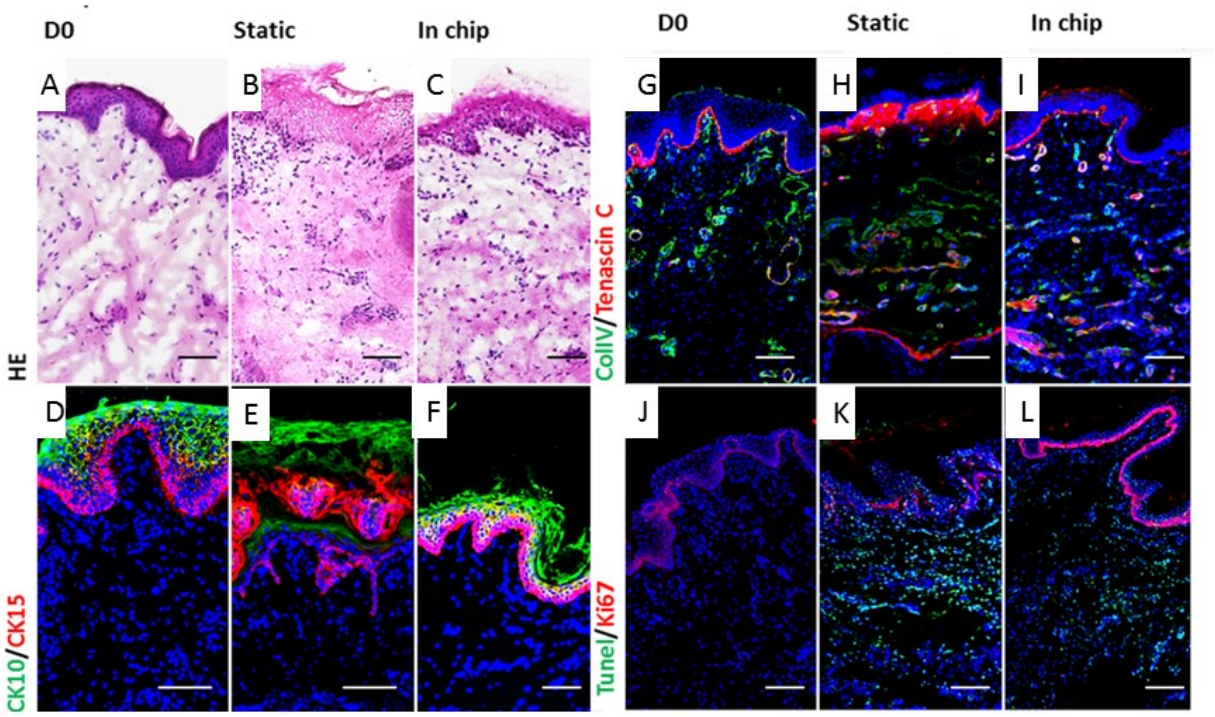

Figure 3.15) Maintenance of *ex vivo* prepuce biopsies for 14 days in MOC culture: Day zero conditions of the tissue are shown in A, D, G, and J. Static cultures are shown in B, E, H, and K, while dynamically cultured tissue in the MOC is indicated with C, F, I and L. H/E staining was applied for histological comparison of the tissues (A–C). Immunofluorescence staining for the epidermal markers cytokeratin 10 and 15 (D– F), the basement membrane markers tenascin C (TenC) and collagen IV (ColIV) (G–I), and Ki67/TUNEL assay for proliferation and apoptosis (J–L) were used for the evaluation of the integrity and viability of the tissues. Overlapping markers are visualised as yellow. Scale bars indicate 100 µm for each picture.

without fluid flow. In static cultures, H/E staining revealed a destructed epidermis and reorganisation of the dermis. MOC-cultured tissues had a slightly damaged, but still existing, epidermis and the dermis had a similar structure to the day 0 controls (Figure 3.15 A-C). Staining for cytokeratin 10 and 15 revealed similar results: the epidermis of the MOC-cultured skin equivalent was thinner than that at day 0, but still expressed both cytokeratins and showed a similar structure to that of day 0. The static control showed a disrupted of the epidermis, wherein the basal keratinocytes were disconnected from the dermis and cytokeratin 10 was only expressed in the cornified layer (Figure 3.15 D-F). In general, type IV collagen and tenascin C are both synthesised and secreted by keratinocytes and fibroblasts and are markers for the extracellular basement membrane. In MOC cultures, both markers were expressed similarly to the day 0 control. In static culture, tenascin C expression was elevated in the dermis, directly under the epidermis (Figure 3.15 G-I). Proliferation in static culture was only visible in some cells, whereas the whole basal layer of the MOC-cultured skin showed positive expression of Ki67 and, therefore, cell proliferation. Apoptosis was slightly upregulated in MOC cultures and more abundant in statically cultured skin (Figure 3.15 J-L).

3.4.3 MOC Adaption to the Philpot Assay

The MOC system was used to culture follicular unit extractions (FUEs) as another step in the attempt to emulate the biology of the skin and its appendages. In contrast to the well-established Philpott assay using single, truncated hair follicles to study hair follicle biology *in vitro* (Philpott *et al.,* 1990), complete hair follicular units were cultured. These almost intact pilosebaceous units include the perifollicular epidermis, dermis and the sebaceous gland(s). We aimed to prolong the culture period of the *ex vivo* hair follicles, taking into account the support of the glands and the surrounding skin tissue on hair follicle maintenance. During the culture period, hair-shaft elongation in growing anagen hair follicles was observed (Figure 3.16 A-C): Within the first 5 days of culture the hair shaft grew 180 µm and grew another 140 µm in the following 4 days.

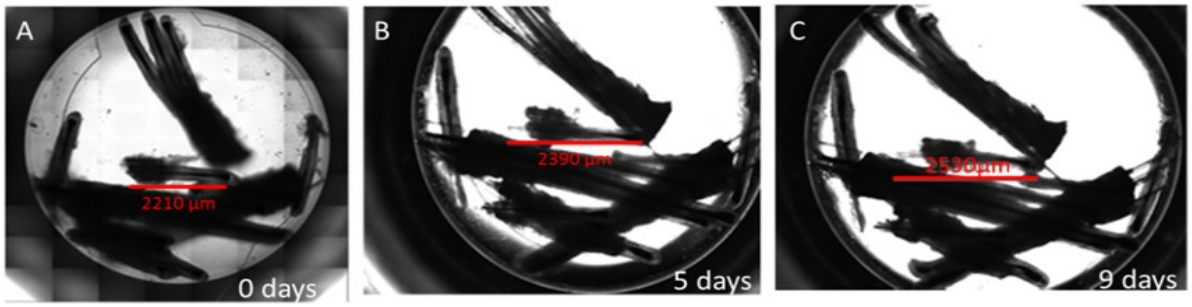

Figure 3.16) Adaption of the Philpott assay to the MOC system: Follicles grew from 2210 µm at day 0 (A) to 2390 µm at day 5 (B) to 2530 µm at day 9 (C).

3.5 MOC Cultivation of Skin and Liver Co-Cultures

The Multi-Organ-Chip was cultured with skin biopsies and liver equivalents to prove its ability of culturing two organs together. Liver was cultured in the compartment closer to the pumps (Figure 3.17, L) while skin (Figure 3.17, S) was cultured in the other compartment. Pumps were triggered so that the medium first passed the liver and then the skin, after it passed the pump. Two cultures were pumped parallel on one MOC. Co-cultivation was performed together with Eva-Maria Materne, who was responsible for liver tissues.

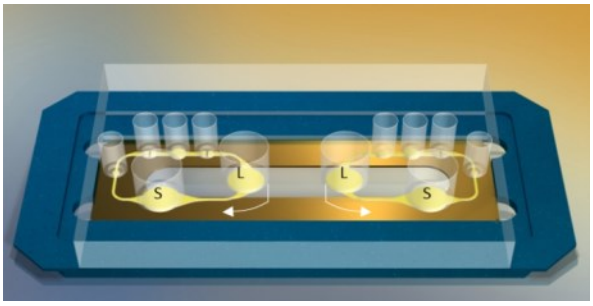

Figure 3.17) 3D drawing of an assembled MOC: With two microfluidic circuits in a PDMS-glass chip attached to a channelplate and placed into a MOC holder (blue). Arrows indicate fluid flow direction of each circuit. S-skin culture compartments, L-liver culture compartments

3.5.1 MOC 14 Day Functionality Test of 2-Tissues-Cultures

In the first co-culture experiment, the functionality of the MOC should be shown for liver and skin co-cultures. The human liver and skin tissue co-cultures were maintained in all MOCs during the experimental period of 14 days (Figure 3.18). Medium samples were taken daily and measured for LDH, glucose and lactate. The oxygen concentration was measured in selected MOCs. After 14 days of cultivation, tissues were analysed by immunohistochemistry. Samples for RNA isolation were taken for the skin, but unfortunately, did not yield enough RNA for further analysis. LDH was measured as an indicator for tissue breakdown. The LDH concentration of liver single-culture decreased continuously from about 40 U/l to 13,5 U/l at day 6, where it stayed, though having a variance of 10 U/l. Skin single-culture, in comparison, had a constant low concentration of about 8 U/l in the first 5 days which then increased linearly to 25 U/l where it stayed with a slight variance of 8 U/l. In the co-cultures of skin and liver the LDH concentration was the sum of each single culture at the beginning and at the end of the cultivation, decreasing from 53 U/l to 28 U/l at day 5. Subsequently, while LDH concentration in skin single-culture increased, the LDH concentration in co-culture stayed constant for another two days and then increased linearly at day 8 and from there on stayed constant as the sum of the single-cultures (Figure 3.18 a). Static cultures had a similar profile as the MOC co-culture, though had a constant slightly higher value (about 10 – 15 U/l more; Figure 3.18 B).

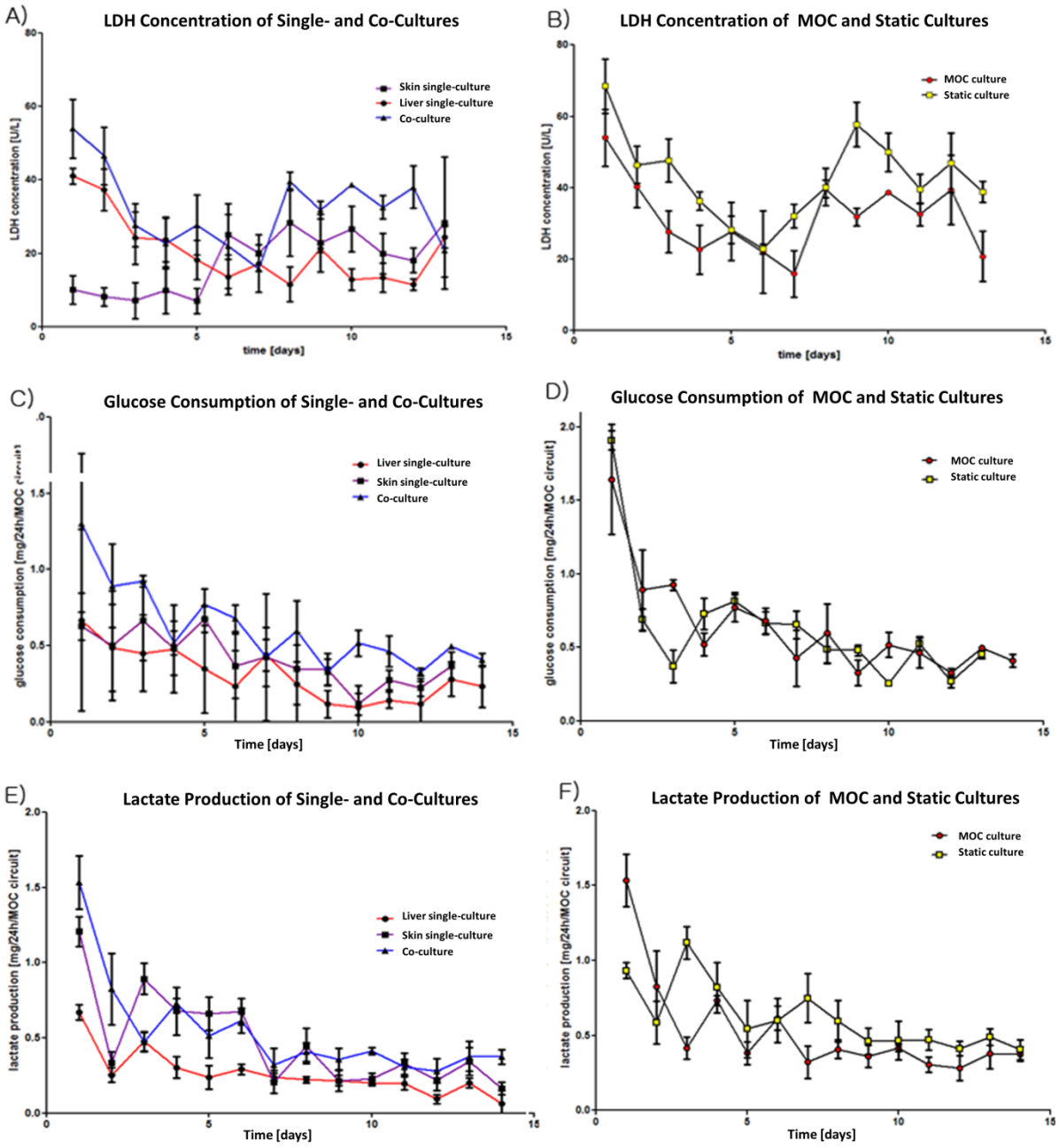

Figure 3.18) Metabolic activity of skin and liver single and co-cultures in the MOC and in comparison to static culture conditions: LDH concentrations of single - and co-cultures (A) and of MOC and static cultures (B).Glucose consumption of single- and co-cultures (C) and of MOC and static cultures (D). Lactate production of single- and co-cultures (E) and in MOC and static cultures (F). Data are +/- SEM (n=4).

Metabolic activity of the MOC co-cultures also showed a biphasic profile with a period of higher but constantly decreasing activity until day 7 and a steady state with low fluctuations both for lactate production and glucose consumption (Fig. 3.18 C and E). Notably, the steady state phase here coincided with the change of the feeding regimen at the same day. Skin and liver single-cultures consumed about the same amount of glucose, where liver always consumed a little less. In the first 3 days the co-culture consumed about twice the

amount as single-cultures, but from day 3 to 10 they only consumed about the same amount or 30% more than the single-cultures. From day 10 on co-cultures again consumed about twice as much as single-cultures (Figure 3.18 C). Comparing the MOC co-cultures to the static controls, the static culture consumed 2.0 mg/24h more in the first day, but consumption dropped straight to 0.4 mg/24h within 3 days. After day 3 glucose consumption of static and MOC-cultures was about the same (Figure 3.18 D). Lactate production decreased in all cultures within the first 3 days. It was most stable in liver single-cultures, where it decreased from 0.6 mg/24h/MOC circuit to 0.3 mg and then stayed constant until day 12 whereon it again decreased to about 0.15 mg. Skin single-cultures had a high lactate concentration at the beginning which decreased from 1,25 mg/24h/MOC circuit to 0.6 mg/24h within 2 days, where it stayed stable until day 8. From day 9 onwards it stayed relatively stable between 0.25 and 0.35 mg/24h/MOC circuit. Lactate production in co-cultures decreased strongly within the first three days from 1,5 mg/24h/MOC circuit to 0.4 mg. It then varied between 0.4 and 0.65 mg/24h/MOC circuit until day 7, whereon it stayed stable at about 0.4 mg/24h/MOC circuit (Figure 3.18 E). Static cultures showed a similar pattern of lactate production as the MOC cultivated co-cultures, though it was a little lower in the first days and lactate production increased on day 3 and from then until the end of the culture it stayed about 1.5 mg higher than in the MOC culture (Figure 3.18 F).

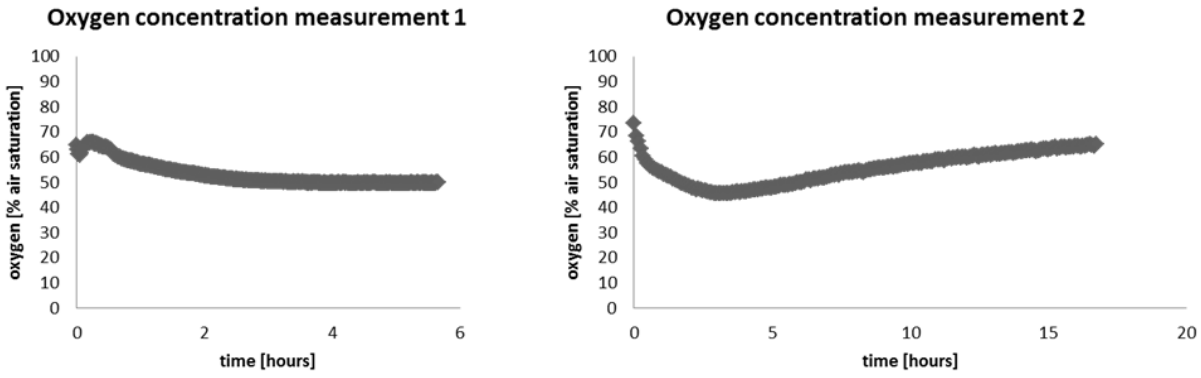

Figure 3.19) Oxygen concentration in MOC: After medium exchange, oxygen concentration showed different trends per measurement but never decreased below 45% air saturation and settled at about 50-60% air saturation.

Another important concern for the design of the MOC was the oxygen concentration in the culture during the devices operation. In preliminary experiments fluorescence quenching was integrated into the MOC culture to analyse oxygen concentration in the circuits. After the medium change, oxygen was measured every minute for 6 hours. Oxygen concentration increased from 60 % air saturation to 65% within the first 15 minutes and then gradually declined until it reached 50 % air saturation where it stayed until the end of measurement

after 6 h. During the second measurement the oxygen concentration showed a different trend: After the start of the measurement, it decreased from 73% air saturation to 45 % within the first 3 hours and then slowly increased to 65% air saturation within the next 13 hours (Figure 3.19).

Albumin synthesis has been selected out of a wide range of functional liver cell activity markers to monitor liver-like activity in the MOC co-cultures (Figure 3.20). A high amount of albumin in the first days of co-culture as well as in skin single-cultures could be seen. This amount decreased from 40 µg/24h/MOC circuit to 0 µg within the first 4 days of culture for both, skin single-cultures and co-cultures, where it stayed constant. In contrast, the liver single-cultures produced about 5-7 µg in the first two days, the production decreased until day 4, where it was nearly 0 and then steadied from day 5 until the end of the culture at day 14 at around 4-6 µg/24h/MOC circuit.

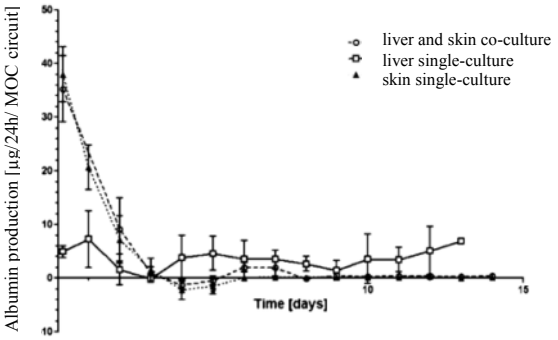

Figure 3.20) 14-day albumin profiles of liver and skin single-cultures and liver and skin co-cultures in the MOC. Data are means ± SEM (n = 6).

3.5.2 MOC 28 Day Long-Term Cultivation of 2-Tissues-Cultures

OECD guidelines for dermal subsystemic repeated dose toxicity testing of chemicals and cosmetics in animals require 21–28 days of exposure (OECD guideline no. 410, ‘‘Repeated Dose Dermal Toxicity: 21/28-day Study’’). Two pivotal aspects to converge our culture system to the current standard animal tests seemed to be most important to analyse the long-term performance of MOC-based human liver and skin co-cultures: i) to provide an air–liquid interface for the skin culture for later dermal substance exposure and ii) to strictly adhere to the required timeline of 28 days of substance exposure. To do so, Transwell® inserts were used to culture liver and skin over this extended period. This ultimately led to reduced shear stress and different nutrient supply characteristics in the MOCs. The cellular metabolism of all tissues was measured for 28 days in the MOC (Figure 3.21E). Glucose consumption of the co-cultures varied between different donors, but showed the same trend throughout the culture period (Figure 3.21 F). Glucose consumption was around 2,1 mg per day and per MOC circuit, decreased to 1 mg at day two and ranged between 0,69 mg and 0,9 mg per day and per MOC circuit from day 3 to 7. After the medium was changed only once a day, the glucose consumption also dropped, ranging between 0,3 and 0,6 mg,

averaging at approximately 0,4 mg per day per MOC circuit. Lactate production was about 1 mg per day per MOC circuit at day one and decreased to an amount of 0,45 to 0,54 mg per day per MOC circuit at day 2 to 6. At day 7 it had a peak of 0,69 mg per day per circuit and after the media change was reduced to once a day, decreased to 0,15 to 0,3 mg per day per circuit with small outliers at day 10 (0,46), day 18 (0,07), day 26 (0,1) and day 28 (0,49 mg per day per MOC circuit) and averaged at 0,2 mg per day per MOC circuit (Figure 3.21 E). This is about 40% lower than the corresponding values of the 14-day studies which were cultured directly exposed to the fluid flow.

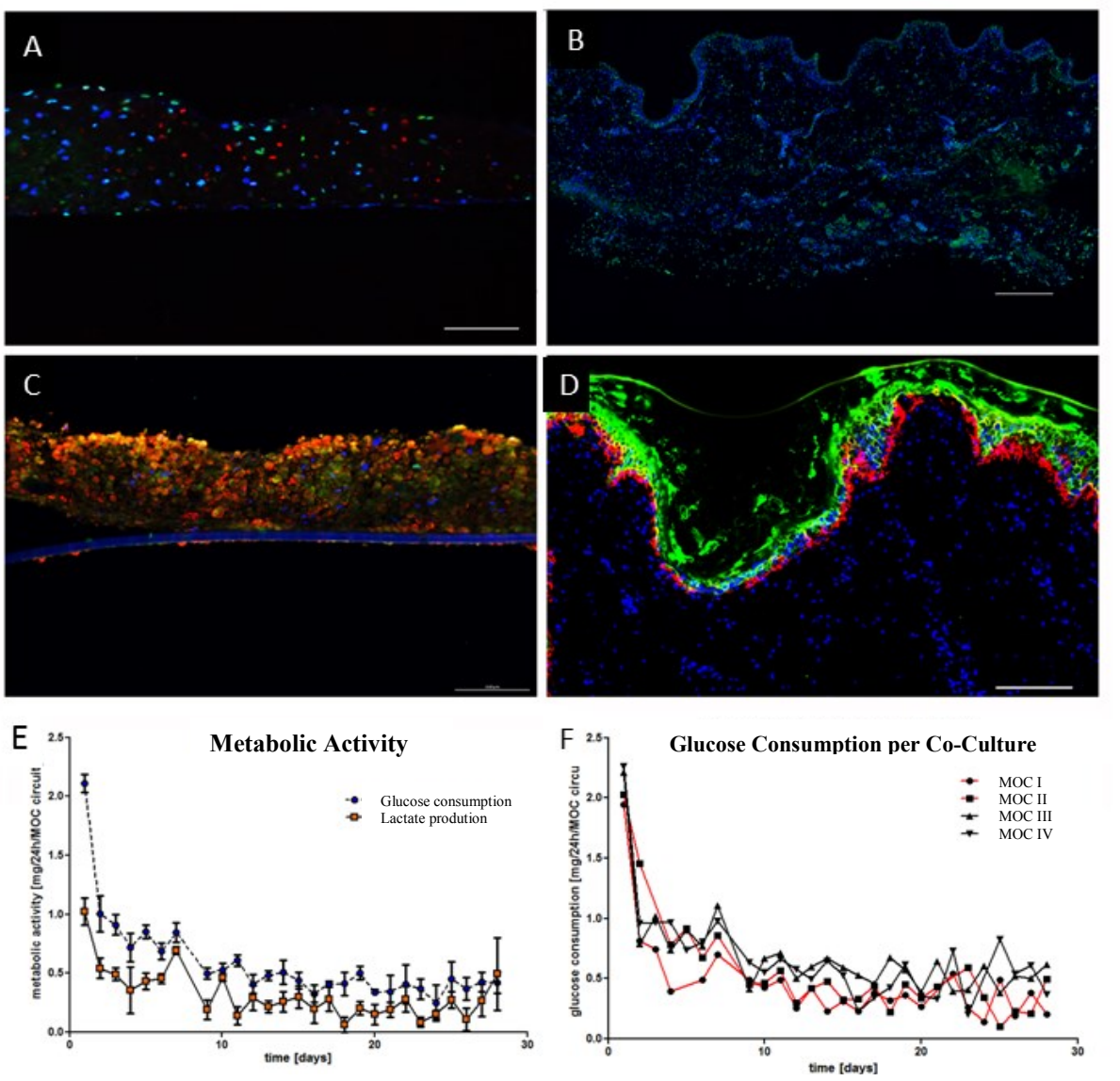

Figure 3.21) Performance of Transwell® multi-tissue cultures over 28 days. Evaluation of cell viability by TUNEL/Ki67 staining of liver tissue (A) and TUNEL staining of skin tissue (B) after 28-day co-culture in the MOC. Cell functionality was shown by immunhistostaining of Phase I enzymes cytochrome P450 3A4 (red) and cytochrome P450 7A1 (green) in liver tissue (C) and cytokeratin 15 (red) and cytokeratin 10 (green) showing both basal and stratified keratinocytes (D), nuclei: blue. Metabolic activity of the co-culture analysed in culture supernatants (E) and parallel trend of glucose consumption per co-culture (F). Data are means ±SEM (n = 4). Scale bars: a, b and d = 100 µm; c = 300 µm.

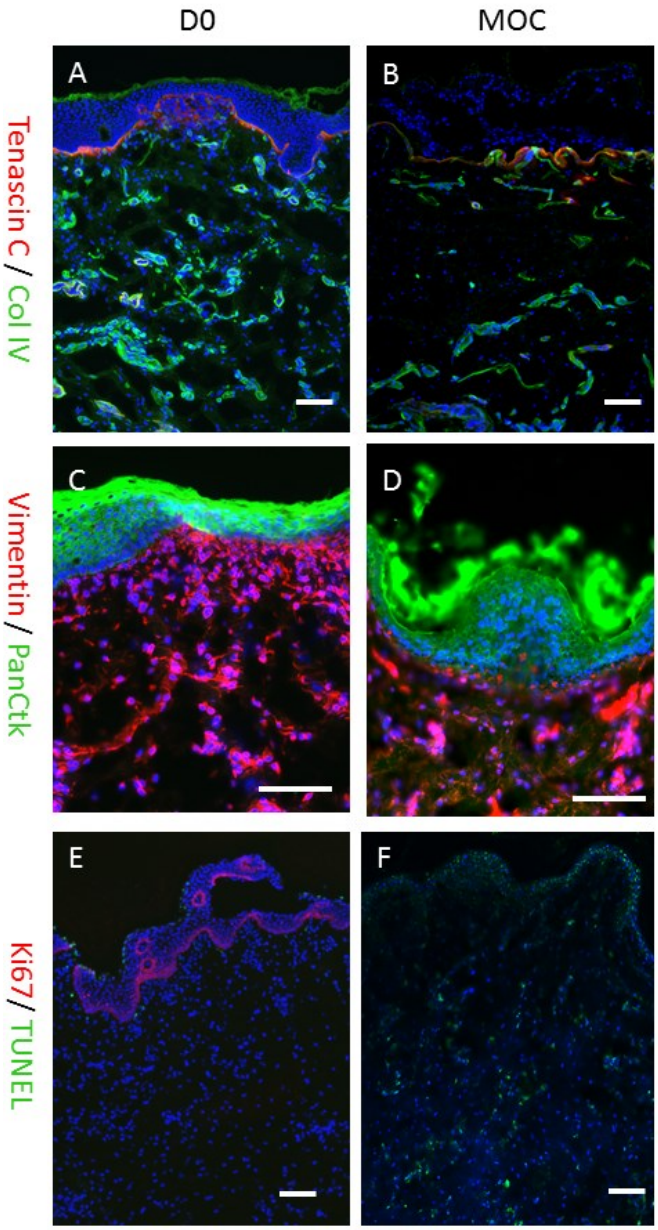

Figure 3.22) Long-term co-culture of skin and liver tissues: skin biopsies in day 0 control (A, C, E) and after 28 days of co-culture (B, D, F) stained for tenascin C and type IV collagen for expression of basal lamina showed slight decrease in expression after long-term culture (A, B) vimentin and panCytokeratin expression of fibroblasts in the dermis and keratinocytes in the epidermis was similar to control (C, D). Ki67 and TUNEL showed proliferation and apoptosis. In day 0 controls proliferation could be seen in the basal layer of the epidermis. In long-term culture no proliferating but several apoptotic cells were visible (E, F). Scale bars indicate 100 µm.

Immunohistochemistry of the tissues was performed to reveal further insights into their biology: Apoptosis was low in both liver and skin tissues (Figure 3.21 A and B). Liver equivalents were stained for the expression of cytochrome P450 3A4 and cytochrome P450 7A1 and skin biopsies for cytokeratin 10/ 15, tenascin C/collagen IV and vimentin/panCytokeratin to individually analyse the functions and thus, the degree of success, of the *in vivo* imitation of each organ. Cytochrome P450 3A4 is an enzyme related to the biotransformation of many xenobiotics, whereas cytochrome P450 7A1 is involved in bile acid synthesis. Both proteins were expressed in the liver equivalents at day 28 (Figure 3.21 C). The skin's epidermis exhibited both basal and stratified keratinocytes after 28 days of culture in the MOC (Figure 3.21 D). Tenascin C and collagen IV are both markers for the basal lamina, though tenascin C is also a marker in wound healing and fibrosis. In the MOC the expression of both was slightly reduced compared to the day 0 controls and was found in the basal lamina between the epidermis and the dermis. Collagen IV was also expressed in the basal lamina surrounding blood vessels

(Figure 3.22 A, B). Vimentin and panCytokeratin were similarly expressed in the day 0 control and in the skin biopsy cultivated in the MOC (Figure 3.22 C, D). Comparing TUNEL/Ki67 staining, apoptotic and proliferating cells, the day 0 control did not show any apoptotic cells, but in the basal layer of the epidermis proliferating cells were visible. The TUNEL staining of the skin biopsy cultured in the MOC showed several apoptotic cells (Figure 3.22 E, F).

3.6 MOC Cultivation of Skin, Liver and Endothelial Cell Co-Cultures

3.6.1 MOC Cultivation of 3-Tissues-Cultures for 15 Days

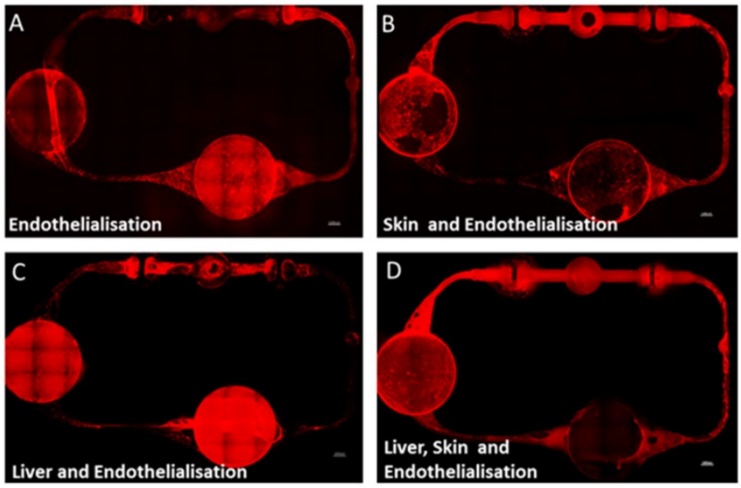

Figure 3.23) Calcein AM viability staining of endothelial cells in the MOC cultures after removal of skin and liver tissues: Endothelial cell culture (A), skin and endothelial cell co-culture (B), liver and endothelial cell co-culture (C) and liver, skin and endothelial cell co-culture (D). Scale bars indicate 1000 µm.

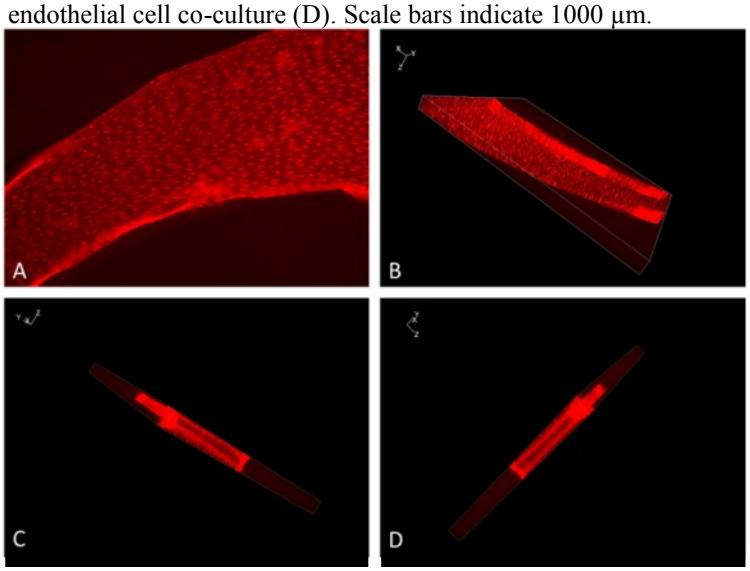

Figure 3.24) 3D view of Calcein AM viability staining of 3-tissues- culture at day 15: View from top (A), front (B), left (C) and right (D). Channels were completely populated with endothelial cells: bottom, top and sides.

Recent studies have shown the significant impact of endothelial cell co-culture on „organ-on-a-chip“ cultures (Kane *et al.,* 2006, Khetani *et al.,* 2008). Therefore, we have included endothelial cells into our MOC culture system. Endothelial cells were inserted into the MOC by a syringe and were allowed to attach to the surface without fluid flow before pumps were connected. After 15 days of cultivation, cultures were stopped and skin and liver tissues were removed for further analysis. Endothelial cells in the MOC channels were stained with CalceinAM to reveal viable cells in the culture. All MOC cultures showed a complete viable endothelialisation at every point of the MOC (Figure 3.23). Different success rates of

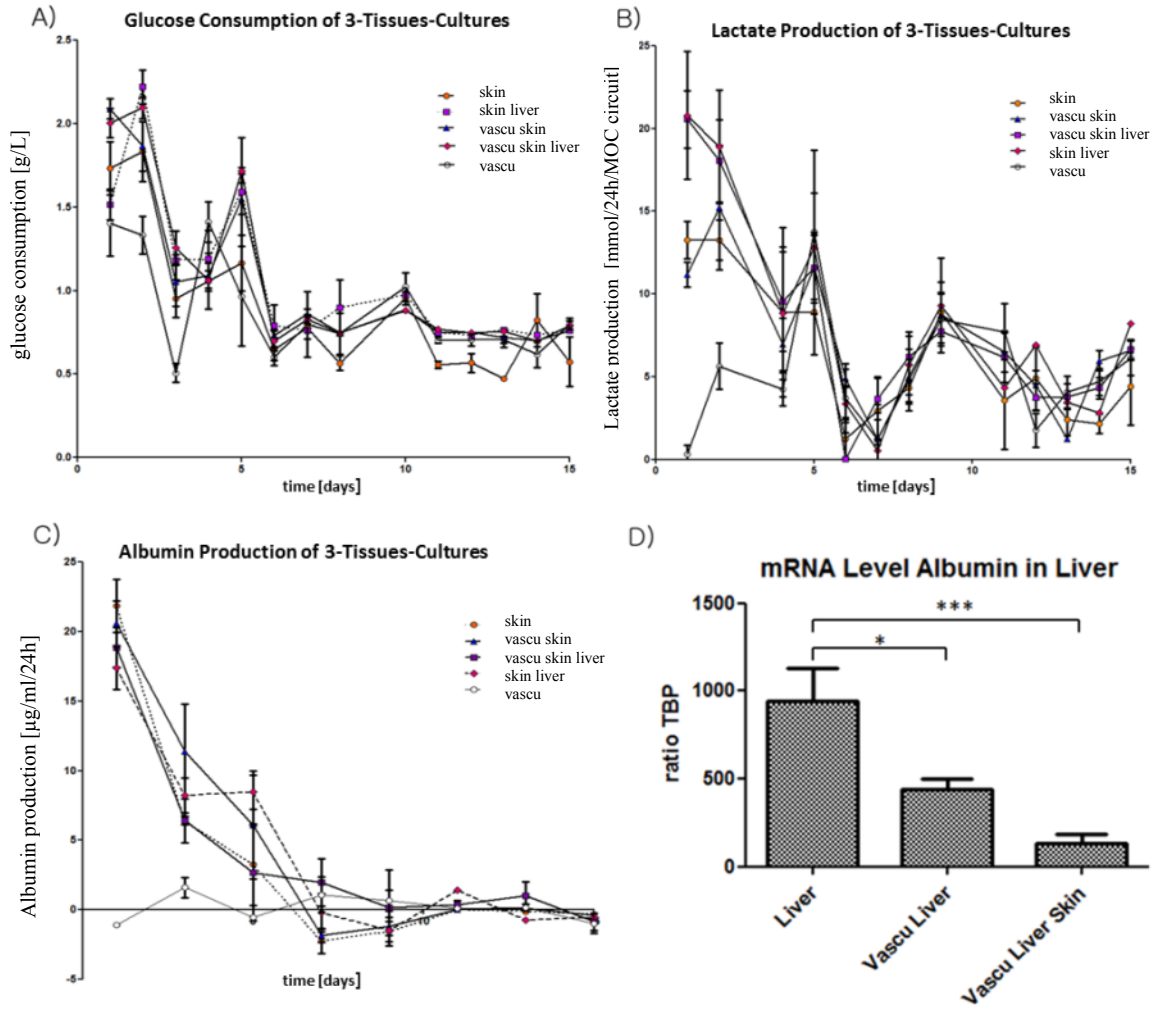

Figure 3.25) Metabolic activity of 3-tissues-cultures in comparison to single and co-cultures: Glucose consumption showed same trends in all cultures (A). Lactate production showed 3 groups in the first 4 days and then all cultures showed same trend (B). Albumin production in cultures with skin dropped in the first 5 days and then stayed around 0, while in endothelial single-culture it constantly stayed around 0 (C). mRNA level of albumin in the liver differed significantly between single-cultures and co-cultures (D). Data are means ±SEM (n=4). Statistical analysis was performed by one-way analysis of variance (ANOVA), followed by post-hoc Dunnett's pairwise multiple comparison test. *P ≤ 0.05, *** P ≤ 0,001 versus liver.

endothelialisation could be seen between the cultures, but were also visible within one group. 3D visualisation of the 3-tissues-cultures was performed from one spot of the channel and showed a successful endothelialisation of the complete channel: the top, the bottom and the sides were completely covered with endothelial cells. Cells aligned themselves and their microfilaments in the direction of the flow (Figure 3.24). Glucose consumption in all cultures showed the same trend (Figure 3.25 A), the first 5 days consumption shifted between 2.2 and 0.5 g/l and was slightly lowen in endothelial cell single-cultures than in all other cultures. From day 6 onwards, all cultures consumed about the same amount of glucose, around 0.7 g/l, though skin single-cultures consumed slightly

less (about 0.15 g/l less) than the other cultures. Lactate production showed 3 different trends in the first 4 days (Figure 3.25 B): endothelial cell single-cultures produced the least in the beginning, starting with 0.3 mmol at the first day and increased 5 mmol each, on the days 2 and 4 before it showed the same trend as for all other cultures from day 5 on. Skin single-cultures and skin and endothelial cell co-cultures started with a lactate production of about 13 mmol/MOC circuit what decreased a little on day 4 before it showed the same trend and values as all other cultures. Skin and liver co-cultures as well as skin, liver and endothelial cell 3-tissues-cultures had the highest lactate production in the first 4 days, starting at 21 mmol/MOC circuit and going down to 9 mmol at day 4, before the same values and trends were seen as in all other cultures. On day 5 all cultures had a value of about 12 mmol and decreased drastically on day 6, whereon it slowly increased again to 7 mmol at day 9 and then decreased slightly to 5 mmol/24h/MOC circuit at day 15. Albumin production was comparable for all cultures including skin, decreasing from 29 µg to around 0 µg within the first 5 days and then stayed around 0. This decrease was about 2 days slower than seen in previous experiments of skin and liver co-cultures exposed to fluid flow. Endothelial cell single-cultures had a constant value around 0 µg/24h/MOC circuit (Figure 3.25 C). Comparing the albumin expression in liver on mRNA level, liver equivalents in co-culture with endothelial cells expressed significantly less albumin then in single-culture ($P \leq 0,5$) and even less in 3-tissue-culture ($P \leq 0,001$; Figure 3.25 D).

3.6.2 MOC Cultivation of 3-Tissues-Cultures for 28 Days

In order to test the applicability of the endothelialised skin and liver co-culture to fulfil the criteria of the OECD guidelines no. 410, the culture was prolonged to 28 days for two parallel cultures. Glucose consumption and lactate production were showing the same trends as the co-culture of skin and liver, though glucose consumption of the endothelialised chip was mostly about 0.1 g/24h/MOC circuit higher than that of the skin and liver co-culture (Figure 3.26 E), while the lactate production stayed the same in both cultures (Figure 3.26 F). Immunohistochemistry staining of the skin biopsies showed an expression of tenascin C and collagen IV in the basal membrane, comparable to that of day 0 controls (Figure 3.26 A). Expression of cytokeratin 15 showed an intact, single layered basal layer of the epidermis (Figure 3.26 B) and staining for TUNEL showed some apoptotic cells, though less than in the co-culture without endothelialisation and the tissue seemed to be viable and functional (Figure 3.26 C).

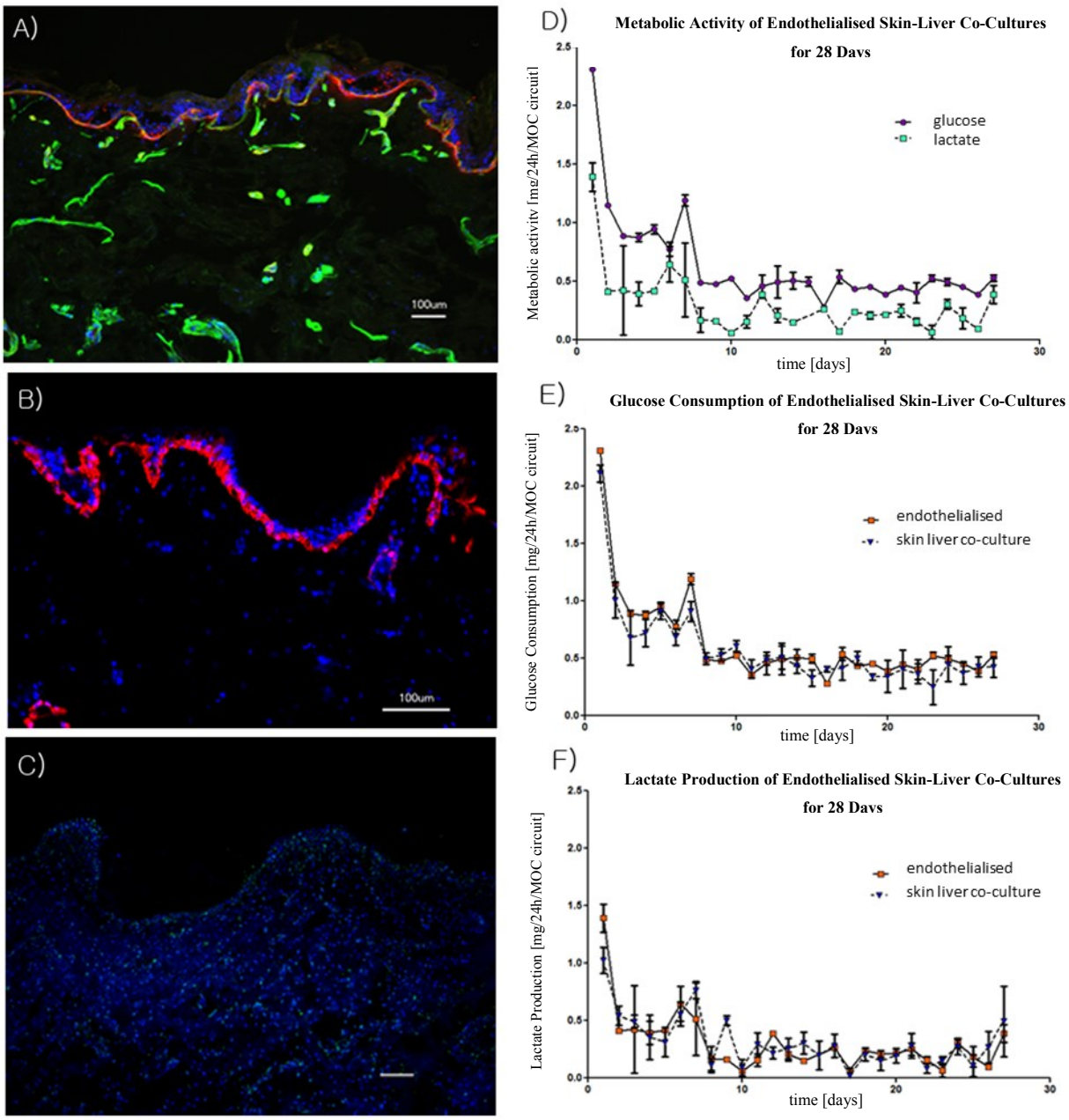

Figure 3.26) MOC Cultivation of 3-tissues-culture for 28 days: Skin biopsies stained for collagen IV and tenascin C showed expression in basal membranes (A). Cytokeratin 15 stained basal layer of the epidermis (B). TUNEL staining showed few apoptotic cells in the tissue (C). Metabolic activity of MOC 3-tissues-cultures in comparison to 2-tissues-cultures: Glucose consumption and Lactate production of MOC 3-tissues-cultures (D), glucose consumption of 3- and 2-tissues-cultures, where 3-tissues-cultures consumed a little more glucose (E). Lactate production of 3- and 2-tissues-cultures, where both cultures produced about the same amount of lactate (F). Data are ± SEM (n=4).

3.7 Toxicity Tests

3.7.1 Troglitazone Exposure to Skin and Liver Co-Cultures for 6 Days

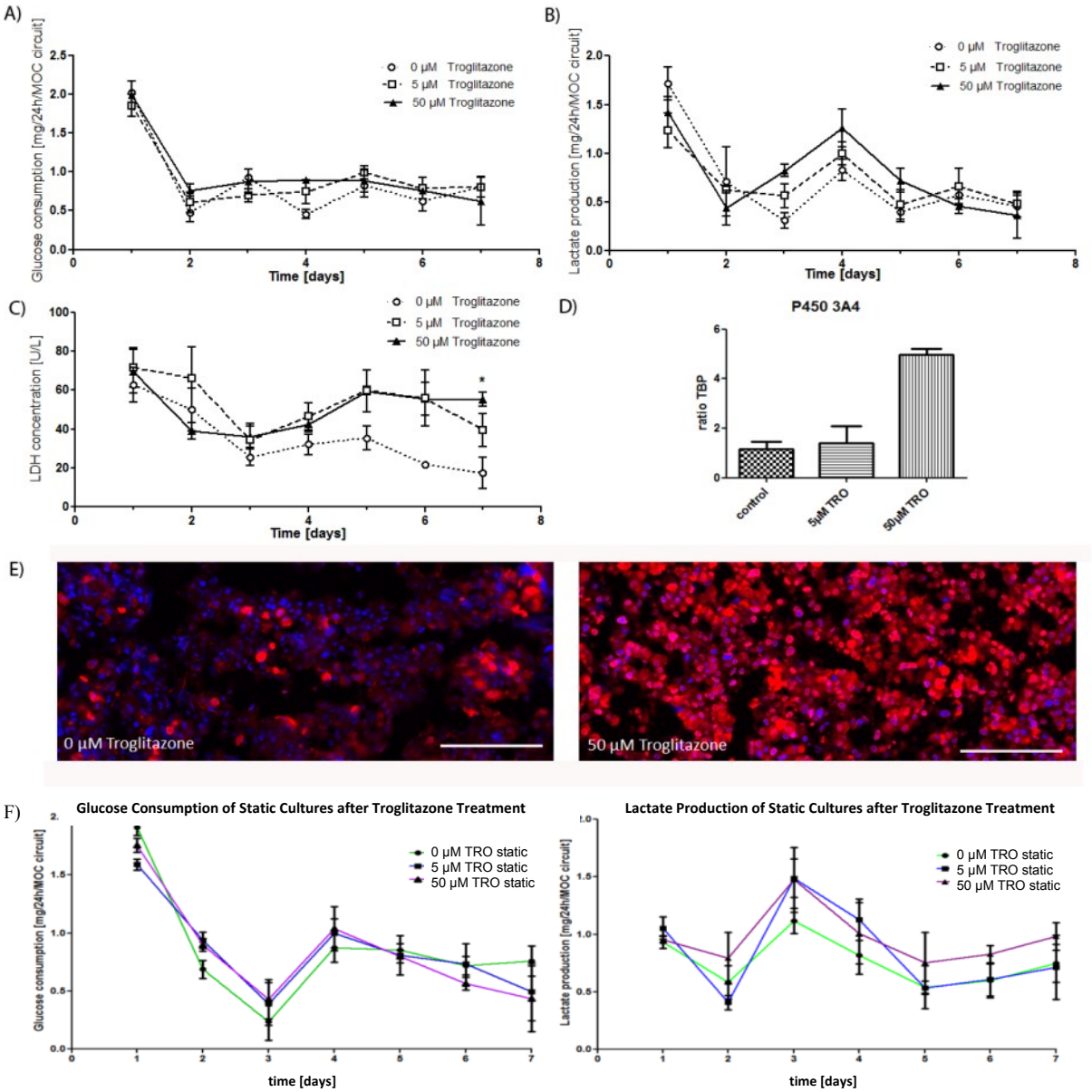

Figure 3.27) Sensitivity to troglitazone after 6 days of daily repeated dose exposure: Glucose consumption (A) and lactate production profiles (B) showed no significant difference between control and troglitazone application. LDH values showed significant increase at day 6 in 50 µM troglitazone exposed cultures (C). Real-time qPCR of the cytochrome P450 3A4 (D) and immunostaining of cytochrome P 450 3A4 in the control (left) compared to the 50 µM troglitazone exposed group (right), nuclear stain blue, showed increased expression in 50 µM exposed cultures: Scale bar 100 µm (E). Metabolic activity of static cultures treated with troglitazone: Glucose (left) and lactate (right) showed no differences between control and troglitazone exposed cultures (F). C) Statistical analysis was performed by one-way analysis of variance (ANOVA), followed by post-hoc Dunnett's pairwise multiple comparison test. *P ≤ 0.05 versus control. (A, B and C) Data are means ± SEM (n = 4).

Troglitazone was chosen to explore whether the MOC system is suitable for daily repeated dose substance testing. Its dose-dependent toxicity on HepaRG cells *in vitro* has been described before (Rogue *et al.,* 2011). MOC co-cultures were exposed to troglitazone during the first 7 unsettled days of co-culture, because a higher sensitivity to a toxic agent at this stage was hypothesised. Nevertheless, troglitazone had no significant effect on the metabolic activity of liver and skin co-cultures, neither in MOC nor in static cultures (Figure 3.27 A, B and F). Within the first 2 days of troglitazone application, LDH concentrations did not differ for different doses, but after 3 days of culture, an increase of LDH activity and after 7 days a significant 60% increase was observed in 50 µM troglitazone treated cultures when compared to DMSO-treated controls (Figure 3.27 C). The most sensitive indicator for dose-dependent sensitivity was seen in the MOC co-cultures on the mRNA levels in the respective liver micro-tissues after 7 days of cultivation. qPCR analysis of cytochrome P450 3A4 and immunohistochemistry showed increased expression of this enzyme on mRNA and protein levels in cultures exposed to 50 µM troglitazone (Figure 3.27 E). An even distributed overexpression of cytochrome P450 3A4 could be detected in all MOCs exposed to 50 µM troglitazone, whilst only minute expression was detectable in the control group. The experiments showed a sensitivity of the MOC co-cultures of liver and skin equivalents to a liver toxic substance at different levels of analyses.

4. Discussion

4.1 Skin Equivalents

Skin equivalents are widely used to replace animal-testing in cosmetic and drug testing. However, existing skin equivalents are only reliable for acute testing, not exceeding 72 hours. A perfusion of the skin equivalent could increase the viability of these skin models to also allow testing chronic application of substances. So far, only little research has been successful to perfuse skin equivalents. One aim of this study is, to achieve a perfusion of the skin equivalents. For this purpose the skin equivalent should be integrated into the MOC which required down-scaling of the skin equivalent to a size of 14.3 mm². The down-scaling has two main advantages: less material is needed for the matrix of the dermis and fewer cells have to be cultivated. Additionally, a smaller amount of the drug has to be applied when testing substances. This would permit high content assays.

4.1.1 Skin Equivalents Using Fibrin-Gel and Collagen-Gel

Skin equivalents made of fibrin-gel and collagen-gel were down-scaled to 96-well insert size in order to test the applicability of these dermis equivalents. Fibrin is a polymer which is polymerised by the addition of thrombin to fibrinogen, as seen *in vivo* in blood clotting (thrombus). Fibroblasts and endothelial cells enter the thrombus and transform it to extracellular matrix and build new blood capillaries (Clark, 1996). The proangiogenic impact makes it a promising candidate for later migration of the endothelial cells into the skin equivalent. However, aprotinin needs to be added to cultures in fibrin-gel to avoid proteolytic degradation of the gel by fibroblasts. This protease inhibitor also avoids the degradation of enzymes and growth factors which might alter the physiology, functionality and communication in the cell culture system and might lead to wrong assertions (Dietrich *et al.,* 1997). In culture, fibrin-gels were stable in their volume for up to 34 days. However, fibrin-gels adhered to the plastic of the Transwell® insert, due to their gluing activity which is also used in surgery to glue tissue sites together (Dal Pizzol *et al.*, 2009). The high ratio of plastic side to the surface area led to a strong concave formation of the gel in the small culture. Thus, keratinocytes which were added after two days in culture would only adhere to the lowest point of the culture. They could therefore not form an adequate epidermis dispersed over the complete dermis. Even the addition of MaxGel™, a basement membrane extract, prior to the addition of keratinocytes could not prevent the accumulation of

keratinocytes at one point of the dermis. The adherence of fibrin led to a strong deformation and change in the structure of the gel once the gel had to be removed from the insert at the end of the culture. These obstacles prevented the successful preparation of skin equivalents for analytic purposes.

The main part of the extracellular matrix of the skin consists of type I collagen. Therefore, a dermis equivalent made of collagen should be best to emulate and contain the physiological functions of the skin. The stability and robustness of this material is beneficial when cultured in a perfused system, with auxiliary shear stress (Buehler, 2006). Compared to the fibrin-gel, the collagen-gel attached less to the plastic of the Transwell® insert and the equivalent was hardly misshaped or deformed, when taken out of the insert for later analysis. Unfortunately, fibroblasts proliferate in the collagen matrix and tend to reorganise the hydrated collagen-gel, whereupon the collagen-gel can shrink to $^{1}/_{28th}$ of its original size within 24 hours (Bell *et al.,* 1979). Though the reorganisation of the collagen to a more physiological structure is desired, the metabolism and degradation of the collagen as a response to stress is counterproductive. Media compositions had to be diluted slowly, to avoid stressful adaption of the metabolism. Especially FCS, BPE (bovine pituitary extract) or EGF needed to be removed from the medium for better differentiation of keratinocytes. Taking care of these factors, dermis equivalents could be produced that shrank in the z-axis in the first days, but had a stable volume after day 4. On both dermis equivalents, keratinocytes were proliferating and forming different layers in the epidermis. However, the differentiation was not as expected, with a basal layer above the basal membrane, where cells proliferate and differentiated keratinocytes in the upper layers, until they lose their cell nucleus in the *stratum corneum*. A reason can be the small total cell number in the 96-well Transwell® insert. It needs intense contact between epidermal and dermal cells to form an evenly distributed epidermis: El Ghalbzouri and colleagues showed that the amount of fibroblasts in the collagen-gel and their functional state is critical for the establishment of an intact epidermal morphogenesis (el-Ghalbzouri *et al.,* 2002). In addition, cell-cell contact of keratinocytes is a major factor for a well-differentiated epidermis. Given the chosen conditions, the epidermis might need closer contact to neighbouring keratinocytes to allow cell-cell interaction. This could be enhanced by addition of mitogenic growth factors like KGF, FGF, IGF-1 and EGF (Bhora *et al.,* 1995; Sanz Garcia *et al.,* 2000). However, the optimisation of full thickness skin equivalents in 96-well Transwell® inserts will require various trials. Design of experiment (DoE) methods could reduce the number of trials and increase probability of the success. So far no paper has been published about these small full

thickness skin equivalents. Therefore, the optimisation of the skin equivalent is still on-going in our lab, financed by a 3-year DFG project. Another possibility to design a small skin equivalent could be the new method of 3D bio printing. The gel, including cells, is printed in a 2D layer, according to a computer program that has parsed the 3D object. Then, a piston holding the gel layer is lowered, the cycle is repeated and the next layer is printed until, layer by layer, an entire 3D object is fabricated (Griffith and Naughton, 2002). Alternatives to these down-scaled full thickness skin equivalents are punched skin or skin equivalents. Using skin biopsies reduces the work for preparation of skin equivalents, is the most physiological "copy" of the skin and provides donor specificity. This is, of course, only possible for the small quantity which is needed for application in the MOC system, where several punches can be obtained from one small piece of skin. If skin equivalents are needed for substance testing, bigger equivalents can be prepared and punched to a smaller size.

4.1.2 Integration of Hair Follicle Equivalents into Skin Equivalents

Integration of hair follicle equivalents into skin equivalents would help to predict the penetration and, therefore, the impact of a substance in a more realistic manner. Substances can penetrate through the skin on different routes, either inter- or transcellular across the *stratum corneum* or transappendageal through the hair follicles and their sebaceous glands (Scheuplein *et al.,* 1967). For example, a study showed caffeine penetration into the blood through the transfollicular pathway within 5 minutes, whereas relevant concentration of caffeine only appeared after 20-30 minutes in the blood, when follicles were artificially closed. The total caffeine concentration that penetrated through the transcellular pathway was also less than that through the transfollicular pathway (Otberg *et al.,* 2008). For particular substances in the range of 300-400 nm the rigid hair shaft acts as a geared pump, moving the particles deeper into the hair follicle. Thus, the substances showed a 10 times longer storage within the hair follicles compared to the storage reservoir capacity of the *stratum corneum*. This demonstrates how important the hair follicle is in transdermal drug delivery (Lademann *et al.,* 2006). The first step to integrate a hair follicle equivalent is the production of the human artificial hair follicle which was described in our group by Lindner *et al.* in 2010 (Lindner *et al.,* 2010). Therefore the dermal papilla, the "control centre" and the consistent part of the hair follicle which stimulates new hair growth was integrated into skin equivalents (Jahoda *et al.,* 1990). The integration of the dermal papilla occurred in two different ways: 1) seeding on top of the dermis equivalent before addition of the epidermal

keratinocytes or 2) integration by a micromanipulator from the top into a full thickness equivalent. Both ways could successfully integrate the dermal papilla, though the integration with the micromanipulator also led to a hole in the epidermis. With some experience, the hole could be reduced to a small scratch in the epidermis and dermis. However, in none of the approaches a hair shaft formation could be observed. *In vivo,* the dermal papilla is highly vascularised (Lachgar *et al.,* 1998) and nutrition plays a key role in shaft formation. This was also shown by a study on transgenic mice, where the overexpression of VEGF led to a strongly induced perifollicular vascularisation. This resulted in accelerated hair growth and in increased size of hair follicles and hair shafts. There was direct evidence that vascularisation promotes hair growth (Yano *et al.,* 2001). In skin equivalents, however, medium needs to diffuse through the dermis equivalent before it can reach the dermal papilla. It reduces the nutrient supply compared to the cultures swimming in the media and especially compared to the *in vivo* supply. The perfusion and especially the endothelialisation and vascularisation of the skin equivalent are, hence, an important factor for the nutrient supply of the hair follicle to enable hair shaft growth. Therefore, the prime focus was the integration of the skin into the MOC and its endothelialisation. This could later lead to a vascularisation of the skin equivalent and the dermal papilla which would then allow hair shaft growth in future experiments.

4.2 Preparation of Liver Equivalents

The liver is one of the crucial organs in toxicological and pharmaceutical studies, as hepatoxicity is one of the major reasons for withdrawing drugs from the market (Jaeschke *et al.,* 2002). The combination of skin and liver equivalents therefore was another interesting subject arising in the progress of the study. A reliable production of 300 spheres per hanging drop culture plate was achieved. Staining for vimentin and cytokeratin 8/18, ZO-1 and MRP-2 demonstrated an equal distribution of HHSteCs throughout the whole aggregate, the tight junction development during culture, the polarisation of cells and the existence of rudimentary bile canaliculi-like networks in the generated liver micro-tissues. One tissue culture compartment of each MOC circuit was seeded with 20 liver aggregates corresponding to 10^6 cells. This matches a miniaturisation ratio of $^1/_{100.000,}$ equal to that of skin. This is part of the doctoral thesis of Eva-Maria Materne, who was responsible for the production and analysis of the liver equivalents mentioned in this study. More details to liver equivalents will be found in her thesis.

4.3 Development of the Multi-Organ-Chip

The Multi-Organ-Chip design needs to satisfy several requirements:

- be able to perfuse organoids, the smallest functional unit of an organ
- be biocompatible
- microscopable
- chemically resistant
- sterilisable
- cost effective and
- easy to produce

The first design of the MOC was a very extensive design, with 6 parallel cultures, each with three culture compartments designed for liver, brain cortex and bone marrow micro-organoids and different sensors at the bottom of the culture (Sonntag *et al.,* 2010). Even though the chip was biocompatible and most of the other requirements were fulfilled, the small tissue volumes of 0.5 µl made it very difficult to handle. The supply of nutrients was intended to be carried out by separate, unidirectional perfusion of medium through each of the three different micro-organoid segments. However, in the first cultures the segments were flooded with medium from the top, as handling of such small volumes was not possible at that time. The first design was rather expensive, so that prototyping was carried on and a second design was constructed. The culture medium was expanded and a pump diffusor was added to the MOC. Unfortunately, the pump principal was insufficient to culture cells in long-term culture and the cells died due to malnutrition. An on-chip peristaltic pump was included into the next design, to allow better nutrition and avoiding high total fluid to tissue ratios, as seen in most other organ-on-a-chip cultures (Huh *et al.,* 2011, Imura *et al.,* 2010 and others). The third design further included a culture compartment for cultures in a Transwell® insert, allowing tissues, e.g. skin, to be cultured at air/liquid interface and to reduce shear stress. The first version of this design allowed closing and opening of valves to either culture the organoid in a closed or open mode, or combining both modes for a distinct feeding regimen. Here, only one tissue could be cultured on one chip. The second version of the third design enabled the parallel cultivation of two tissue cultures with the same medium supply but different waste tanks for separate analysis. However it was firstly difficult to bond this design, as the channel was close to the edge of the glass slide. Besides, plasma treatment using a plasma pen produced a high number of leaking chips which could not be used for culture. Secondly, the medium did not

split up equally to both tissue culture compartments, as the medium had to take a turn to flow to the upper culture compartment. Putting some pressure on the valve of the lower culture and therefore closing the valve a little to let less medium pass, helped a little but did not solve the problem. This design did indeed allow the parallel culture of two tissues, but the effect of one tissue on the other could not be evaluated, as the metabolites of each organoid never reached one another. Combining all advantages and reducing all disadvantages, the fourth design was established: Two culture compartments were together in one circuit, allowing the respective metabolites to reach both organoids. Additionally, two circuits could be cultured at the same time on one MOC. This doubled the throughput. Preliminary problems with the first-time complete loading of the circuit were solved by screwing injection fittings on top of the culture compartments and fixing a syringe on both compartments. With this method, the pressure was even at all areas of the circuit and the channels could be equally filled with media. An injection port was added to the culture design to allow medium exchange and addition of substances. Unfortunately the design was not practicable. Entering the circuit with a needle was difficult and removing or adding media was not possible: the channel was only 100 µm high and due to the channelplate on top of the culture, needles could only be applied vertically. Thus, only very little medium could be removed or added. Instead, the medium was exchanged at the culture compartments. This was handy for single-cultures but was more difficult for two-tissues-cultures, especially when Transwell® inserts were added or small aggregates were cultured. Regardless, the 4th generation MOC turned out to be the strongest and most successful design and most cultures described in this study were performed with this design. Yet, the next design should include an injection port that can be used to ease media exchange.

4.3.1 MOC Casting

In the first year the PDMS polymerisation was often not complete and the PDMS layer thus had to be produced again. The problem was due to sulphur and sulphur chloride particulates which inhibited the polymerisation of PDMS (Kimoto *et al.,* 2005). Removal of these contaminants, like sulphur residue in latex gloves, avoided the inhibition. Combining this provision with avoiding a humid environment led to a fully polymerised PDMS. Improving the spacer from PFTE to POM and introducing a syringe pump, to inject the PDMS in the casting station, improved the process immensely. In the first year, only one MOC could be casted per day, while now, up to 15 MOCs can be casted per day. Hence, for the fourth design, 30 circuits could be casted per day. The limiting factor here was the existence of

only two master plates, otherwise more MOCs could be casted per day. MOCs could be casted up to one month before bonding without having any influence on the cultures.

4.3.2 MOC Bonding

Bonding follows the process of MOC casting. The medium had to be inserted at the latest 30 min after the bonding process, to sustain the long-term hydrophilic character of the plasma activation (Bhattacharya *et al.,* 2005). After injection of the medium, the MOC should be incubated for 24 to 72 hours. This enabled a diffusion of nutrition and growth factors into the PDMS before the culture was started and therefore avoided a dilution of the final media. However, a longer incubation period should be avoided, as the antibiotics used lose their activity after approximately 3 days at 37°C and would encourage bacterial resistance. If longer pre-incubation periods are favoured, the medium should be changed every two to three days.

4.3.2.1 Plasma Pen

The time consuming treatment with the plasma pen yielded only 30% leakage-free MOCs. The time needed to scan the whole area of the PDMS layer and the glass object slide was too long to keep the plasma activation of the complete surface active. This led to unsatisfying bonding, air bubbles in the channels and insufficient adherence of cells to the surface. The use of tape pads helped to avoid the often occurring case of bonding of the pump membrane to the glass slide which led to the closure of the channels. In addition, it was time consuming to place the pads at the right place and to remove the pads without residues. These factors led to the development of a new method for bonding.

4.3.2.2 Plasma Chamber

The use of a plasma chamber for plasma treatment showed a constant bonding of the whole surface and the process of plasma treatment itself took only 30 seconds. It took less than 10 minutes to complete the bonding process. Exchanging the tape pads with metals pads and magnetic screws avoided the time consuming placing and removing of the pads and left no residues. The success rate was 80 % of leakage-free MOCs. The 20% leaking MOCs were not always explainable. In most cases, MOCs did not bond properly on the side which might have been due to fingerprints on the PDMS layer. Though we tried to avoid touching the PDMS layer, it sometimes was inevitable and happened accidentally. Another problem was the leakage through the membrane. The membrane was in some cases not stable enough and

broke, possibly because it had to endure more pressure than usual, e.g. when a channel was mistakenly partially closed during bonding process or a channel was otherwise blocked for a short time. These leaking MOCs were then discarded and new MOCs were casted and bonded. In total, this system proved to be much more efficient and replaced the plasma pen method.

4.3.3 Setup of MOC Cultivation

The MOC could be setup in two different modes: i) tissues directly exposed to the fluid flow or ii) tissues in Transwells®. Both setups required the same casting, bonding and connection to the peristaltic pump and only differed when tissues were added. Both setups could further be combined with each other, when both culture compartments were in use: One tissue could be cultured in a Transwell® and one directly exposed to the flow. This enhanced the production of the MOC, as both setups were treated identically and demonstrates the flexibility of the MOC system.

4.3.3.1 Transwell®-Based Skin Cultivation vs. Exposed to Fluid Flow

Skin biopsies in Transwell® holders achieved better results for skin maintenance than those placed directly in the flow. This was due to the air–liquid interface of the skin which is only possible in Transwell® cultures and allowed the epidermal differentiation in a similar manner as seen *in vivo*. When the skin biopsies were submerged in the flow, the epidermis was soaked and the shear stress led to a premature degradation of the epidermis. Penetration of cells through the Transwell® and into the channel system of the MOC could further be prevented by choosing a small pore size. If penetration would be needed, for example for migration of endothelial cells, the membrane of the Transwell® could easily be replaced by a membrane with a bigger pore size. In some cases, bubbles formed under the Transwell® insert when closing the lid which needed to be removed and the Transwell® needed to be inserted again. The problem was now solved by a bubble trap in the lid which had two drills, avoiding under pressure under the Transwell® and could be connected with a small tube to close the system.

Figure 4.1) Bubble trap lid

4.4 MOC Cultivation of Skin Tissues

4.4.1 MOC Cultivation of Skin Equivalents

4.4.1.1 MOC Cultivation of Skin Equivalents of Fibrin- and Collagen-Gels

One first step of the MOC cultivation was to include the skin equivalents made in 96-well inserts. When the fibrin-gel was cultured in the MOC, the gel structure was soon completely deformed and was not emulating a human skin structure. Medium was able to pass the gel easily to the top and, therefore, avoided air/liquid interface. If the fibrin-gel, a filamentous biopolymer gel, is compared to flexible polymer gels, it has larger elastic moduli, a pronounced negative normal stress when deformed in simple shear and an increased elastic modulus with increasing strain (Wen *et al.,* 2007). To avoid this deformation, the mesh size should be changed by increasing the fibrinogen concentration. The average mesh size in fibrin-gels increases with the square of fibrinogen concentration, if the networks of fibres are homogeneously distributed throughout the gel (Piechocka, 2010). This might have reduced the amount of deformation, but problems with the fibrin-gel had already occurred in static culture and removal of the fibrin-gel from the Transwell® was problematic. Hence, the focus was set on other skin equivalents, as described below. Collagen-gel based skin equivalents could be cultured in the MOC without deformation. However, hardly any improvement of the epidermal differentiation was visible. As mentioned before, the research on the improvement of the skin equivalent in 96-well size is still on-going but these first results in the MOC already showed that the cultivation of collagen-gels is preferable.

4.4.4.2 MOC Cultivation of MatTek® Skin Equivalents

In a next step to cultivate skin equivalents in the MOC, punches of skin equivalents from MatTek® were produced and added into the MOC. H/E staining revealed a rearrangement and compression of the dermal matrix structure in dynamic MOC cultures. Cell nuclei were located closer to each other with denser extracellular matrix structure compared to day 0 and the static control. The compression might have two sources: one is the pressure from the fluid flow and the other is the screwing of the lid onto the skin model when MOCs were set up. Another reason might be the reorganisation of the matrix by the fibroblasts, as the compressed skin model is morphologically more similar to the *in vivo* skin than the uncompressed skin. The matrix is tighter and the communication between keratinocytes and fibroblasts is eased. Studies have demonstrated that mild compression might counteract the decrease in skin micro-vascular flow (Neuschwander *et al.,* 2012). However, other studies

showed that compression might induce cell damage in engineered muscle tissue (Breuls *et al.,* 2003). Therefore, a small in- and outlet was introduced into the MOC's lid which can be closed with a small tube to allow compression release when closing the lid, if necessary. The different layers of the epidermis were analysed by immunofluorescence, showing the expression of the epidermal markers cytokeratin 10 for differentiating keratinocytes and cytokeratin 15 for undifferentiated keratinocytes. Both were similarly expressed in static and dynamic MOC cultures. The epidermal function seemed to be better preserved in the MOC culture according to the continuous lining of the cytokeratin 15 positive cells at the basal layer of the epidermis and its discontinuity in static culture. Hardly any proliferating or apoptotic cells were seen in the MOC or in day 0 controls according to Ki67/TUNEL double staining. In the epidermal layer of static cultures selected apoptotic cells could be found, suggesting the onset of degradation of this skin equivalent.

4.4.4.3 MOC Cultivation of MatTek® Skin Equivalents in Combination with Subcutaneous Tissue

In the next step, EpiDermFT™ skin equivalents were combined with subcutaneous tissue dissected from prepuce. The subcutaneous tissue is composed mainly of adipocytes, fibroblasts and macrophages. H/E staining revealed more viable cells and a compressed dermal matrix in the samples with subcutaneous tissue cultured in the MOC compared to static cultures with and without subcutaneous tissue. Subcutaneous tissue was well integrated into skin equivalents in the MOC, while its integration was poor in the static culture. The integration of subcutaneous tissue into the skin equivalent has important beneficial effects for the transplantation of skin grafts. It is a sign of sufficient nutrient supply and well-being of the skin equivalent in the MOC (Almeyda *et al.,* 2013). Cytokeratin 15 staining revealed an increase of undifferentiated keratinocytes in static cultures with subcutaneous tissue, compared to those in static culture without subcutaneous tissue. The greatest similarity to the *in vivo* epidermis, however, was seen in the MOC-cultured skin equivalent with subcutaneous tissue. Cytokeratin 15 was expressed in the basal layer of the epidermis, where proliferation took place. The same result could be seen in the Ki67 staining for proliferating cells. The basal layer of the MOC-cultured epidermis showed an increase of proliferating cells compared to the static culture with subcutaneous tissue. Normal static culture without subcutaneous tissue showed no proliferation but instead displayed some apoptotic cells in the epidermis. Taking the absence of proliferating cells in the static epidermis without subcutaneous tissue into account, it seems that epidermal

growth, regeneration and homeostasis was reduced immensely compared to the cultures with subcutaneous tissue. This might be due to the influence of lipid metabolism and the paracrine effects of adipose-derived cells in the subcutaneous tissue (Lee *et al.,* 2012). The subcutaneous tissue of the static cultures showed many dead cells, another sign of poor integrity and malnutrition under static conditions. In MOC cultures, however, less apoptotic cells were visible. It seems that the *ex vivo* subcutaneous tissue has a higher metabolism than the skin equivalents which can only be supplied by perfusion, as provided by the MOC system.

4.4.2 MOC Cultivation of Skin Biopsies

Since integration of the subcutaneous tissue into the MOC system worked well, the next step was the integration of a skin biopsy. These days, much research on transdermal drug diffusion is performed using porcine skin as a substitute for human skin, due to its high morphological similarity (Barbero and Frasch, 2009). However, human skin would, of course, be the better choice. Considering its reliable source, prepuce tissue was used for these skin biopsies. Unlike commercially available skin models, the prepuce contains apocrine glands which produce lysozymes, neutrophil elastases and cytokines. In addition, it has numerous specialised nerve endings *in vivo*. Furthermore, adult stem cells which are capable of regenerating the epidermis are present in their specific quiescence-promoting niches in the prepuces (Fleiss *et al.,* 1998). The heterogeneity of the original tissue supports different cellular and molecular events in the respective biopsies. Therefore, skin biopsy maintenance in culture in comparison to skin equivalents was evaluated for future substance testing. H/E staining of the epidermis showed disruption and dermal reorganisation in the static cultures. In contrast, MOC-cultured skin showed a similar distribution as seen in the control at day 0. Cells in the epidermis of the static culture seemed to have differentiated and built an unnatural thick layer of cornified envelop but did not proliferate further to provide new cells for differentiation, as only few cell nuclei could be seen in the epidermis. Staining of cytokeratin 10 and 15 likewise showed the disruption of the epidermis. Even though cells expressed cytokeratin 15, these cells were clustered and were hardly connected to the dermis. Some positive staining of cytokeratin 15 could even be seen in the dermis. This part of the dermis was also positive for tenascin C. Type IV collagen and tenascin C which are both synthesised and secreted by keratinocytes and fibroblasts, were used as markers for the extracellular basement membrane (Marionnet *et al.,* 2006). Type IV collagen is mainly found in the basement membrane of the skin, in the epidermal-dermal

border and the dermal endodermal border including blood vessels (Abreu-Velez and Howard, 2012). Tenascin C is an extracellular matrix component known to be important for cell shape and migration behaviour. It has a pro-migratory role for epidermal cells around the basement membrane in skin and has been shown to be upregulated during wound healing, inflammatory processes and fibrosis (Sidgwick and Bayat, 2012 and Chiquet-Ehrismann, 2004). The upregulation, indicating inflammatory processes and fibrosis, could be clearly seen in the static culture. In MOC-cultured skin, however, tenascin C was only expressed in the basal lamina, comparable to the control at day 0. Cytokeratin 10 and 15 expressions also resembled the day 0 control, even though the epidermis shrank a little during the culture period of 14 days. The epidermis and the basal lamina were still intact, representing a solid barrier function and allowing chronic *in vitro* substance testing for 14 days, including penetration studies. This was also proven by staining for proliferation and apoptosis. Static cultures showed many apoptotic cells and no specific staining for proliferating cells. MOC-cultured skin, however, showed proliferation and less apoptotic cells in the basal layer of the epidermis, suggesting a small amount of cell loss. Being able to cultivate biopsies of skin has huge advantages compared with skin equivalents. The biopsies combine all cell types of the human skin, including fibroblasts and keratinocytes which are usually the only cell types in skin equivalents and others, such as Langerhans cells, melanocytes, endothelial cells and the natural extracellular matrix. Due to its originality, the skin can mimic the *in vivo* situation best once its characteristics can be maintained *in vitro*. Therefore, the MOC system allows analysing the effect of cosmetic and pharmaceutical substances on the skin. Prepuce biopsies are especially suitable for eye cosmetics due to the similarity of its structure to the eyelid and similar bacterial flora (Fleiss, 1998). In addition, other skin biopsies, for example from the scalp or the abdomen could be implemented, depending on the appendages and glands needed for application and substances tested. Being able to prepare and maintain biopsies in a reproducible and robust manner encourages the transfer of other organs into the system.

4.4.3 MOC Adaption of the Philpot Assay

The aim of the MOC adaption of the Philpot assay was to prolong the culture period of the *ex vivo* hair follicles, taking into account the support of the glands and the surrounding skin tissue for hair follicle maintenance. During the culture period a hair-shaft elongation in growing anagen hair follicles was observed. Further analysis by Beren Ataç revealed signs of advancing regression phase, an intact appearance of the basement membrane, connective

tissue and dermal papilla, proliferative cells in the follicular bulb as well as apoptotic cells within the dermal papilla and the proximal connective tissue sheath (Ataç *et al.,* 2013). These results suggest a catagen progression in the hair follicle in the MOC culture and a successful extended culture period of *ex vivo* hair follicles by dynamic perfusion without loss of hair follicle morphology. Moreover, the initiation of catagen was postponed compared to the Philpott assay (Philpott *et al.,* 1990). This allows longer performance of the Philpott assay and, therefore, extended periods of observance of hair growth-modulation effects of agents.

4.5 MOC Cultivation of Skin and Liver Co-Cultures

4.5.1 MOC 14 Day Functionality Test of 2-Tissues-Cultures

The human liver and skin tissue co-cultures were maintained successfully in all MOCs during the experimental period of 14 days. A constant LDH level of about 20 U/l from cultivation day 6 onwards indicated an artificial but stable tissue turnover in the system. Cell death within the steady state happened primarily in the skin culture compartment, as data from MOC single tissue cultures of skin suggested. A possible explanation might be an increased epidermis turnover induced by the artificial culture conditions, such as artificial shear stress and lack of air exposure to the epidermal surface of skin biopsies. It is interesting that the steady tissue turnover was not affected when the daily MOC feeding rate was reduced by half starting on day 7 of culture. LDH measurement of static culture showed an increased apoptosis compared to MOC cultures, indicating the advantage of perfusion in the MOC system. Glucose consumption was similar in both single-cultures, though skin single-cultures had slightly higher consumption than the liver. Though the skin had about 5 times more cells compared to the liver equivalent, liver cell lines generally consume a greater amount of glucose than primary cultures (Bissell *et al.,* 1978). Glucose consumption in co-cultures, however, was not constantly the sum of both single-cultures. This was the first indication for different behaviour in single- and co-culture which later became more obvious, when albumin production was analysed. In all cultures the glucose consumption decreased, when the medium exchange rate was lowered. As about 50% of the existing glucose in the medium was usually consumed, the glucose concentration in the medium might have been insufficient. The medium contained 2 g/l, twice as much as the average physiological blood glucose level, so an increase of glucose concentration would be possible, but would also diminish the similarity to the physiological conditions. Extended medium

changes per day would be possible, though as the number of MOCs cultured increases, the medium change is difficult to handle by one person. Therefore, to cope with the further expansion of MOCs cultured and the concomitant increase of medium changes per day, an automated robot will be inevitable for media change. This robot is currently developed in cooperation with the Fraunhofer IWS. From day 8 onwards, the consumption of glucose and production of lactate by the co-cultures reached a near to steady state which indicates the establishment of a stable artificial co-existence between the two tissues. Lactate production was highest in the first 3 days for all cultures. It might be related to the stress the cells experienced, by changing the culture conditions from static to dynamic culture or, in case of skin from *in vivo* to *ex vivo*. The lactate production within the first 9 days was highest in skin single-culture. This effect might be due to the punching of the skin biopsies which induced wounds. Lactate is known to participate in the healing process, in stimulation of collagen production by fibroblasts and in promoting angiogenesis. Experiments with scratched monolayers revealed a faster cell migration in response to increased lactate concentration (Matthew *et al.,* 2001, Britland *et al.,* 2012 Porporato *et al.,* 2012). In co-cultures with liver the lactate production was reduced. This result seems to be related to the communication between the two cultures and matches the studies where albumin enhanced wound healing in rats (Kobayashi *et al.,* 2004). Lactate concentration in cultures including skin decreased significantly in the first three days. This might be the lactate which was released from the skin's damaged blood capillaries and got washed out. It also occurred during the time period, when albumin concentration in cultures was high and might be explained by enhanced wound healing. After day 9, lactate concentrations were higher in co-cultures than in single-cultures, as expected. Interestingly, static cultures of skin and liver co-cultures consumed a similar amount of glucose, but produced more lactate than the MOC-cultivated co-cultures. This could be a proof of the advantage of a perfused system over a static system. Nevertheless, in both static and perfused cultures, the lactate production to glucose consumption ratio was rather high, so it might be possible that an oxygen limitation and, therefore, anaerobic conditions existed in the cultures. To assure that this is not the case oxygen was measured with the fluorescence quenching method. Oxygen gradients varied for different measurements, though the oxygen concentration never left the range of 50-70 % air saturation. These differences might be caused by the handling of the fibre optic probe which was difficult to position below the MOC system in the incubator. The sensor spots which were added to the culture were about the size of the culture compartment and were therefore cut into half. This did not influence the spots productivity,

but worsened the handling with the fibre optic probe. It might be advantageous to use the complete spot. It reduces the microscopablity of the culture compartment, but would increase the range where the fibre optic probe could measure and, therefore, would improve the handling. The handling might further be improved by an incubator independent MOC support which can keep the temperature of the MOC culture at 37°C without an incubator. Such a system has already been successfully tested, but due to equipment shortage could not be applied to more than six parallel running MOC systems. Therefore, it was not used in these experiments. More experiments will be needed to improve the oxygen measurement in the MOC system and to assure an appropriate oxygen concentration in the medium. However, the availability of oxygen might be limited for the cultures even though the air saturation of the medium is sufficient, as calculations by Stevens suggest. His studies showed that hepatocytes would not be able to grow, due to oxygen availability limitation in medium overlay that exceeds 0.34 mm (Stevens, 1965). One other possibility to measure oxygen in the MOC is a system of Colibri photonics, where micro and nano probes can be added to the culture and be measured in a miniaturised space. An optical instrument allows the oxygen measurement with spatial resolutions down to cell scale. With this tool the oxygen concentration at every position of the MOC could be determined. Additionally, the oxygen concentration within the tissue could be measured, if beads can be included into the tissue and fluorescence light could reach the beads for absorption and emission of radiation. Thus, any possible oxygen limitation in the medium or the tissue could be detected. This system is currently tested in our lab.

Focussing on the albumin production in the MOC system, an unexpected high amount of albumin in the first 2–3 days of co-culture was observed. This can be clearly explained by albumin released from the skin biopsies, as the single-skin cultures exhibited exactly the same profile. These amounts of albumin were eventually released from the inner lumen of the damaged micro-vessels of the skin and the extra-capillary depots. Strikingly, the albumin profile of the single skin cultures at days 4, 5 and 6 substantiated a pronounced consumption of albumin by the skin. This observation was perfectly matched by the parallel albumin profile of the co-culture at slightly higher absolute amounts. It suggested that the albumin consumed by the skin in the co-cultures was provided by the active production of the respective liver compartment. The constant albumin production in single liver tissue culture further supported this hypothesis. Finally, the crosstalk between liver and skin within the co-culture steadied and albumin concentration stayed close to zero (0.15 mg per day per circuit at day 7 and 0.13 mg per day per circuit at ay 14). It might be interpreted as

equilibrium between albumin production by the liver and immediate consumption of the same amount of albumin by the skin. This result matches the well-known fact that albumin is degraded by skin fibroblasts and, furthermore, that nearly 50% of the extravascular albumin in humans is stored in the skin (Peters, 1996). Albumin is absorbed by the network of collagen, proteoglycans and hyalurons *in vivo* and its concentration increases with overhydration in human skin by 20–30% (Peters, 1996). Therefore, skin biopsies in submerged culture can act as an albumin depot. However, it remains unclear if skin would be able to absorb even larger amounts of albumin. Surprisingly, further analysis of mRNA of albumin in another experiment, using different media, showed a reduced mRNA expression of albumin in co-culture compared to liver single-cultures. This finding underscores the stable coexistence between the two tissues. It is interesting that albumin synthesis in liver single-organ MOC cultures exhibits values (3.5 µg per day per circuit at day 7 and 6.8 µg per day per circuit at day 14) consistent with those shown in the literature (Lübberstedt *et al.,* 2010).

Unfortunately, RNA isolation from the skin in this experiment was not possible. RNA isolation was first performed with the RNeasy kit which yielded a very low RNA concentration for skin biopsies. The more tissue was added for isolation, the less RNA was obtained. This outcome seemed to be related to the abundance of extracellular matrix rich in glycosaminoglycan and collagens which decreased the success rate of RNA isolation immensely. Therefore for later experiments the method was changed to trizol isolation, but could not yield a sufficient mRNA amount for further analysis, either.

4.5.2 MOC 28 Day Long-Term Cultivation of 2-Tissues-Cultures

Skin and liver were cultured in a co-culture in the MOC for 28 days. This time period is required by OECD guidelines for dermal subsystemic repeated dose toxicity testing of chemicals and cosmetics (OECD guideline no. 410). At the end of the culture liver tissues were stained for the expression of cytochrome P450 3A4, an enzyme related to the biotransformation of many xenobiotics and cytochrome P450 7A1, an enzyme involved in bile acid synthesis. Both enzymes were expressed in the liver tissue, indicating the preservation of its metabolic activity over the culture period of 28 days. In the skin, staining for cytokeratin 10 and 15 revealed a thinned, but still intact epidermis, showing both cells in the basal layer and the differentiated layers of the epidermis. The expression of tenascin C and type IV collagen decreased during the culture period, so a decreased function of the basal lamina might need to be taken into account. Staining for vimentin, for cells of

mesenchymal origin and panCytokeratin, for all keratinocytes in the epidermis, revealed a sound relation of epidermis and dermis. Staining for apoptosis revealed several apoptotic cells, leading to the conclusion that the skin is not perfectly unimpaired as it was on day 0, but for a culture of 28 days still very viable. The cellular metabolism of the culture was measured for 28 days in the MOC. A robust steady state metabolic activity from day 8 onwards throughout the entire culture process of 28 days was observed. It was about 40% lower than the corresponding values of the 14 day studies in the MOC cultures and might be an indicator of a slightly less efficient nutrient supply through the Transwell® membrane. Nevertheless, the tissues accommodate a stable long-term performance and, therefore, are very well suited for relevant substance testing protocols in the near future. Hence, the MOC system is well-qualified for long-term skin penetration efficacy and toxicity studies of 2-tissues-cultures.

4.6 MOC Cultivation of Skin, Liver and Endothelial Cell Co-Cultures

4.6.1 MOC Cultivation of 3-Tissues-Culture for 15 Days

After the successful combination of a skin and liver equivalent co-cultures in the MOC, the next experiment was the addition of a third tissue: endothelialised channels in the MOC, to support the other two tissues with a vessel network, as *in vivo*. Endothelialised MOCs showed a fluid-tight layer in all tissue combinations for 15 days. The combination of William's E medium and endothelial cell medium seemed to have worked for all tissues, though some small differences in metabolic behaviour were seen. All channels were covered with viable endothelial cells, proving the successful integration of endothelial cell vessels into the MOC system culturing skin and liver tissues. 3D view of the 3-tissues-culture further proves the coverage of all channel-walls by endothelial cells, illustrating blood vessel-like coverage. Glucose consumption in co-cultures hardly varied for different co-cultures and 3-tissues-cultures did not consume more glucose than 2-tissues-cultures. In addition, the reduction of glucose consumption accompanied with the lowered feeding rate, might suggest a glucose limitation in the system. However, it seems like the less glucose was supplied the lower was the relative production of lactate. Lactate was also highest in the first days, but here differences between combined cultures were visible. It is, therefore, questionable, if it is better to increase the glucose content to 4 g/l in the medium and to increase the feeding rate, or, to keep a glucose content of 2 g/l, if glucose limitation is the desired condition, i.e. if the homeostasis of cultures is preferred instead of high proliferation.

The comparable amount of glucose in the blood *in vivo* is 1 g/l, though glucose level increases when nutrition is taken up, but usually does not exceed 1.65 g/l (Rizza *et al.,* 1980) and remains above 0.55 g/l even after exercise or moderate fasting (Wahren *et al.,* 1978 and Consoli *et al.,* 1987). Therefore, in my opinion, it is advantageous, to keep the glucose level in the medium at 2 g/l to keep the cells in homeostasis, as long as apoptosis in cells is not seen and glucose is not entirely depleted below 0.55 g/l. Albumin concentration in the 3-tissues-cultures differed a little compared to the skin and liver co-culture described above: the albumin concentration dropped slower and reached a level around 0 not before day 5 instead of day 3. In the experimental setup in the 2-tissues-cultures described earlier, both tissues, skin and liver, were cultured directly exposed to the fluid flow. In this experiment the liver equivalents were still cultured directly exposed to the fluid flow, the skin biopsies, however, were cultured in Transwell® inserts. Hence, the above described wash out of albumin in the blood was slowed down, due to less shear stress and less direct contact to the fluid and the flow and albumin got diluted less rapid. mRNA analysis further showed a lower expression of albumin, indicating a crosstalk between the different tissues. It emphasises the importance of systemic culture.

4.6.2 MOC Cultivation of 3-Tissues-Culture for 28 Days

For two MOC circuits, the cultivation of the 3-tissues-cultures was prolonged to 28 days. Again, a mix of William's E medium and endothelial cell medium of 80% to 20% was applied, but as in the 28 days 2-tissues-cultures of skin and liver, both tissues were cultured in Transwell® inserts. Glucose consumption in 3-tissues-cultures was slightly higher than in 2-tissues-cultures, though both were lower than in the 15 day culture, where only skin was cultured in the Transwell® insert. It seems that the glucose concentration of the medium was not limiting glucose uptake, but the supply of the tissues was reduced due to Transwell® inserts. Though more glucose was taken up compared to 2-tissues-cultures, the same amount of lactate was produced, indicating a healthy, aerobe environment. This finding was further supported by the immunohistochemistry evaluation. Slightly less apoptotic cells were seen in skin biopsies in 3-tissues-cultures compared to 2-tissues-cultures, demonstrating the well-being of the cells in the skin. Tenascin C and collagen IV were strongly expressed in basal membranes, but tenascin C did not show any overexpression and was therefore not indicating wound healing or fibrosis in the tissue, as seen in static cultures earlier. Staining for cytokeratin 15 showed a small line at the bottom of the epidermis, indicating proliferating cells in the basal layer only, as in day 0 controls.

4.7 Toxicity Tests

Troglitazone is an anti-diabetic and anti-inflammatory drug which was prescribed for diabetes mellitus type 2 patients, but led to drug-induced hepatitis. Soon after its approval the adverse liver effects showed up in several patients and the drug had to be withdrawn from the market. This drug was chosen for application in the MOC system for repeated dose substance testing

4.7.1 Troglitazone Exposure to Skin and Liver Co-Cultures for 6 Days

Troglitazone was added daily to the skin and liver co-culture for 6 days, following 1 day of normal cultivation. Troglitazone showed no significant effect on the metabolic activity of liver and skin co-cultures. However, after 4 days of culture an increase of LDH activity was observed and after 7 days a significant 60% increase was seen compared to DMSO-treated controls. Analysis on the mRNA level of the liver micro-tissues revealed a dose dependent increase of cytochrome P450 3A4 in cultures exposed to 50 µM troglitazone compared to the control. The upregulation following troglitazone treatment has been shown before (Rogue *et al.,* 2011 and Ramachandran *et al.,* 1999) and is a typical reproduction of toxicity *in vivo*. Metabolic activity did not show any pronounced increase of glucose consumption induced by troglitazone in any concentration, neither in static nor in MOC-cultivated cultures. This is in contrast to what has been reported by Hewitt (Hewitt *et al.,* 2002). Immunhistochemical staining of skin tissue did not show any difference in treated or untreated cultures, as was expected. To my knowledge, no evidence of toxic impact of troglitazone on the skin has been reported so far.

5. Outlook

During this study a multi-organ-chip system has been developed capable of maintaining 3D tissues derived from cell lines, primary cells and biopsies of various human organs. The system was approved for skin equivalents as well as for skin biopsies and skin biopsies in combination with liver equivalents and even an additional endothelialisation of the complete channel setting in the chip. For the first time we provide a system that allows maintaining multiple organoids, including skin and liver, viable for more than 28 days. Aside from multiple dose skin toxicology studies truly pharmacodynamic evaluations can now be performed. The effects of systemic and topical dosage of drugs and cosmetics on skin and skin combined with liver can be analysed. *Ex vivo* samples of diseased skin can be used to evaluate or develop new and established dermal therapies, either systemic or topic. In the future, this chip could further be tested with an *ex vivo* epidermis which could be imposed on the insert to assure a leak-proof air/liquid interface to allow authentic penetration of substances and, therefore, to give more evidence on the substance's transepidermal diffusion. When combining the system with the liver equivalent the penetration of possible liver toxic substances in cosmetics and creams through the skin and their liver toxicity could be tested in one system (e.g. for mercury(II)chloride in whitening creams). Another possibility for skin equivalents in the MOC system is its combination with dendritic cells, currently on-going under my supervision, using monocyte derived dendritic cells isolated from buffy coats. The setup is especially interesting for substances which are metabolised by keratinocytes before their contact with dendritic cells. Hence, sensitising substances can be distinguished from non-sensitisers. A further step to improve the MOC system is the embedding of more organs into another prototype. A first approach is currently tested in our laboratory, combining liver, kidney and intestine in a two-level system. One circulation will include the intestinal barrier, where substances and nutrition can penetrate to the second circulation below, passing the liver and kidney

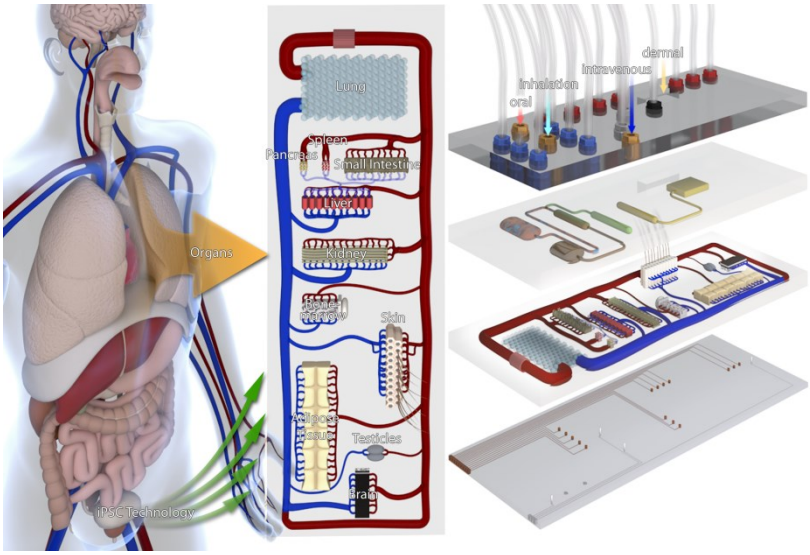

Figure 6.1) Concept of the eleven-organoid-chip

equivalent. Further plans are the production of an eleven-organoid-chip system (Figure 6.1). It will include separate substance and medium application sides, representing oral, inhalational, intravenous and dermal application and waste tanks for urine, bile, faeces, etc. Production of these organoids might include iPS technology to provide all organoids from the same donor. Sensors at the bottom glass slide of the MOC will automatically measure pO_2, pH, temperature and possibly also glucose, lactate and LDH concentration. This system will provide a systemic as well as human test system for drugs, replacing animal models in drug testing and predicting drugs' safety and efficacy more efficiently.

6. Zusammenfassung

Vorhandene Test zur Substanztestung versagen überdurchschnittlich häufig, die Toxizität von Medikamenten hervorzusagen. Die *in vitro* Tests im Zellkulturlabor scheitern daran, die Komplexität des Menschen nachzubilden. Die Tierversuche hingegen, scheitern an der schlechten Vorhersage der Medikamente im Menschen. Um dieses ständig wachsende Dilemma von mangelhafter prädiktiver präklinischer Substanzevaluation zu verhindern, sind neue Lösungen nötig. Diese sollten die phylogenetische Distanz zwischen Labortieren und Menschen vermeiden und die Diskrepanz zwischen heutigen *in vitro* Testsystemen und dem menschlichen Körper eliminieren. Bisher wurden nur sehr wenige multi-Kompartiment Zellkultur Flusssysteme beschrieben, noch weniger in miniaturisierter Form. Der entworfene Multi-Organ-Chip besteht aus einem gewöhnlichen Mikroskopobjektträger aus Glas, das über Plasmabonding an eine Silikonschicht gebunden wird, die das Negativ der Kulturfläche der Organäquivalente, die verbindenden Kanäle, und die Pumpmembranen beinhaltet. Darüber ist eine Channel-Platte verbunden, die die Zugänge und Befestigungen für die Pumpschläuche sowie Nährmedienreservoire und Zugang zu den Organäquivalenten beinhaltet. Dieser Multi-Organ-Chip soll zur Verbesserung der bisherigen Zellkulturbedingungen führen. Zum Beispiel hat die Entwicklung von Hautäquivalenten in den letzten Jahrzehnten erheblichen Fortschritt gemacht. Trotz alledem limitiert die statische Kultivierung der Haut die essentiellen physiologischen Eigenschaften, die entscheidend sind für Toxizitätsstudien und Medikamenten-Screening. Der dynamisch, perfundierte Multi-Organ-Chip Bioreaktor ist im Stande variable, mechanische Schub- und Scherspannung anzuwenden und kann daher die Lebensdauer der Haut in Kultur verlängern. Durch diese Verbesserung der Kultivierungsbedingungen, konnte die Lebensdauer der Haut auf bis zu 14 Tage verlängert werden. Bisherige Kulturen haben im Vergleich 3 Tage selten überschritten. Das Design des Multi-Organ-Chips erlaubt es weiterhin, die Organoide, die kleinste funktionelle Einheit eines Organs, entweder direkt im Strom zu kultivieren oder in einem Transwell®, wobei das Organ an einer Luft/Flüssigkeit Grenze wachsen kann. Versuche unter beiden Bedingungen zeigten erstaunliche Unterschiede der Barriere Funktion der Haut, die deutlich besser ausgebildet war, wenn die Oberfläche der Haut der Luft ausgesetzt wurde. Da die Hautkultivierung in dem Multi-Organ-Chip erfolgreich war, wurde anschließen ein Leberäquivalent hinzugefügt. Für toxikologische und pharmazeutische Studien, ist die Leber mit eines der kritischen Organe, da Lebertoxizität eines der häufigsten Gründe ist, derentwegen Medikamente vom Markt genommen werden

müssen. Die Kombination der beiden Organäquivalente, je $^{1}/_{100.000}$ der Biomasse des Menschen, zeigte eine erstaunlich gute Kompatibilität der beiden Organoide. Es möglich beide Organäquivalente zusammen stabil 28 Tage zu kultivieren. Funktionalität, Struktur und Überleben der Organoide in dieser Langzeit Kultivierung war erheblich besser als im Vergleich zu bisher beschriebenen Kultivierungsbedinungen. Weiterhin konnte ein Crosstalk der beiden Organoide beobachtet werden. Um die Funktionalität des Systems weiter zu testen, wurde eine Substanz beaufschlagt. Die Substanz wurde täglich beaufschlagt und bereits nach 3 Tagen konnte eine erhöhte LDH Konzentration beobachtet werden, die an Tag 6 der Beaufschlagung signifikant höher war als die Kontrolle. Um die Dissertation zu vervollständigen, wurden die Kanäle des Multi-Organ-Chips weiterhin mit Endothelzellen ausgekleidet. Die Endothelzellen besiedelten die Kanäle vollständig, oben, unten und an den Seiten sowie die komplette Fläche der Kanäle und streckten sich mit dem Strom. Auch die Kombination von den drei verschiedenen Organoiden konnte erfolgreich für 28 Tage durchgeführt werden, und brachte sogar bessere Ergebnisse in Überleben und Funktionalität als in der zwei-Organoid Kultur. In dieser Arbeit wurde demnach ein potentielles, neues Instrument zur Substanztestung entwickelt.

8. References

Abreu-Velez M. and Howard M. S., North American Journal of Medical Sciences, 2012, 4, 1–8.

Almeyda R, van der Eerden P, Vuyk H. Skin graft survival on subcutaneous hinge flaps: an algorithm for nasal reconstruction. Laryngoscope. 2013 Mar;123(3):605-12.

Anderson, H and Berg, A.v.d., Microfabrication and microfluidics for tissue engineering: state of the art and future opportunities. Lab Chip, 2004, 4, 98-103.

Barbero AM, Frasch HF. Pig and guinea pig skin as surrogates for human in vitro penetration studies: a quantitative review. Toxicol In Vitro. 2009 Feb;23(1):1-13.

Bell E, Ehrlich HP, Buttle DJ, Nakatsuji T. Living tissue formed in vitro and accepted as skin-equivalent tissue of full thickness. Science. 1981 Mar 6;211(4486):1052-4..

Bell, E., Ivarsson, B. & Merrill, C. Production of a tissue-like structure by contraction of collagen lattices by human fibroblasts of different proliferative potential in vitro. Proc Natl Acad Sci U S A. 1979 Mar;76(3):1274-8.

Bhattacharya, S., Datta, A., Berg, J.M., Gangopadhyay, S. Studies on surface wettability of poly(dimethyl) siloxane (PDMS) and glass under oxygen-plasma treatment and correlation with bond strength. Journal of Microelectromechanical Systems. 2005, 14(3), S. 590–597.

Bhora FY, Dunkin BJ, Batzri S, Aly HM, Bass BL, Sidawy AN, Harmon JW. Effect of growth factors on cell proliferation and epithelialization in human skin. J Surg Res. 1995 Aug;59(2):236-44.

Bissell DM, Levine GA, Bissell MJ. Glucose metabolism by adult hepatocytes in primary culture and by cell lines from rat liver. Am J Physiol. 1978 Mar;234(3):C122-30

Blanpain C, Fuchs E Epidermal stem cells of the skin. Annu Rev Cell Dev Biol. 2006;22:339-73.

Boulais N, Misery L. The epidermis: a sensory tissue. Eur J Dermatol. 2008 Mar-Apr;18(2):119-27.

Bowden, P. E., Stark, H. J., Breitkreutz, D. & Fusenig, N. E. Expression and modification of keratins during terminal differentiation of mammalian epidermis. Curr Top Dev Biol. 1987;22:35-68.

Boyce, S. T., Christianson, D. J. & Hansbrough, J. F. Structure of a collagen-GAG dermal skin substitute optimized for cultured human epidermal keratinocytes. J Biomed Mater Res. 1988 Oct;22(10):939-57.

Breuls R. G. M., Bouten C. V. C., Oomens C. W. J., Bader D. L., Baaijens F. P. T. Compression Induced Cell Damage in Engineered Muscle Tissue: An In Vitro Model to Study Pressure Ulcer Aetiology. Ann Biomed Eng. 2003 Dec;31(11):1357-64.

Britland S, Ross-Smith O, Jamil H, Smith AG, Vowden K, Vowden The lactate conundrum in wound healing: clinical and experimental findings indicate the requirement for a rapid point-of-care diagnostic. P.Biotechnol Prog. 2012 Jul;28(4):917-24.

Buehler M.J. Nature designs tough collagen: explaining the nanostructure of collagen fibrils Proc Natl Acad Sci USA, 103 2006, pp. 12285–12290

Cannon C.L., Neal P.J., Southee J.A., Kubilus J., Klausner M., New epidermal model for dermal irritancy testing, Toxicol. Vitro 8 1994 889–891.

Chiquet-Ehrismann R., Tenascins. Int. J. Biochem. Cell Biol., 2004, 36, 986–90.

Clark, RAF: Wound repair: Overview and general considerations. In: RAF Clark, ed. The Molecular and Cellular Biology of Wound Repair. New York: Plenum, 1996, pp. 3–50

Consoli A, Kennedy F, Miles J, Gerich J. Determination of Krebs cycle metabolic carbon exchange in vivo and its use to estimate the individual contributions of gluconeogenesis and glycogenolysis to overall glucose output in man. J Clin Invest. 1987;80:1303–1310.

Coulomb B, Lebreton C, Dubertret L., Influence of human dermal fibroblasts on epidermalization. J Invest Dermatol (1989). 92: 122-125.

Council Directive 86/609/EEC of November 1986 on the approximation of laws, regulations and administrative provisions of the Member States regarding the protection of animals used for experimental and other scientific purposes. Official Journal of the European Union L358, 18.12.1986, 1–28.

Dal Pizzol, MM; Roggia, MF; Kwitko, S; Marinho, DR; Rymer, S (2009). Use of fibrin glue in ocular surgery. Arq Bras Oftalmol. 2009 May-Jun;72(3):308-12.

Dietrich W, Spath P, Ebell A, Richter JA: Prevalence of anaphylactic reactions to aprotinin: Analysis of two hundred forty-eight reexposures to aprotinin in heart operations. J Thorac Cardiovasc Surg 1997; 113:194–201

el-Ghalbzouri A, Gibbs S, Lamme E, Van Blitterswijk CA, Ponec M. (2002) Effect of fibroblasts on epidermal regeneration. Br J Dermatol. 2002 Aug;147(2):230-43.

Elias, P. M. Stratum corneum defensive functions: an integrated view. J Invest Dermatol. 2005 Aug;125(2):183-200.

EU, Regulation (EC) No 1907/2006, in: E.P.A.T.C.O.T.E. UNION (Ed.), Official Journal of the European Union, 2006, pp. L 396/391.

EU, Seventh Amendment to the EU Cosmetics Directive 76/768/EEC, in: The European Parliament and the Council of the European Union (Ed.), Brussels, 2003

European Parliament Directive 2010/63/ EU of the European Parliament and of the Council of 22 September 2010 on the protection of animals used for scientific purposes. Official Journal of the European Union L276, 20.10.2010, 33–79.

Fleiss P. M., Hodges F. M. and Van Howe R. S., Sex. Transm. Infect., 1998, 74, 364–7.

Fuchs, E. & Green, H. Changes in keratin gene expression during terminal differentiation of the keratinocyte. Cell. 1980 Apr;19(4):1033-42.

Fusenig NE, Breitkreutz D, Lueder M, Boukamp P, Worst PKM. Keratinization and structural organization in epidermal cell cultures. In: International cell biology 1980-1981 (Schweiger HG ed) Springer-Verlag; Berlin Heidelberg New York, pp 1004-1014.

Fusenig NE., Mammalian epidermal cells in culture. In: Biology of the integument 1986 (Bereiter-Hanh J, Matoltsy AG, Richards KS eds) Springer-Verlag; Berlin Heidelberg New York Tokyo, pp 409-442.

Giangreco A, Qin M, Pintar JE, Watt FM. Epidermal stem cells are retained in vivo throughout skin aging. Aging Cell. 2008 Mar;7(2):250-9.

Griffith LG, Naughton G. Tissue engineering--current challenges and expanding opportunities. Science. 2002 Feb 8;295(5557):1009-14

Grimme J. M. and Cropek D. M. Biomimetic Sensors for Rapid Testing of Water Resources, 2013, ISBN 978-953-51-1035-4

Groeber F. ,Kahlig, A., Loff, S., Walles, H., Hansmann, J. A bioreactor system for interfacial culture and physiological perfusion of vascularized tissue equivalents. Biotechnol J. 2013 Mar;8(3):308-16.

Häckel, M. Oberflächen nach Maß Modifizierung von Kunststoffen mit Atmosphärendruck-Plasmajets. Chemie & More. 2010, 6, S. 42-45.

Huh, D., Hamilton, G.A., Ingber, D., From 3D cell culture to organs-on-chips. Trends Cell Biol., 2011, 21, 745-754.

Huh, D., Matthews, B. D., Mammoto, A., Montoya-Zavala, M., Hsin, H. Y., & Ingber, D. E. (2010). Reconstituting organ-level lung functions on a chip. Science (New York, N.Y.), 328(5986), 1662–8.

Imura Y, Yoshimura E, Sato K. Micro total bioassay system for oral drugs: evaluation of gastrointestinal degradation, intestinal absorption, hepatic metabolism and bioactivity. Anal Sci. 2012;28(3):197-9.

Imura, Y., Sato, K., & Yoshimura, E. Micro total bioassay system for ingested substances: assessment of intestinal absorption, hepatic metabolism, and bioactivity. Analytical chemistry, 82(24), 9983–8.

Imura, Y., Yoshimura, E., & Sato, K. Micro total bioassay system for oral drugs: evaluation of gastrointestinal degradation, intestinal absorption, hepatic metabolism, and bioactivity. Anal Sci. 2012;28(3):197-9.

Jaeschke H, Gores GJ, Cederbaum AI, Hinson JA, Pessayre D, Lemasters JJ. Mechanisms of hepatotoxicity. Toxicol Sci. 2002 Feb;65(2):166-76.

Jahoda CAB, Oliver RF. The dermal papilla and the growth of hair. In: Hair and Hair Diseases . (Orfanos CE, Happle R, eds). 1990 Springer-Verlag (Berlin and New York)

Jang KJ, Mehr AP, Hamilton GA, McPartlin LA, Chung S, Suh KY, Ingber DE. Human kidney proximal tubule-on-a-chip for drug transport and nephrotoxicity assessment. Integr Biol (Camb). 2013 Aug 19;5(9):1119-29.

Johnston LJ, Halliday GM, King NJ. Langerhans cells migrate to local lymph nodes following cutaneous infection with an arbovirus. J Invest Dermatol. 2000 Mar;114(3):560-8..

Kalluri R. Basement membranes: structure, assembly and role in tumour angiogenesis. Nat Rev Cancer. 2003 Jun;3(6):422-33.

Kalyanaraman, B. & Boyce, S. Assessment of an automated bioreactor to propagate and harvest keratinocytes for fabrication of engineered skin substitutes. Tissue Eng. 2007 May;13(5):983-93.

Kalyanaraman, B., Supp, D. M. & Boyce, S. T. Medium flow rate regulates viability and barrier function of engineered skin substitutes in perfusion culture. Tissue Eng Part A. 2008 May;14(5):583-93.

Kane B. J., Zinner M. J., Yarmush M. L. and Toner M. Liver-specific functional studies in a microfluidic array of primary mammalian hepatocytes. Anal. Chem., 2006, 78, 4291–8.

Khademhosseini, A., Langer, R., Borenstein,J., Vacanti, P. Microscale technologies for tissue engineering and biology. Proc. Natl. Acad. Sci.U.S.A., 2006, 103, 2480-2487.

Khetani S. R. and Bhatia S. N. Microscale culture of human liver cells for drug development. Nat. Biotechnol., 2008, 26, 120–6.

Kim HJ, Ingber DE. Gut-on-a-Chip microenvironment induces human intestinal cells to undergo villus differentiation. Integr Biol (Camb). 2013 Aug 19;5(9):1130-40.

Kimoto K, Tanaka K, Toyoda M, Ochiai K. Indirect latex glove contamination and its inhibitory effect onvinyl polysiloxane polymerization. J Prosthet Dent. 2005 May;93(5):433-8.

Klein MB, Pham H, Yalamanchi N, Chang J. Flexor tendon wound healing in vitro: The effect of lactate on tendon cell proliferation and collagen production. J Hand Surg Am. 2001 Sep;26(5):847-54.

Kobayashi N, Nagai H, Yasuda Y, Kanazawa K. The early influence of albumin administration on protein metabolism and wound healing in burned rats. Wound Repair Regen. 2004 Jan-Feb;12(1):109-14.

Lachgar, Charveron, Gall, Bonafe. Minoxidil upregulates the expression of vascular endothelial growth factor in human hair dermal papilla cells Br J Dermatol. 1998 Mar;138(3):407-11.

Lademann J., Richter H., Schaefer U.F., Blume-Peytavi, U., Teichmann A., Otberg N., Sterry W. Hair Follicles – A Long-Term Reservoir for Drug Delivery. Skin Pharmacol Appl Skin Physiol 2006;19:232–236

Lampe, M. A., Williams, M. L. & Elias, P. M. Human epidermal lipids: characterization and modulations during differentiation. J Lipid Res. 1983 Feb;24(2):131-40.

Lee SH, Jin SY, Song JS, Seo KK, Cho KH. Paracrine Effects of Adipose-Derived Stem Cells on Keratinocytes and Dermal Fibroblasts Ann Dermatol. 2012 May;24(2):136-143.

Lindner, G., Horland, R., Wagner, I., Ataç, B., & Lauster, R. De novo formation and ultra-structural characterization of a fiber-producing human hair follicle equivalent in vitro. J Biotechnol. 2011 Mar 20;152(3):108-12..

Lübberstedt M., Müller-Vieira U., Mayer M., Biemel K. M., Knöspel F., Knobeloch D., Nüssler A. K., Gerlach J. C. and Zeilinger K., HepaRG human hepatic cell line utility as a surrogate for primary human hepatocytes in drug metabolism assessment in vitro. J. Pharmacol. Toxicol. Methods, 2010, 63, 59–68.

Luepke NP: Hen's egg chorioallantoic membrane test for irritation potential.. Fd Chem Toxic, 23/1985, S. 287–91.

Magerl, M., Kauser, S., Paus, R. & Tobin, D. J. Simple and rapid method to isolate and culture follicular papillae from human scalp hair follicles. Exp Dermatol. 2002 Aug;11(4):381-5.

Mahler, G. J., Esch M. B., Glahn R. P., and Shuler M. L.. Characterization of a gastrointestinal tract microscale cell culture analog used to predict drug toxicity. Biotechnol Bioeng. 2009 Sep 1;104(1):193-205.

Mahler, G. J., Shuler M. L., and. Glahn R. P. Character ization of Caco-2 and HT29-MTX co-cultures in an in vitro digestion/cell culture model used to predict iron bioavailability. J. Nutr. Biochem 2009. 20:494–502,

Manson, S.M., Simplifying complexity: a review of complexity theory. Geoforum, 2001, 32, 405-414.

Marionnet C., Pierrard C., Vioux-Chagnoleau C., Sok J., Asselineau D. and Bernerd F., Interactions between fibroblasts and keratinocytes in morphogenesis of dermal epidermal junction in a model of reconstructed skin. J. Invest. Dermatol., 2006, 126, 971–9.

Marionnet, C., Pierrard, C., Vioux-Chagnoleau, C., Sok, J., Asselineau, D. & Bernerd, F. Interactions between fibroblasts and keratinocytes in morphogenesis of dermal epidermal junction in a model of reconstructed skin. J Invest Dermatol, 2006, 126, 971-9.

McGrath, J.A.; Eady, R.A.; Pope, F.M. (2004). Rook's Textbook of Dermatology (7th ed.). Blackwell Publishing. pp. 3.1–3.6. ISBN 978-0-632-06429-8.

McMillan JR, Akiyama M, Shimizu H. Epidermal basement membrane zone components: ultrastructural distribution and molecular interactions. J Dermatol Sci. 2003 May;31(3):169-77.

N. J. Hewitt, S. Lloyd, M. Hayden, R. Butler, Y. Sakai, R. Springer, A. Fackett and A. P. Li, Correlation between troglitazone cytotoxicity and drug metabolic enzyme activities in cryopreserved human hepatocytes. Chem.-Biol. Interact., 2002, 142, 73–82.

Neuschwander T. B., Macias B. R., Hargens A. R., and Zhang Q., Mild External Compression of the Leg Increases Skin and Muscle Microvascular Blood Flow and Muscle Oxygenation during Simulated Venous Hypertension. ISRN Vascular Medicine, vol. 2012, Article ID 930913, 6 pages.

Odland, G. F. A submicroscopic granular component in human epidermis. J Invest Dermatol. 1960 Jan;34:11-5.

OECD Guidelines for the Testing of Chemicals Test No. 410: Repeated Dose Dermal Toxicity: 21/28-day Study (1981)

OECD Guidelines for the Testing of Chemicals Test No. 431: In Vitro Skin Corrosion: Human Skin Model Test (2004)

O'Guin, W. M., Galvin, S., Schermer, A. & Sun, T. T. Patterns of keratin expression define distinct pathways of epithelial development and differentiation. Curr Top Dev Biol. 1987;22:97-125.

Otberg N., Patzelt A., Rasulev U., Hagemeister T., Linscheid M., Sinkgraven R., Sterry W., Lademann J. The role of hair follicles in the percutaneous absorption of caffeine. Br J Clin Pharm 2008; 65(4):488-492

Parenteau NL, Nolte CM, Bilbo P, Rosenberg M, Wilkins LM, Johnson EW et al.. Epidermis generated in vitro: practical considerations and applications. J Cell Biochem. 1991 Mar;45(3):245-51.

Peters T., Jr, All About Albumin: Biochemistry, Genetics, and Medical Applications, Academic Press, San Diego, CA, 1996.

Philpott M. P., Green M. R. and Kealey T., Human hair growth in vitro. J. Cell Sci., 1990, 97, 463–71.

Piechocka, I. K., Bacabac, R. G., Potters, M., Mackintosh, F. C., & Koenderink, G. H. Structural hierarchy governs fibrin gel mechanics. Biophys J. 2010 May 19;98(10):2281-9.

Ponec M, Weerheim A, Kempenaar J, Mommaas AM, Nugteren DH. Lipid composition of cultured human keratinocytes in relation to their differentiation. J Lipid Res. 1988 Jul;29(7):949-61.

Ponec, M. Skin constructs for replacement of skin tissues for in vitro testing. Adv Drug Deliv Rev. 2002 Nov 1;54 Suppl 1:S19-30.

Porporato PE, Payen VL, De Saedeleer CJ, Préat V, Thissen JP, Feron O, Sonveaux P. Lactate stimulates angiogenesis and accelerates the healing of superficial and ischemic wounds in mice. Angiogenesis. 2012 Dec;15(4):581-92.

Prunieras M, Regnier M, Woodley D. Methods for cultivation of keratinocytes with an air-liquid interface. J Invest Dermatol. 1983 Jul;81(1 Suppl):28s-33s..

Ramachandran V., Kostrubsky V. E., Komoroski B. J., Zhang S., Dorko K., Esplen J. E., Stromand S. C.. Venkataramanan R, Troglitazone increases cytochrome P-450 3A protein and activity in primary cultures of human hepatocytes. Drug Metab. Dispos., 1999, 27, 1194–1199.

Ramadan V. A., Jafarpoorchekab, Q., Huang, H., Silacci, C., Carrara, P., Ghaye, S. NutriChip: nutrition analysis meets microfluidics. Lab Chip. 2013 Jan 21;13(2):196-203.

Rizza RA, Gerich JE, Haymond MW, Westland RE, Hall LD, Clemens AH, Service FJ. Control of blood sugar in insulin-dependent diabetes: comparison of an artificial endocrine pancreas, subcutaneous insulin infusion and intensified conventional insulin therapy. N Engl J Med. 1980 Dec 4;303(23):1313-8.

Rogue A, Lambert C, Jossé R, Antherieu S, Spire C, Claude N, Guillouzo A. Comparative gene expression profiles induced by PPARγ and PPARα/γ agonists in human hepatocytes. PLoS One. 2011 Apr 18;6(4):e18816.

Rosdy M., Clauss L.C., Terminal epidermal differentiation of human keratinocytes grown in chemically defined medium on inert filter substrates at the air–liquid interface, J. Invest. Dermatol. 95 1990 409–414.

Rovida C, Hartung T. Re-evaluation of animal numbers and costs for in vivo tests to accomplish REACH legislation requirements for chemicals - a report by the transatlantic think tank for toxicology (t(4)). ALTEX. 2009;26(3):187-208.

Russell, W.M.S. & Burch, R.L.. The Principles of Humane Experimental Technique, 1959, 238pp. London, UK: Methuen.

Sanz Garcia S, Santos Heredero X, Izquierdo Hernandez A, Pascual Peña E, Bilbao de Aledo G, Hamann C. Experimental model for local application of growth factors in skin re-epithelialisation. Scand J Plast Reconstr Surg Hand Surg. 2000 Sep;34(3):199-206.

Schaefer H, Lademann J. The Role of Follicular Penetration Skin. Pharmacol Appl Skin Physiol 2001;14(suppl 1):23–27

Scheuplein R.J., Mechanism of percutaneous absorption. II. Transient diffusion and the relative importance of various routes of skin penetration, J. Invest. Dermatol. 48 (1967) 79–88.

Schimek K, Busek M, Brincker S, Groth B, Hoffmann S, Lauster R, Lindner G, Lorenz A, Menzel U, Sonntag F, Walles H, Marx U, Horland R. Integrating biological vasculature into a multi-organ-chip microsystem. Lab Chip. 2013 Aug 13;13(18):3588-98.

Shahabeddin, L., Berthod, F., Damour, O. & Collombel, C. Characterization of skin reconstructed on a chitosan-cross-linked collagen-glycosaminoglycan matrix. Skin Pharmacol 3, 107-14 (1990).

Shuler, M., Modeling Life. Ann Biomed Eng. 2012 Jul;40(7):1399-407..

Sidgwick G. P. and Bayat A., Extracellular matrix molecules implicated in hypertrophic and keloid scarring. J. Eur. Acad. Dermatol. Venereol., 2012, 26, 141–152.

Sin, A., Chin, K. C., Jamil, M. F., Kostov, Y., Rao, G., & Shuler, M. L. The design and fabrication of three-chamber microscale cell culture analog devices with integrated dissolved oxygen sensors. Biotechnol Prog. 2004 Jan-Feb;20(1):338-45.

Sonntag, F., Schilling, N., Mader, K., Gruchow, M., Klotzbach, U., Lindner, G., Horland, R., Wagner, I., Lauster, R., Howitz, S., Hoffmann, S., Marx, U., (2010). Design and prototyping of a chip-based multi-micro-organoid culture system for substance testing, predictive to human (substance) exposure. J Biotechnol. 2010 Jul 1;148(1):70-5.

Stevens K. M. Oxygen requirements for liver cells in vitro. Nature. 1965 Apr 10;206(980):199

Strobel, M, Lyons CS, Mital KL. Plasma Surface Modification of Polymers Relevance to Adhesion Utrecht : VSP, 1993. ISBN-10: 9067641642.

US7288405B2: Devices and methods for pharmacokinetic-based cell culture system, Patent

Wahren J, Felig P, Hagenfeldt L. Physical exercise and fuel homeostasis in diabetes mellitus. Diabetologia. 1978;14:213–222.

Wen Q., Basu A., Winer J. P., Yodh A. and Janmey P. A. Local and global deformations in a strain-stiffening fibrin gel. New J. Phys. 2007 9 428

Woodley DT, Chen M. The basement membrane zone In: The Biology of the Skin. (Freinkel RK, Woodley DT eds) The Parthenon Publishing Group Inc.;2001, New York, pp 133-156.

Wu M.-H., Huang S.-B., Cui Z., Cui Z. and Lee G.-B., Development of perfusion-based micro 3-D cell culture platform and its application for high throughput drug testing. Sens. Actuators, B, 2008, 129, 231–240.

Yano K, Brown LF, Detmar M. Control of hair growth and follicle size by VEGF-mediated angiogenesis. J Clin Invest. 2001 Feb;107(4):409-17.

Zhang, C., Zhao, Z., Abdul Rahim, N. A., Van Noort, D., & Yu, H. Towards a human-on-chip: culturing multiple cell types on a chip with compartmentalized microenvironments. Lab Chip. 2009 Nov 21;9(22):3185-92.

9. Appendix

Publications

- **Wagner I***, Materne EM*, Brincker S, Süßbier U, Frädrich C, Busek M, Sonntag F, Sakharov DA, Trushkin EV, Tonevitsky AG, Lauster R, Marx U. (2013)
  A dynamic multi-organ-chip for long-term cultivation and substance testing proven by 3D human liver and skin tissue co-culture. Lab Chip. Aug 13;13(18):3538-47
- **Wagner I*,** Ataç B*, Horland R, Lauster R, Marx U, Tonevitsky AG, Azar RP, Lindner G. (2013)
  Skin and hair on-a-chip: in vitro skin models versus ex vivo tissue maintenance with dynamic perfusion. Lab Chip. Aug 13;13(18):3555-61.
- Sonntag F, Schilling N, Mader K, Gruchow M, Klotzbach U, Lindner G, Horland R, **Wagner I**, Lauster R, Howitz S, Marx U (2010)
  Design and prototyping of a chip-based multi-micro-organoid culture system for substance testing, predictive to human (substance) exposure. Journal of Biotechnology, Volume 148, Issue 1, 70-75
- Lindner, G., Horland, R., **Wagner, I.,** Ataç, B., Lauster, R. (2011)
  De novo formation and ultra-structural characterization of a fiber-producing human hair follicle equivalent *in vitro*. Journal of Biotechnology, Volume 152, Issue 3, 108-112
- Sonntag, F., Gruchow, M., **Wagner, I.**, Lindner, G., Marx, U. (2011)
  Miniaturisierte humane organtypische Zell- und Gewebekulturen. Biospektrum 04/2011

Eidesstattliche Erklärung

Ich erkläre an Eides Statt, dass die vorliegende Dissertation in allen Teilen von mir selbstständig angefertigt wurde und die benutzen Hilfsmittel vollständig angegeben worden sind

Ilka Wagner
Berlin, den 11.10.2013